Winter 12-15-2017

The Regulation of Extracellular Amyloid-β Levels by Ionotropic Glutamatergic Transmission in an Alzheimer's Disease Mouse Model

Jane Cecelia Hettinger
Washington University in St. Louis

WASHINGTON UNIVERSITY IN ST. LOUIS

Division of Biology and Biomedical Sciences
Neurosciences

Dissertation Examination Committee:
John Cirrito, Chair
Jin-Moo Lee
Steven Mennerick
Erik Musiek
Karen O'Malley

The Regulation of Extracellular Amyloid-β Levels by Ionotropic Glutamatergic Transmission in an Alzheimer's Disease Mouse Model

by
Jane Hettinger

A dissertation presented to
The Graduate School
of Washington University in
partial fulfillment of the
requirements for the degree
of Doctor of Philosophy

December 2017
St. Louis, Missouri

Table of Contents

List of Figures

Chapter 2

Chapter 3

Acknowledgments

First, I would like to extend profound gratitude to my thesis mentor and friend, Dr. John Cirrito. John has been an incredibly patient and generous mentor for the past six years. From my very first days in the lab, John has actively taught me both how to do and how to think about science, and has even jumped in to help out with early morning time points or collecting microdialysis samples in odd hours of the night. His door is always open for science, life questions, conversation, and adorable cat and/or toddler pictures. When I had to take months out of the lab for surgery, he was amazingly supportive, with only the occasional gibe about my early-onset old age. Almost no dry ice bombs were deployed in the making of this PhD.

I owe so much to the denizens of the Cirrito lab, past and present. Thank you for patiently teaching me techniques, chatting with me about science and life, listening to all my cat stories, telling me your own cat (and dog) stories, stepping in to help me out with lab chores. Special thanks to Hyo Lee for the qPCR experiments, Todd Davis for the histology, and Clare Wallace for being a microdialysis comrade-in-arms. And, of course, I couldn't have done it (sanely) without Carla Yuede. Carla, your friendship has meant so much to me. Thank you for the talks, scientific and otherwise.

I would also like to warmly thank the members of my thesis committee, Steve Mennerick, Jin-Moo Lee, Erik Musiek, and Karen O'Malley for the scientific knowledge they've shared, for the hours they patiently listened to me talk, for the helpful feedback each member provided, and for the understanding and flexibility they showed me.

Lastly, I have to thank my family for holding me up and keeping me on my feet. You are everything and I wouldn't make it out the door without you backing me up. The hours of phone

calls, the group texts, the cards, the emails, the many, many, many cat/dog/baby pictures, and the visits remind me how loved and supported and lucky I am, all the time.

Mom and Dad, you are my biggest supporters and constant cheerleaders. You never doubt me, even when I lose confidence in myself. Without the traits you instilled in me I never would have made it through graduate school, or really though much of anything. To you I owe my perseverance, my work ethic, my ability to laugh it off and keep going, my curiosity, and much, much more. How two accountants raised daughters with careers in higher education, policy, and science is a bit of a mystery, but I think it means you gave us the skills and attitudes to succeed in whatever area we chose. How lucky are we?

Mary Beth and Margaret, it is an incredible privilege to have you as my older sisters. My entire life, I've had two built-in companions looking out for me. It's so incredible to have people that instantly understand and validate how I feel. I love what we share, from life experiences to identical senses of humor. Your pride in me throughout grad school made me feel like I was doing something much cooler than staying in school to 23rd grade. Jay and Alyssa, our family is stronger, happier, fuller, and, of course, more decisive with the two of you in it. Both of you have been incredibly enthusiastic supporters of my progress, and it makes my heart happy.

Lastly, I would like to thank my grandparents for the lessons and values and love they shared with me. In many ways, this dissertation is dedicated to them.

Jane Hettinger

Washington University in St. Louis

December 2017

ABSTRACT OF THE DISSERTATION

The Regulation of Extracellular Amyloid-β Levels by Ionotropic Glutamatergic Transmission in an Alzheimer's Disease Mouse Model

by

Jane Cecelia Hettinger

Doctor of Philosophy in Biology and Biomedical Sciences

Neurosciences

Washington University in St. Louis, 2017

Professor John R Cirrito, Chair

Brain extracellular concentration of the peptide amyloid-β (Aβ) is a major contributor to Alzheimer's disease (AD) pathogenesis. High Aβ levels in the extracellular space precipitate aggregation of the peptide into soluble and insoluble toxic species. This process begins decades before cognitive impairment and triggers the cascade of pathology that eventually leads to AD. Synaptic activity is key to the regulation of extracellular Aβ levels. Presynaptic activity drives the production of Aβ, while postsynaptic receptor activation exhibits more nuanced regulation. For example, high levels of NMDA receptor (NMDA-R) activation have been shown to decrease Aβ production through the extracellular signal-regulated kinase (ERK). The studies outlined in this document sought to determine the pathways by which Aβ levels are influenced by NMDA-Rs as well as the other major ionotropic glutamate receptors, AMPA-Rs. We found that NMDA-Rs activate ERK and decrease Aβ production through a pathway non-specific to NMDA-R subtype or ERK isoform and that does not rely on calcium/calmodulin-dependent protein kinase II (CaMKII), protein kinase A (PKA), or protein kinase C (PKC) signaling. We also found that

though basal AMPA-R activity increases Aβ levels, evoked activation of AMPA-Rs reduces extracellular Aβ through distinct NMDA-R-dependent and independent pathways. Unexpectedly, NMDA-R-independent AMPA-R regulation decreases Aβ levels by reducing its half-life in the extracellular fluid. Because previous studies describe synaptic activity-mediated Aβ regulation through altered production, this finding presents a novel link between synaptic transmission and Aβ clearance. The work described here aims to explore the mechanisms by which normal brain activity influences Aβ homeostasis in an effort to more fully understand AD pathogenesis.

EPIGRAPH

"My strength lies solely in my tenacity."

- Louis Pasteur

Chapter 1

Introduction and Perspective

Alzheimer's Disease

Alzheimer's disease (AD) accounts for 60 to 80 percent of dementia, affecting an estimated 5.4 million Americans as of 2016 (www.alz.org). The prevalence of AD is only expected to grow due to an aging population, with estimates projecting 13.8 million affected Americans by 2050 barring significant scientific progress. The cost of dementia healthcare is overwhelming and untenable; 2016 healthcare costs are estimated to be $236 billion even without incorporating secondary costs to care providers. Out of the top ten causes of death, AD is the only disease without a cure, prevention, or even a way to slow disease progression. There are currently only five FDA-approved pharmaceuticals for AD, and all are designed to temporarily ease symptoms. Clearly, there is an exigent need for AD therapeutic development.

In the ten-year period between 2002 and 2012, over 400 AD clinical trials were performed with a disheartening 0.4% rate of success (Cummings et al., 2014). A variety of factors have contributed to the failure of these trials, including a lack of clear and sensitive outcome criteria, complications with drug delivery, and the protracted trial length required for such studies (Becker 2008). A further obstacle to progress is that the presentation of AD symptomatology occurs at least 10-20 years after disease pathogenesis (Morris and Price, 2001). On a positive note, recent advances have characterized AD biomarkers that now allow clinicians and researchers to quantify presymptomatic AD pathology.

The Alzheimer's diseased brain exhibits extensive neuronal death and synaptic loss throughout the cortex as well as two major lesions: amyloid plaques and neurofibrillary tangles. Amyloid plaques are composed of the peptide amyloid-β (Aβ) aggregated within the extracellular space of the brain. Aβ that has folded into traditional amyloid β-sheet secondary

structures are called fibrillar plaques, whereas diffuse plaques are composed amorphous deposits of Aβ. Fibrillar plaques, also called neuritic plaques, are usually surrounded by a corona of dystrophic neurites and activated glia. Neurofibrillary tangles, on the other hand, are intracellular deposits of hyperphosphorylated tau. Normally, tau serves as a tubulin binding protein that stabilizes microtubules. In AD, however, tau is hyperphosphorylated, dissociates from microtubules, and accumulates as paired helical filaments. Cognitive impairment is highly correlated with the presence of neurofibrillary tangles, though the same is not true of amyloid plaques (Nagy et al., 1995; Guillozet et al., 2003; Bennett et al., 2004; Mocanu et al., 2008). These two AD pathologies share a complex relationship that is still an active area of research. The presence of Aβ plaques appears to drive tau pathology. Tau pathology is not seen in the neocortex without coexisting Aβ pathology, though amyloid plaques can occur without the presence of tau (Price and Morris, 1999). In addition, tau pathology is greatly exaggerated in mice with mutant human tau following injection of Aβ fibrils (Götz et al., 2001). In cognitively-impaired transgenic mice with both human Aβ and tau, however, the removal of Aβ pathology is not sufficient to ameliorate cognitive loss (Oddo et al., 2006). Furthermore, tau aggregation can directly cause neurotoxicity and synaptic loss in mouse models with mutant tau, while amyloid-only AD mouse models do not exhibit neurodegeneration (Mocanu et al., 2008). It appears that Aβ is necessary to initiate disease pathology but not sufficient to explain the entirety of AD pathology or symptomology. The relative importance of both Aβ and tau aggregates in AD progression continues to be hotly debated, a topic that I will discuss in greater detail below.

Amyloid Cascade Hypothesis

Amyloid-β (Aβ) was first discovered by isolating and purifying the principal component of cerebral amyloid angiopathy (CAA) and then amyloid plaques from Alzheimer's disease and Down's syndrome brains (Glenner and Wong, 1984; Masters et al., 1985). In 1987, genetic analysis revealed the amino acid sequence of Aβ, isolated the amyloid precursor protein (APP) from which Aβ is cleaved, and mapped *APP* to chromosome 21 (Goldgaber et al., 1987; Tanzi et al., 1987; Tanzi, 2012). After the first causative early onset-familial AD (EO-FAD) mutation in *APP* was discovered in 1991 (Goate et al., 1991), many began to view Aβ as the initiating factor in AD pathology, a concept that was presented by Hardy & Higgins (1992) as the amyloid cascade hypothesis. In the 15 years since this seminal paper was published, mountains of data has been generated in support and against this hypothesis, making it arguably the most controversial topic in AD research today.

One of the strongest arguments bolstering the amyloid cascade hypothesis is made using the genetic data gathered from AD patients, particularly from those patients with EO-FAD. EO-FAD is extremely rare and numbers regarding its prevalence are vague. Approximately 1-5% of all AD cases are thought to be early onset, both familial and sporadic (alzforum.org). EO-FAD is characterized by an autosomal dominant inheritance of fully penetrant mutations in any one of three genes: *APP*, *presenilin-1* (*PSEN1*), and *presenilin-2* (*PSEN2*) (for review see: Tanzi, 2012). Importantly for the amyloid cascade hypothesis, inheritance of any of the approximately 225 mutations identified for EO-FAD (http://www.molgen.ua.ac.be/ADMutations) causes AD by influencing Aβ aggregation. In these rare cases, Aβ clearly drives pathology, which begins with the appearance of fibrillar amyloid plaques later followed by tau pathology and neuronal loss (Musiek and Holtzman, 2015).

Though EO-FAD genes clearly indicate Aβ as a causative factor in AD, late-onset AD (LOAD) compromises the vast majority of AD cases. LOAD susceptibility is much more complex than EO-FAD and includes a myriad of genetic risk factors as well as environmental influences. Currently, numerous large, worldwide, case-controlled genome-wide association studies (GWAS) have identified 12 genes associated with LOAD. Only one of these gene variants, however, is an established risk factor with a strong association with AD – the ε4 allele of the apolipoprotein gene (*APOE*; Strittmatter et al., 1993; Tanzi, 2012). Though *APOE* ε4 is not a causative factor in AD, one copy of the allele increases the risk of 4-fold and two copies increase the risk 12-fold (Corder et al., 1993). ApoE has a multitude of roles in the CNS, primarily involving lipid metabolism and transport. Its relevance to AD, apoE has shown to bind Aβ directly and studies have found that earlier and greater Aβ deposition occurs in individuals with two ε4 alleles. Furthermore, studies using transgenic Alzheimer mouse models have found that apoE alleles can influence the amount and structure of Aβ deposits in the brain (Holtzman et al., 2000, 2011). As with EO-FAD, the genetic factors for LOAD yield strong evidence that Aβ has an important and potentially causative role in AD.

Despite these strong genetic arguments for the amyloid cascade hypothesis, there remain a number of concerns regarding the importance of Aβ and its initiating role in pathology. The first argument against the hypothesis is the lack of correlation between the amount of Aβ deposition and neuronal loss and clinical symptoms, both temporally and spatially. Where Aβ plaques begin to form in the precuneus and frontal lobes, neuronal loss occurs in the entorhinal cortex and hippocampus (Braak and Braak, 1991). Tau pathology, on the other hand, overlaps with neuronal loss and correlates more strongly with cognitive impairment (Arriagada et al., 1992; Nagy et al., 1995; Mocanu et al., 2008). The lack of correlation between plaque load and

AD symptoms has been made clear following the unfortunate failure of clinical trials that have targeted Aβ. Notable is the Elan AN1792 active Aβ immunization study in which amyloid plaques were successfully cleared from the brains of AD patients without a resulting improvement in cognition (Holmes et al., 2008).

Although these findings certainly cast doubt on the concept that Aβ causes AD symptomology on its own, there is still a strong argument for the importance of Aβ in AD. While overall amyloid burden might not correlate with cognitive impairment, a number of studies suggest that it is soluble oligomeric Aβ species that are neurotoxic and cause synaptic dysfunction, not monomeric Aβ or fibrillar amyloid plaques (De Felice et al., 2007; Lacor et al., 2007; Benilova et al., 2012; Talantova et al., 2013). Oligomer quantification is difficult, but it could be that the number of oligomers has a stronger correlation with cognitive decline than plaque load. Moreover, evidence suggests that Aβ-related pathology has the ability to initiate downstream AD pathology. Mice generated with both mutant human APP and mutant human tau show increased formation of tau tangles compared to mice that only express human tau, though the number of plaques is unchanged (Lewis et al., 2001). Furthermore, human biomarker data shows that Aβ pathology precedes alterations in tau pathology by years (Bateman et al., 2012). In light of the genetic data previously described, the fact that Aβ deposition occurs before other AD pathology suggests that Aβ production and aggregation is the causative, initiating factor of AD pathogenesis. Initial clinical trials targeted Aβ using participants within the later stages of AD who already exhibit cognitive decline. By this point in the disease progression, Aβ has already initiated an entire cascade of downstream pathology that will likely not be ameliorated once Aβ is removed. Thus, when targeting Aβ, the earlier, the better to intercede prior to substantial

pathology, cell loss, or brain damage. Naturally, the difficulty with this notion is identifying and recruiting asymptomatic participants who may or may not develop AD.

One ongoing study, the Dominantly Inherited Alzheimer Network (DIAN) treatment trial, seeks to address this issue by recruiting participants from OE-FAD families who carry a causative mutation and beginning anti-amyloid treatment early in the pathological cascade (Bateman et al., 2012). Another ongoing trial, the Anti-Amyloid Treatment in Asymptomatic Alzheimer's Disease (A4) study, is using cognitively normal, older participants who show evidence of amyloid pathology with the same concept of targeting Aβ early to prevent further AD pathology and cognitive decline (https://clinicaltrials.gov). Results from these studies will give insight into the amyloid hypothesis, and will particularly indicate the viability of therapeutically targeting Aβ.

The amyloid cascade hypothesis has stood as one of the fundamental concepts guiding Alzheimer's research since its conception in 1992(Hardy and Higgins, 1992; Hardy and Selkoe, 2002; Selkoe and Hardy, 2016). Since this time, we have found that AD comprises a complex confusion of pathological events, such as tau phosphorylation, neuroinflammation, mitochondrial damage, synaptic dysfunction, oxidative stress, and neuronal loss (Musiek and Holtzman, 2015). Though Aβ is clearly not acting on its own to bring about the changes observed in the AD brain, neither its importance in AD pathogenesis nor its potential as an AD therapeutic can be denied.

Amyloid Precursor Protein Processing

Amyloid-β is a 37-43 amino acid peptide produced from the cleavage of the amyloid precursor protein (APP). The APP family of proteins, which includes the APP-like protein 1 and 2 (APLP1, 2), are type 1 membrane proteins with large extracellular domain and short cytoplasmic tails (Zheng et al., 2011). These APLPs do not produce Aβ; though the family is highly conserved, APLPs lack the Aβ sequence. While the specific physiological function of APP is not known, the fact that Aβ is not conserved suggests that it is unrelated to APP's primary function. APP is ubiquitously expressed throughout the body and is highly enriched in the brain. Within the CNS, APP is strongly expressed in neurons, with little to no expression in non-neuronal cell types (Guo et al., 2012). Once APP is produced, it leaves the ER and is sorted through the trans-Golgi network and trafficked to the plasma membrane. APP is then internalized and trafficked through the endocytic pathway to either be recycled back to the membrane or degraded in the lysosome (Thinakaran and Koo, 2008). When APP reaches the membrane, it is subject to processing through the amyloidogenic or non-amyloidogenic pathways.

Amyloidogenic Pathway

Amyloidogenic APP processing occurs when APP is sequentially cleaved by β-and γ-secretases to produce the Aβ peptide. APP is first cleaved by β-secretase, resulting in the shedding of most of the ectodomain, a fragment called sAPPβ. The resulting C-terminal, membrane-bound fragment is termed C99 or β-CTF. C99 can then be cleaved by γ-secretase to produce Aβ and the APP intracellular domain (AICD; Haass et al., 2012). Cleavage by β-secretase is the rate-limiting process in Aβ production. The enzyme within β-secretase responsible for cleaving at the β-site, a transmembrane aspartyl protease, has been identified and

named BACE1 (β-site APP cleaving enzyme). BACE1 is optimally active in acidic environments, such as found in the lumen of endosomes, suggesting that BACE1 preferentially cleaves APP once endocytosed (Turner et al., 2003; Haass et al., 2012). Given its role in producing Aβ, BACE1 is clearly an attractive target for drug development. Many BACE inhibitors have been developed, and there are clinical trials ongoing whose outcomes are yet to be seen (www.alzforum.org).

The γ-secretase complex is composed of four subunits: presenilin-1 (PS1), presenilin-2 (PS2), nicastrin, APH-1, and PEN-2. Presenilin-1 and -2 make up the catalytic domain of the complex. γ-Secretase is a sloppy proteinase and cleaves at multiple sites within the transmembrane domain of Aβ between amino acids 37 and 43, producing different Aβ species (Thinakaran and Koo, 2008). Most of the Aβ produced is 40 residues in length ($A\beta_{40}$), but the longer $A\beta_{42}$ residue is more prone to aggregation and thus the major component of amyloid plaques (Miller et al., 1993). Mature γ-secretase is principally located at the plasma membrane and in endosomes. Interestingly, of the three genes with mutations linked to EO-FAD, two involve the γ-secretase complex. Mutations in PS-1 and -2 alter cleavage site specificity, leading to the preferential production of $A\beta_{42}$ over $A\beta_{40}$. The resulting increased $A\beta_{42}/A\beta_{40}$ ratio leads to increased amyloid aggregation.

Of all the secretases, γ-secretase has proven to be the most tractable target for drug development. There have been multiple effective γ-secretase inhibitors (GSIs) developed that decrease Aβ production in both mice and humans, though toxicity has been an issue. Enthusiasm for GSI clinical trials has been low following the dramatic failure of Eli Lilly's phase III semagacestat in which there were both significant toxic effects as well as clinical worsening (Doody et al., 2013). To date, all GSI clinical trials have been stopped due to mechanism-based

toxicities. A new class of drug targeting γ-secretase is now in development. Gamma-secretase modulators (GSMs) modify the activity of the enzyme so that less $A\beta_{42}$ is produced without changing the processing of other γ-secretase substrates. Currently, these drugs are still only tested in animal models in an effort to combine potency with safe drug-like properties but are expected to move into proof-of-mechanism human clinical trials (Bursavich et al., 2016).

As mentioned above, BACE1's increased activity in low pH environments suggests that the amyloidogenic processing of Aβ occurs within endosomes. Indeed, multiple groups have found that clathrin-mediated endocytosis of APP is essential for Aβ generation (Koo and Squazzo, 1994; Cirrito et al., 2008). Further, Aβ elimination is not affected when endocytosis is blocked. Once Aβ is cleaved from APP, it is released into the endosomal lumen and then released into the extracellular space following exocytosis. Once in the extracellular space, Aβ can begin to aggregate. Importantly, greater extracellular concentrations of Aβ result in elevated aggregation and vice versa (Meyer-Luehmann et al., 2003).

Non-amyloidogenic Pathway

The production of Aβ can be precluded if APP is cleaved by α-secretase instead of β-secretase. This non-amyloidogenic processing occurs because α-secretase cleaves APP within the Aβ domain, resulting in the large ectodomain sAPPα and the membrane-tethered C83 or α-CTF. C83 can then be cleaved by γ-secretase to produce the 3kDa p3 and AICD, similarly to C99 (Zheng et al., 2011). There are several zinc metalloproteinases, members of the "a disintegrin and metalloproteinase" family (ADAM), that can function as α-secretases; however, ADAM10 has been identified as the primary α-secretase in neurons (Kuhn et al., 2010). Non-amyloidogenic APP processing predominantly occurs at the plasma membrane (Haass et al.,

2012). Studies that overexpress or knockout BACE1 have found that there may be substrate competition between α- and β-secretase such that enhancing the amyloidogenic pathway depresses the non-amyloidogenic pathway and vice versa (Turner et al., 2003). The therapeutic implication of this fact is that increasing α-secretase activity and the non-amyloidogenic pathway leads to decreased Aβ production. In support of this concept, overexpression of ADAM10 in an amyloidosis mouse model results in decreased amyloid pathology (Postina et al., 2004; De Strooper et al., 2010). Despite this, α-secretase is not an ideal therapeutic target due to a high degree of redundancy between the ADAM proteases, making direct activators difficult to develop. However, drugs that indirectly activate α-secretase by targeting a regulator of its activity show more promise (De Strooper et al., 2010).

Synaptic Activity and Aβ Production

Production of Aβ is influenced by a number of regulators, chief among them being synaptic activity. In 2003, Kamenetz et al. tested the role that neuronal activity plays in APP processing by using pharmacology to increase or decrease activity in organotypic hippocampal slices from an AD mouse model and measuring the Aβ levels in the medium. When activity was decreased, levels of both $A\beta_{40}$ and $A\beta_{42}$ were reduced. Conversely, levels were elevated with enhanced neuronal activity. Further experimentation found that levels of C99 (β-CTF) were increased with increased activity, suggesting that β-secretase is involved in the elevation of Aβ levels.

Following this intriguing paper, Cirrito et al. (2005) used in vivo microdialysis to test the relationship between synaptic activity and Aβ production in awake, freely moving AD mouse

models. Both pharmacological manipulators of activity (tetrodotoxin and tetanus toxin to decrease activity, picrotoxin to increase) and perforant pathway electrical stimulation were used and interstitial fluid (ISF) Aβ levels were measured. As in the study by Kamenetz et al., synaptic activity was determined to drive Aβ generation. The study further identified that synaptic vesicle exocytosis alone, even without an action potential, was enough to increase Aβ levels. Cirrito et al. (2005) proposed that synaptic vesicle membrane recycling that occurs during synaptic activity is linked to APP endocytosis, which, as previously discussed, is known to increase Aβ production and release (Koo and Squazzo, 1994; Cirrito et al., 2008). In fact, inhibiting clathrin-mediated endocytosis with a dominant negative version of dynamin, an endocytosis GTPase, completely blocked the effect of synaptic activity on Aβ levels. The opposite is not true; inhibiting action potentials only partially blocks the effect of endocytosis, meaning that there is a percentage of Aβ produced through endocytosis not caused by synaptic activity (Cirrito et al., 2008). In line with these findings, Das et al. (2013) were able to visualize APP and BACE1 trafficking in cultured neurons to show that synaptic activity causes the convergence of APP and BACE1 in recycling endosomes, resulting in increased Aβ production.

Further studies have gone on to test the relationship between synaptic activity and Aβ generation in more physiological settings. For example, endogenous neuronal activity was induced in the barrel cortex through manual vibrissal stimulation, resulting in localized increases in ISF Aβ levels (Bero et al., 2011). Similarly, unilateral ablation of whiskers lead to depressed activity in the corresponding barrel cortices and thus reduced plaque load (Tampellini et al., 2010a). Another piece of physiological evidence comes from studies showing that Aβ levels in the ISF follow a diurnal pattern with highest levels during periods of wakefulness and lowest levels during sleep. Furthermore, acute sleep deprivation resulted in increased ISF Aβ and

chronic sleep deprivation lead to increased Aβ plaque deposition (Kang et al., 2009). These results were supported and furthered by a recent study showing that disruption of slow wave activity, which occurs during non-REM sleep and represents decreased synaptic activity, increased Aβ levels in the cerebrospinal fluid of cognitively normal human participants (Ju et al., 2017).

Observations in human patients support synaptic activity-dependent Aβ generation. Temporal lobe tissue removed from non-demented epileptic patients was found to have a greater incidence of senile plaques than non-epileptic autopsy controls, indicating that elevated synaptic activity can drive amyloid pathology (Mackenzie and Miller, 1994). Studies using both positron emission topography (PET) and functional magnetic resonance imaging (fMRI) have identified a network of cortical regions that are active during rest, when the participants are not actively performing a task, termed the default mode network (Raichle et al., 2001). Revealingly, this network of brain regions that maintain a high level of synaptic activity closely correlate with the pattern of amyloid deposition in AD brains (Buckner et al., 2005). Buckner et al. (2009) continued on to identify that these default mode regions are actually part of a map of cortical hubs, areas that provide nodes of convergence for interconnecting and distinct systems through high levels of connectivity. These hubs maintain high levels of activity continuously regardless of task state. The study found that high levels of connectivity in the brain, i.e., hubs, strongly correlate with levels of Aβ deposition (Buckner et al., 2009). Finally, a study using patients undergoing intracranial monitoring following acute brain injury was able to demonstrate that, as in mice, human brain ISF Aβ concentrations correlate with neuronal function (Brody et al., 2008).

Post-synaptic Signaling and Aβ Production

Synaptic activity regulates of Aβ production through increased endocytosis at the presynaptic membrane, as discussed previously. In addition to this presynaptic pathway of regulation, synaptic activity can also modulate APP processing and Aβ production through postsynaptic receptor signaling. This modulation can occur in opposition to presynaptic-dependent Aβ release, resulting in decreased Aβ production. Compared to the presynaptic pathway discussed before, postsynaptic regulation is complex and frequently involves multiple signaling events.

Agonists for muscarinic acetylcholine receptors (mAChRs) have been used to ameliorate cognitive impairment in humans for many years. This limited clinical value has inspired a number of studies investigating the relationship between mAChRs and AD pathology, including Aβ production. These studies found that M1 mAChR stimulation increased the production of sAPPα, indicating increased non-amyloidogenic processing of APP (Fisher, 2012). M1 AChRs act on APP processing through protein kinase C (PKC) activation, which activates ADAM17 in turn. Blocking mAChR signaling either by chemically lesioning the cholinergic nucleus basalis magnocellularis or by using a specific inhibitor decreased Aβ plaque load in an AD mouse model. mAChR inhibition both activated α-secretase and inhibited BACE1 (Fisher, 2012). Furthermore, deletion of M1 mAChRs enhanced cognitive impairment and resulted in greater plaque load (Davis et al., 2010).

Throughout the brain, glutamate serves as the primary excitatory neurotransmitter. There are multiple subtypes of glutamate receptors, both ionotropic and metabotropic. Within the context of AD, the ionotropic N-methyl-D-aspartate (NMDA) receptor is the most studied due to

its pivotal role in mediating long-term potentiation (LTP), the cellular correlate for memory. There is a great deal of evidence linking Aβ to NMDA-R dysfunction (for review see Zhang et al., 2016), but there are a number of studies that describe a reciprocal relationship in which NMDA-R signaling affects APP processing and Aβ production. Low concentrations of NMDA applied to primary cortical neurons promoted Aβ release via increased BACE processing (Lesné et al., 2005). A different group, however, found that an acute, sublethal pulse of NMDA treatment *in vitro* resulted in increased trafficking of ADAM10 to the postsynaptic membrane through an interaction with the synapse-associated protein97 (SAP97), which would increase non-amyloidogenic APP processing (Marcello et al., 2007). In concurrence with this study, Hoey et al. (2009) found that NMDA receptor signaling increases C83 (CTF-α) by 2.5-fold, indicating an increase in α-secretase APP cleavage. Indeed, these effects were blocked by treatment with an α-secretase inhibitor (Hoey et al., 2009). In 2011, our group published a paper addressing these incongruent findings using *in vivo* microdialysis to address the question in a more physiological context. A mouse model of AD was treated with a range of NMDA concentrations. We found that the effect of NMDA on Aβ levels in the ISF is dependent on concentration such that low concentrations of NMDA increase ISF Aβ while higher doses appear to do the opposite. Further experiments showed that the increase in Aβ found with low levels of NMDA activation is dependent on action potentials in a manner identical to previous findings that presynaptic activity drives Aβ (Cirrito et al., 2005b; Verges et al., 2011), though higher levels of NMDA do not require synaptic activity to affect Aβ. Instead, high doses of NMDA lead to calcium-dependent activation of extracellular regulated kinase (ERK), which initiates a signaling cascade that promotes α-secretase activity. Thus, this study reconciled previous conflicting reports on NMDA-Rs relationship to Aβ production by positing that the end result of NMDA-R activation

depends on the level of ERK activation (Verges et al., 2011). The pathway through which ERK ultimately acts on α-secretase activity is unknown and will be addressed later in this document.

Another group of glutamatergic postsynaptic receptor shown to regulate Aβ production is the metabotropic glutamate receptors (mGluRs), although its actions on Aβ are more complex. Broad mGluR activation in primary cultures and in slices resulted in increased sAPPα; however, a more selective agonism of the mGluR subtype mGluR5 has the opposite effect, increasing Aβ production. This indicates that specific receptor subtypes have opposing effects on Aβ generation. In fact, activation of postsynaptic Group I mGluRs was found to produce $A\beta_{40}$ release while Group II mGluR stimulation triggered $A\beta_{42}$ production (Kim et al., 2010). In support of these results, the genetic deletion of mGluR5 in AD mouse models resulted in significantly decreased Aβ aggregation and plaque number along with improved cognition (Hamilton et al., 2014).

The final postsynaptic receptor to discuss is the serotonin (5-HT) receptor. Using *in vivo* microdialysis to treat Alzheimer's mouse models of AD with selective serotonin reuptake inhibitors (SSRIs) that increase serotonergic signaling, drugs that are commonly used to treat depression, lead to decrease ISF Aβ levels, as does direct treatment with serotonin (Cirrito et al., 2011). Like the effect of NMDA-Rs on Aβ, this serotonergic effect is dependent on ERK signaling and increased α-secretase activity. This pathway appears to rely on the activation of the $5\text{-}HT_5R$, $5\text{-}HT_6R$, and $5\text{-}HT_7R$ subtypes, which are all coupled to G_s-signaling and activate protein kinase A (PKA; Fisher et al., 2016). Chronic SSRI administration to AD mouse models for four months decreased both soluble and insoluble Aβ levels in brain lysates and decreased plaque load. These findings were supported by similar findings in humans. Cognitively normal participants with a history of antidepressant use underwent PET Aβ imaging, a method used to

quantify cortical plaque load. Compared to participants with no antidepressant usage reported, treated participants exhibited much less cortical amyloid (approximately half). Given that SSRIs are FDA-approved and well-tolerated, the authors of this study propose that SSRIs could make an ideal preventative anti-Aβ therapy (Cirrito et al., 2011; Sheline et al., 2014)

Amyloid-β Clearance

As mentioned previously, the steady-state concentration in the extracellular space is a key determinant in the propensity of monomeric Aβ to begin the toxic process of aggregation (Meyer-Luehmann et al., 2003). While much of the research on Aβ focuses on its production, increased steady-state Aβ levels spring from an imbalance between production and clearance. In fact, evidence is beginning to indicate that impaired Aβ clearance may be a key factor in both EO-FAD and LOAD. In a study by Mawuenyega et al. (2010), used a technique called stable isotope labeling kinetics (SILK) to compare the kinetics of Aβ turnover in the CSF of participants with symptomatic LOAD to cognitively normal controls. Briefly, participants were infused with a non-radioactive isotope-labeled leucine, which is soon incorporated into most newly made leucine-containing proteins. CSF samples are collected from the participants through lumbar puncture hourly and analyzed for labeled Aβ using tandem mass spectrometry. Both production and clearance kinetics can be calculated using this method, making it a powerful tool. Surprisingly, the researchers found a 30% impairment in the clearance of both $A\beta_{40}$ and $A\beta_{42}$ in the Alzheimer's patients compared to controls, though no change in production was measured (Mawuenyega et al., 2010). The same technique was used in EO-FAD participants carrying *PSEN* mutations. Compared to sibling noncarrier controls, the *PSEN* mutation carriers

exhibited a 24% increase in CNS $A\beta_{40}$ and $A\beta_{42}$, suggesting that EO-FAD and LOAD have different disease mechanisms (Potter et al., 2013).

The prominence of impaired clearance in LOAD is supported by genetic evidence. The strongest risk factor for LOAD, the apoE ε4 allele, is thought to involve alterations in Aβ clearance, although the exact mechanism behind apoE's link to AD remains controversial (Bell et al., 2007). In addition to apoE, GWAS have identified several other genetic variants that increase the risk of LOAD. At least two of these gene, *PICALM* and *CLU*, are thought to be related to Aβ clearance (De Strooper and Karran, 2016). Aβ clearance is a complex process mediated through multiple processes and molecular players. Below I will outline the four major pathways responsible for clearing Aβ from the extracellular space: proteolytic degradation, transport into the blood or lymph, bulk flow of the CSF, and cellular uptake and subsequent intracellular degradation.

Aβ Transport across the BBB

By comparing Aβ levels in time-matched arterial, peripheral venous, and central venous blood samples from human participants, Roberts et al. (2014) were able to calculate the net transport of Aβ across a capillary bed from the CNS to the plasma. Based on these findings, the researchers conservatively estimated that approximately 25% of Aβ clearance results from direct transport of Aβ across the BBB (Roberts et al., 2014). Movement of Aβ across the BBB is primarily mediated by two receptor proteins: the low-density lipoprotein receptor related protein-1 (LRP1) and the receptor for advanced glycation end products (RAGE). LRP1 is associated with Aβ efflux from the brain into the periphery, whereas RAGE is implicated in influx.

LRP1 is a member of the LDL receptor family involved in signal transduction that has been shown to interact with Aβ. LRP1 is highly expressed in neurons, glia, and vascular cells in the brain; notably, its expression within brain capillaries is reduced during normal aging and in AD brains (Kanekiyo and Bu, 2014). It is thought that LRP1 directly binds to Aβ in the ISF and allows Aβ to be transcytosed across the BBB into the bloodstream (Deane et al., 2004; Bell et al., 2007). Inhibiting LRP1 function with either antagonists or inhibiting antibodies significantly impairs Aβ clearance and deletion of *LRP1* in vascular smooth muscle cells exacerbated Aβ deposition (Kanekiyo et al., 2012). LRP1 preferentially binds $A\beta_{40}$ over the more aggregation-prone $A\beta_{42}$ as well as a more amyloidogenic mutant Aβ, suggesting that fibrillogenic Aβ may be more difficult to remove from the ISF (Tanzi et al., 2004). The ATP-binding cassette transporter p-glycoprotein (Pgp, also known as ABCB1) has also been implicated in Aβ efflux. Acute inhibition of Pgp in an Alzheimer's mouse model resulted in a 30% increase in ISF Aβ levels. Furthermore, Pgp-null mice show decreased Aβ transport across the BBB and, like LRP-1, $A\beta_{40}$ is preferentially targeted. Pgp deletion leads to increased Aβ deposition in a mouse model (Cirrito et al., 2005a).

Opposing the actions of LRP1 and Pgp, RAGE actively transports soluble Aβ from the bloodstream back into interstitium. Transgenic APP models and AD brains exhibit upregulated RAGE, implicating it as a physiologically relevant player in AD pathology (Deane et al., 2004).

ISF Bulk Flow

Aβ residing in the ISF can be cleared from the brain alongside other ISF solutes. The ISF is the fluid found in the miniscule gaps between cells in the brain, occupying the extracellular space that contacts the basement membranes of the capillaries making up the BBB. The ISF

makes up approximately 15-20% of volume of an adult brain (Lei et al., 2016). Following tracers injected into the brain, researchers have identified a bulk flow of ISF along the basement membranes of capillaries and arteries that relies on diffusion. This pathway, the perivascular drainage pathway, eventually moves ISF towards the cervical lymph nodes. Drainage along this pathway is estimated to occur at a rate of 0.11-0.29μL/minute/g of brain tissue. This movement is driven by pulsations of intracranial arteries (Weller et al., 2007). Motive force may decrease with age as arteriosclerosis results in stiffening vessels, reducing ISF clearance, which could exacerbate Aβ deposition (Bakker et al., 2016).

Another pathway for Aβ clearance was recently defined by Maiken Nedergaard's group, termed the glymphatic pathway (Iliff et al., 2012). This pathway is characterized by the influx of CSF along arteries into the ISF, which then drains along large caliber paravenous spaces (e.g. internal cerebral and caudal rhinal veins). The glymphatic pathway is heavily dependent on the expression of aquaporin4 (AQP4), a water-selective channel on astrocytic end-feet responsible for regulating water homeostasis. These channels facilitate fluid movement in the interstitium, creating a current that drives ISF clearance. By imaging the movements of fluorescent-tagged Aβ injected into the brain parenchyma, researchers found that *Aqp4* deletion reduced Aβ clearance by over 50% (Iliff et al., 2012). Another important factor affecting the rate of clearance is sleep. During sleep, the volume of the interstitial space increases, resulting in increased convective flow and enhanced Aβ clearance (Xie et al., 2013). This volume change is proposed to occur due to changes in astrocyte cell volume.

Proteolytic Aβ Degradation

Aβ in the ISF is the target of peptidases that reside both in the ISF and on cell membranes. One of the most studied of these is the neutral metalloendopeptidase, neprilysin (NEP). NEP is a type II membrane protein whose catalytically active domain is exposed to the extracellular space. Catabolism of Aβ as measured by injected radiolabeled Aβ into the hippocampus is greatly minimized following treatment with thiorphan, a NEP inhibitor (Iwata et al., 2001). Additionally, disruption of NEP expression results in increased levels of soluble Aβ as well as increased Aβ deposition. In line with these findings, AD brains exhibit lower levels of NEP, particularly in regions vulnerable to AD pathology (Baranello et al., 2015).

Another enzyme associated with Aβ degradation is the insulin-degrading enzyme (IDE). Though IDE is primarily a cytosolic protease, it can reside in the plasma membrane and in the extracellular space. IDE knock-out in Alzheimer's mouse models display a significant increase in Aβ levels as compared to wild-type littermates, where IDE overexpression results in a 50% reduction in both soluble and insoluble Aβ levels (Tanzi et al., 2004). Like NEP, IDE expression is increased with age (Baranello et al., 2015).

Beyond NEP and IDE, other enzymes linked to Aβ catabolism include endothelin-converting enzyme (ECE), angiotensin converting enzyme (ACE), and the matrix metalloproteinases (MMPs). ECE-1 preferentially cleaves $A\beta_{40}$ over $A\beta_{42}$, raising the 40:42 ratio of Aβ production, though not influencing levels of externally introduced Aβ. *In vitro* studies demonstrated that ACE has the ability to degrade Aβ, but its inhibition or genetic disruption do not regulate Aβ levels *in vivo*. MMP-2 and MMP-9 have both been found to directly cleave Aβ. MMP-9, in fact, can degrade both soluble and fibrillar Aβ and is found in astrocytes surrounding

amyloid plaques in AD mouse models, potentially acting to reduce plaque load (Yan et al., 2006). Furthermore, MMP expression in AD patients is increased and is stimulated by Aβ (Tanzi et al., 2004).

Cellular Uptake and Degradation

The final pathway for Aβ clearance is its uptake by surrounding neurons and glia and intracellular degradation. Neurons can take up Aβ from the extracellular space using a number of potential receptors, including LRP1. As discussed earlier, LRP1 is expressed on the epithelial cells of the BBB and aids in Aβ transcytosis from the ISF to the blood (Storck et al., 2015). In addition to this, LRP1 is expressed in the postsynaptic region of cell body of neurons where it can bind and internalize soluble Aβ (Kanekiyo et al., 2011). Neuron-specific deletion of LRP1 results in slowed ISF Aβ clearance and increased Aβ deposition. Once Aβ is internalized through endocytosis, the majority is trafficked through early and late endosomes to the lysosomal pathway where it is degraded through enzymes such as cathepsin B and cathepsin D (Li et al., 2012). If lysosomal activity is impaired, such is observed in the early stages of AD, Aβ that would otherwise be degraded can aggregate in the acidic microenvironment of lysosomes, possibly seeding additional Aβ aggregates (Li et al., 2012).

Similar to neurons, astrocytes can also endocytose and degrade Aβ (Wyss-Coray et al., 2003). Extracellular Aβ can be taken up by astrocytes through receptor-mediated endocytosis using such receptors as formyl peptide receptors (FPRs), leucine-rich glioma inactivated protein 3 (LGI3), and LRP1 (Ries and Sastre, 2016). Enhancing astrocytic lysosomal machinery, including enhanced cathepsin B and cathepsin D activity, accelerates Aβ clearance, lowers soluble Aβ levels in the ISF, and ameliorates amyloid plaque load (Xiao et al., 2014). LRP-1 is

expressed in astrocytes as well as in neurons. Conditional astrocytic knockdown of LRP-1 impaired Aβ clearance and accelerated Aβ pathology without altering production (Liu et al., 2017). Astrocytic activation, characterized by cellular hypertrophy and an enhanced expression of glial fibrillary acidic protein (GFAP), is a key pathological feature in AD brains, observable early in disease progress (Verkhratsky et al., 2010). Within the degenerating brain, activated astrocytes can be found surrounding plaques, suggesting a relationship between these two pathologies. Whether or not activation of astrocytes is protective or harmful in the context of AD is still under debate (De Strooper and Karran, 2016). Upon activation, many of the normal functions astrocytes provide become impaired. It is possible that the ability of astrocytes to clear Aβ may be diminished as well. In support of this concept, a study by Kamphuis et al. (2015) found that prohibiting astrocyte activation lead to increased expression of genes involved in lysosomal degradation and the inflammatory response induced in AD mouse models. No change in amyloid pathology was observed. However, these findings directly conflict with another study showing that blocking astrocyte activation lead to increased plaque load that they propose may be due to decreased clearance since Aβ production was unchanged (Kraft et al., 2013). It seems likely that astrocytes play various roles in modifying AD pathology, and that their overall function in regard to AD changes throughout disease progression.

Microglia are the final cell type to actively take up and degrade Aβ. Microglia act on soluble or fibrillar forms of Aβ through both fluid-phase pinocytosis and by phagocytosis, and activation of microglia with lipopolysaccharide (LPS) leads to a robust increase in Aβ clearance (Herber et al., 2007). As with astrocytes, there is continued debate over the role of microglia in AD as well as the broader role of inflammation (De Strooper and Karran, 2016). For example, the complement system, which initiates the inflammatory response, has both been found to

increase Aβ load in Alzheimer's mice or to have no effect on Aβ accumulation (Wyss-Coray, 2006). One pro-inflammatory cytokines, TNF-α, enhances Aβ deposition (Wang et al., 2015). However, a similar cytokine, IL-6, has an opposing effect. Overexpression of IL-6 results in extensive gliosis and microglial activation, boosting levels of Aβ phagocytosis and decreased plaque burden (Chakrabarty et al., 2010). In the past few years, the microglial transmembrane protein TREM2 has garnered a great deal of attention in the AD following the discovery that loss-of-function *TREM2* mutations increase the risk of LOAD by 3- to 5-fold. 5XFAD Alzheimer's mouse models with *TREM2* deletion show increased Aβ plaques in a gene dose-dependent manner as well as reduced microglial activation, arguing for a protective role of microglia (De Strooper and Karran, 2016). Though the role of microglia throughout AD progression is still debated, these immune cells clearly possess the ability to phagocytose and degrade Aβ.

In Vivo Brain Microdialysis

In the experiments detailed in the following pages, the predominant experimental technique used is *in vivo* microdialysis, specifically in the mouse hippocampus. Microdialysis is a very useful technique to monitor the concentration of neurotransmitter and other molecules under a certain size in the ISF of awake, freely moving animals. Microdialysis was originally developed in the 1960s and 70s to measure neurotransmitter levels in the brain (for review see Chefer et al., 2009). This technique relies on the microdialysis probe, which is composed of a tubular cannula with a semi-permeable tip of dialysis membrane. A solution lacking the analyte of interest (i.e. Aβ) is constantly perfused through the probe via pump. In my experiments, the

perfusion buffer is artificial CSF supplemented with bovine serum albumin (BSA) to block the binding of Aβ to the walls of the tubing and probe. A guide cannula for the probe is surgically implanted in the brain, and the probe is later carefully inserted into this cannula and into the brain. Once inserted, the dialysis membrane allows for the free diffusion of molecules of and under a specific molecular weight in and out of the perfusion buffer. In the experiments described here, Aβ monomers in the ISF are able to move down their concentration gradient from the ISF into the perfusion buffer, while compounds added to the perfusion buffer (e.g. AMPA) flow from the probe into the ISF simultaneously. The perfusate then moves past the dialysis membrane into the outflow tubing where it is collected and analyzed for Aβ concentration. The percentage of analyte that is collected in the perfusate, the relative recovery rate, is affected by a number of factors such as the surface area of the probe membrane, membrane material, diffusional characteristics of the analyte, flow rate of the perfusion buffer, hydrophobicity of the analyte, and analyte molecular weight (Shippenberg and Thompson, 2001). The molecular weight cut-off (MWCO) of the probe refers to the highest molecular weight an analyte can be at which 90% is retained by the membrane. A higher MWCO means that a probe can reliably collect larger analytes. For my thesis work, I used a microdialysis probe with a MWCO of 32kDa, meaning that the 4kDa Aβ peptide can easily diffuse across the membrane. Recovery is proportional to flow rate, such that a slower flow rate results in greater recovery. A faster flow rate, however, results in greater collected perfusate volume, which may be necessary for analyte analysis. The choice of flow rate, then, is a compromise between a greater rate of recovery and temporal resolution.

Recovery of ISF Aβ via microdialysis was pioneered by Cirrito et al. in 2003. The authors used *in vitro* experiments to characterize the recovery of Aβ by microdialysis in a

controlled environment. The percentage recovery coefficient of the probe was calculated using the interpolated zero flux method. In this method, a range of flow rates were used and the concentration of Aβ collected at each were collected. These data were plotted to construct a recovery curve from which the theoretical recovery from a zero flow rate can be extrapolated. The mean percentage recovery of recoverable, soluble Aβ in the solution was approximately 10%. Furthermore, the study showed that they were able to collect and measure $A\beta_{40}$ and $A\beta_{42}$, as well as both transgenic and murine Aβ (Cirrito et al., 2003).

Aβ measurement using microdialysis has a number of advantages over other sampling techniques. Primarily, microdialysis allows us to monitor changes in Aβ levels dynamically, ever hour, in response to treatment within the context of an intact brain. As discussed in this introduction, the regulation of Aβ levels in the ISF is incredibly complex and involves neurons, glia, and the circulatory system working together, something that cannot be properly recapitulated *in vitro*. The main technique used to quantify changes in Aβ levels in animal models is done in brain lysates. Besides the loss of temporal resolution, tissue lysis captures all pools of Aβ, and the ISF pool of Aβ most faithfully reflects local production and clearance (Cirrito et al., 2003). In addition to these advantages, microdialysis always us to use reverse microdialysis to directly perfuse drugs and other compounds through the probe and into the hippocampus, bypassing the troublesome blood brain barrier.

Microdialysis does come with its disadvantages, however. The temporal resolution is limited by recovery efficiency and the amount of sample needed for analyte analysis. To measure $A\beta_{40}$ levels in an Alzheimer's mouse model, this requires sampling every hour. However, to measure analytes of lower concentrations such as $A\beta_{42}$ or murine Aβ, even more temporal resolution must be given up in favor of a larger sample volume. Microdialysis is an invasive

technique and tissue damage is unavoidable. Furthermore, we have observed a significant level of gliosis surrounding the probe after a few days of sampling. The size of the microdialysis probe is such that the technique is limited to areas sufficiently capacious to surround the probe. The murine hippocampus is large enough to accommodate a probe, but any regional differences within the structure are undetectable. When using reverse microdialysis, the delivery efficiency of the drug or compound is difficult to measure, as is its rate of diffusion through the target tissue. Thus, the drug concentrations stated are always the starting concentrations and not the actual concentration delivered. Despite these drawbacks, microdialysis remains a useful tool to identify factors that regulate ISF Aβ levels in awake mice over a period of days.

Alzheimer's Disease Mouse Models

Murine Aβ exists in the rodent brain in picomolar range (human Aβ in AD brains is in the nanomolar range) and, due to only three substitutions, does not aggregate into amyloid formations (Price et al., 1995; Cirrito et al., 2003; Esquerda-Canals et al., 2017). The discovery of EO-FAD genes, therefore, was pivotal to developing an animal model for AD. The first transgenic mouse model that developed AD-type neuropathology overexpressed human mutant V717F APP and exhibited neuritic plaques, synaptic loss, astrocytosis, and microgliosis (Games et al., 1995). Since then, approximately 80 mouse models using EO-FAD genes have been generated utilizing various combinations of mutations in human APP, PSEN1, and PSEN2 (www.alzforum.org/research-models). Mice that overexpress human mutant APP, like the Games et al. model, develop diffuse and dense amyloid plaques within around 6-12 months of age, depending on the level of overexpression and the mutation used. The most commonly used

APP mutations include the K670N/M671L (Swedish), V717F (Indiana), E693G (Artic), E693K (Dutch), and V717I (London) mutations(Kitazawa et al., 2012). The most used of these is the Swedish double mutation, which increases overall APP expression by increasing β-secretase cleavage of APP (Haass et al., 1995). Presenilin transgenic mice do not develop plaque pathology, although the ratio of $A\beta_{42}/A\beta_{40}$ is increased. Therefore APP and PSEN mutations are often combined, leading to mice that form plaques at earlier ages than single APP transgenic mice.

We chose to use a double transgenic mouse in the following experiments, specifically the APPswe/PSEN1dE9 mouse model (also known as APP/PS1 or Borchelt mice). These mice were developed by co-injecting two vectors encoding a chimeric mouse/human APP harboring the Swedish mutation and a human PSEN1 with a ΔE9 mutation (Jankowsky et al., 2001). These mice begin developing Aβ deposits around the age of six months and exhibit hippocampal and cortical plaques by nine months (Jankowsky et al., 2004). Gliosis, LTP impairment, dysfunctions in learning and memory, and limited neuronal loss are also observed (Li et al., 2015). The mice used in these studies are hemizygous on the congenic C57Bl/6J background. Because we sought to investigate factors that influence AD pathogenesis that, by definition, occur prior to plaque development, the mice used in these experiments were two to four months of age. By using young mice, we were able to examine levels of soluble Aβ without having to account for the amyloid sink that occurs around plaques or for Aβ escaping plaques. These mice do not develop any tau pathology.

Of course, these mouse models are unable to completely recapitulate the full pathology and symptomology seen in true AD. For example, the appearance of plaques and exhibition of cognitive deficits seen in the models do not follow the same temporal pattern seen in human AD.

Importantly, these mice fail to exhibit neurodegeneration. Mice made utilizing EO-FAD mutations alone do not develop neurofibrillary tangles. In some mice, phosphorylated tau does occur, but no paired helical filaments of tau are observed. Mice with tau mutations have been made and crossed with EO-FAD mutations, resulting in mice that exhibit both plaques and tangles. While these models show both fundamental AD pathologies, they still represent a composite of two distinct diseases and do not follow the same temporal and spatial properties in the human disease (Oddo et al., 2003; Elder et al., 2010). Though mouse models of AD clearly fail to faithfully represent human AD, these models are still invaluable tools for understanding particular aspects of the disease and have helped us gain a greater understanding of AD pathogenesis and pathology.

Summary

Alzheimer's disease (AD) is a pressing issue, affecting one in ten people aged 65 and older. While most other major causes of death have decreased in prevalence, AD has experienced an 89% increase in deaths (www.alz.org/facts). Increasing research and failed clinical trials demonstrate that early prevention of AD, starting years before symptoms emerge, might be the most effective way to combat this devastating disease. Understanding how AD develops and the factors that contribute to its pathological origins will be vital to develop preventative therapeutics. Though Aβ does not drive many of the symptoms and pathology displayed in AD progression, its toxic aggregation clearly plays an important role in pathogenesis. The regulation of extracellular Aβ levels, which determine the probability of aggregation, is complex and involves both pre- and postsynaptic neuronal signaling. The work described in this document

explores the regulation of Aβ by NMDA and AMPA receptors, the glutamate receptors responsible for mediating synaptic plasticity. We aim to describe how these two prominent and abundant glutamate receptors affect AD pathogenesis so that we may identify new therapeutic strategies.

Chapter 2

NMDA Receptor Regulation of Amyloid-β Levels through Extracellular Signal-Regulated Kinase

ABSTRACT

The extracellular concentration of soluble, monomeric Aβ is a critical factor for the initiation and rate of aggregation into toxic species, such as oligomers, fibrils, and plaques. Factors that influence Aβ production, therefore, have the potential to modulate disease progression. Research from our lab has shown that high levels of NMDA-R activation result in a significant decrease in Aβ levels dependent on the activation of the MAP kinase/extracellular signal-regulated kinase (ERK) signaling cascade by calcium influx through the NMDA-R. Evidence suggests that activated ERK decreases Aβ production by altering APP processing. Certain other receptors that activate ERK do not show this decrease in Aβ production, suggesting that NMDA-Rs act on ERK and Aβ through a selective pathway. Defining this pathway may undercover molecules that can selectively decrease Aβ in a way that global NMDA-R or ERK activation cannot. By selectively antagonizing the NMDA-R subunits GluN2A and GluN2B during NMDA treatment, I found that neither subunit is responsible for the effect of NMDA-Rs on Aβ levels. Using virally driven RNA interference to knockdown expression of the two ERK isoforms, ERK1 and ERK2, I determined that ERK signaling to regulate APP processing is not isoform-specific. Furthermore, I found that NMDA-Rs do not act on ERK and Aβ production through calcium/calmodulin-dependent protein kinase II (CaMKII), protein kinase A (PKA), or protein kinase C (PKC) signaling.

INTRODUCTION

The *N*-methyl-D-aspartate (NMDA) receptor is an ionotropic glutamate receptor activated by the concurrent binding of glutamate and postsynaptic depolarization, with either

glycine or D-serine acting as coagonist. NMDA-Rs are nonselective cation channels, allowing the flow of sodium (Na^+) and calcium (Ca^{2+}) into the cell and potassium (K^+) out. These heterotetrameric receptors are composed of two GluN1 subunits and two GluN2A-D subunits. Which GluN2 subunits make up the receptor help determine its electrophysiological and pharmacological properties (Hunt and Castillo, 2012).

NMDA-R's permeability to Ca^{2+} and its coincidence-dependent activation make these receptors critical to synaptic plasticity and memory formation. Calcium is highly buffered within the cytoplasm so that even very small changes in Ca^{2+} concentration can have dramatic effects. Depending on the level of Ca^{2+} influx induced by NMDA-R activation, Ca^{2+} signaling can lead to either synaptic plasticity and cell survival pathways or excitotoxicity and cell death pathways. These opposing roles of NMDA-Rs are thought to be mediated by the cellular localization of the channels; synaptic NMDA-Rs are associated with neurotrophic effects while extrasynaptic NMDA-Rs seem to activate pro-death pathways (Hardingham et al., 2002; Hardingham and Bading, 2010). The concept that only extrasynaptic receptors are responsible for NMDA-R-mediated excitotoxicity is not without contention. Wroge et al., for example, found that synaptic NMDA-Rs are toxic in response to certain endogenous and exogenous insults, indicating that NMDA-R functions are more complex than proposed by the extrasynaptic NMDA-R hypothesis (Wroge et al., 2012).

Another possible explanation for the dichotomous roles of NMDA-Rs might lie in their subunit composition. Synaptic sites seem to be primarily composed of GluN2A-containing NMDA-Rs, which preferentially bind with postsynaptic density protein-95 (PSD-95). On the other hand, extrasynaptic sites are enriched with GluN2B-NMDA-Rs, which interact with synapse-associated protein-102 (SAP-102) (Papouin et al., 2012; Papouin and Oliet, 2017). This

distinction is not perfect, however, and GluN2A and GluN2B can be found at both cellular locations (Wang et al., 2016). The subunit composition of NMDA-Rs does appear to affect their signaling pathways. Importantly, presence of either GluN2A or GluN2B determines the direction by which the NMDA-R regulates ERK activity, though there are conflicting studies on this issue. Multiple groups have found that GluN2A-containing receptors signal to activate ERK while GluN2B-containing receptors inhibit ERK (Hardingham, 2006; Ivanov et al., 2006a; Li et al., 2006; Wang et al., 2015). Other studies, however, link GluN2B-containing receptors to ERK activation (Krapivinsky et al., 2003).

Given that NMDA-Rs are implicated in both memory formation and cell death, it is not surprising that these receptors have been linked with AD pathophysiology. Numerous studies have shown that certain forms of Aβ have toxic effects on synapses (for review see Malinow, 2012; Zhang et al., 2016). Overproduction of Aβ results in depressed glutamatergic signaling in hippocampal CA1 pyramidal neurons both through reduced receptor transmission as measured by electrophysiology and decreased dendritic spine density (Kamenetz et al., 2003; Shrestha et al., 2006). Amyloid-β appears to enhance long-term depression (LTD)-like synaptic weakening, acting through common signaling molecules such as calcineurin and caspase-3, while simultaneously diminishing long-term potentiation (LTP; Kamenetz et al., 2003; Malinow, 2012). Interestingly, Aβ-mediated impairments in LTP can be blocked using NMDA-R antagonists, directly linking Aβ toxicity to NMDA-Rs. Brains from AD animal models express lower levels of glutamate transporters, which would result in decreased glutamate uptake and more glutamate in the synapse (Zhang et al., 2016). In support of this concept, Aβ decreases glutamate uptake by cultured astrocytes (Matos et al., 2008). Lastly, memantine, a low-affinity

NMDA-R antagonist, has been approved by the FDA for treatment of AD patients and appears to mitigate some aspects of cognitive loss in certain patients.

Knowing that NMDA-Rs are implicated in later stage AD pathology, our lab and others asked if they might also be involved in AD pathogenesis, specifically in Aβ production. As discussed in the introduction to this document, conflicting studies conducted *in vitro* reported that NMDA-R activation either increased Aβ production through increased BACE activity (Lesné et al., 2005) or decreased Aβ levels by boosting α-secretase activity (Hoey et al., 2009). Using microdialysis in an AD mouse model, our lab found that NMDA-Rs actually have opposing effects on Aβ levels depending on the level of receptor activation and the amount of Ca^{2+} conducted through the channel (Verges et al., 2011). Lower levels of NMDA increased Aβ levels by increasing synaptic activity-dependent APP processing. This effect was blocked by inhibiting action potentials with tetrodotoxin (TTX). Conversely, high NMDA levels reduced the amount of Aβ produced, despite the presence of TTX. This effect was shown to require activation of extracellular signal-regulated kinase (ERK), which signals through an undefined pathway to increase α-secretase APP processing (Verges et al., 2011). Defining the steps from NMDA-R activation and ERK signaling is one of the questions addressed in this chapter.

The ERKs (ERK1, ERK2, ERK3/4, ERK5, and ERK7) are part of a family of mitogen-activated protein kinases (MAPKs) that are activated by a variety of signals and mediate myriad cellular processes. ERK1/2 are the most common isoforms expressed in the CNS and express 84% sequence homology. ERK2 is expressed relatively more than ERK1, though the expression ratio is region-specific. In the hippocampus, the ratio of ERK1 to ERK2 levels is 0.33 (Ottiz et al., 1995). Both isoforms are expressed throughout the brain and both are primarily neuronal (Samuels et al., 2009). Traditionally thought to have identical roles, the recent ability to

genetically inhibit individual ERK isoforms has revealed distinct functions for ERK1 and ERK2 (Yu, 2012). For example, ERK1 has been implicated in protection against NMDA-induced neuronal distress (Nakazawa et al., 2008) while ERK2 is involved in AMPA-R-mediated cell death (Yu et al., 2010).

Once ERK is phosphorylated and activated by MAP kinase kinase (MEK), it phosphorylates its many cellular targets or translocates into the nucleus to regulate gene expression (Samuels et al., 2009). There are over 160 substrates for ERK already identified that regulate a huge variety of cellular tasks, sometimes even mediating opposing processes (Yoon and Seger, 2006). In order to maintain signaling specificity, the timing of ERK activation as well as its subcellular localization must be highly regulated (Pouysségur et al., 2002).

ERK signaling has been strongly implicated in synaptic plasticity related to learning and memory, particularly the induction of LTP (English and Sweatt, 1996). As part of these studies, a number of signaling molecules that activate ERK in the context of LTP have been identified. Bading and Greenberg (1991) established that NMDA-R signaling leads to ERK activation, and subsequent studies have found that this pathway involves multiple possible signaling molecules (Bading and Greenberg, 1991). Which of these possible signaling pathways are responsible for linking NMDA-Rs to Aβ production remains unknown. By reviewing the literature, we have identified the four most likely candidates that link NMDA-R activation to ERK in our system: 1) calcium/calmodulin-dependent protein kinase II (CaMKII; (Chen et al., 1998; Zhu et al., 2002a) 2) protein kinase C (PKC; Kurino et al., 2002; Gangarossa and Valjent, 2012) 3) protein kinase A (PKA; English and Sweatt, 1996) and 4) Ras-specific guanine nucleotide-releasing factor (RasGRF), a guanine-nucleotide exchange factor for Ras (Krapivinsky et al., 2003; Feig, 2011). Calcium influx through NMDA-Rs causes activation of CaMKII, PKC, and PKA-dependent

signaling pathways that can activate the ERK signaling cascade. In contrast, RasGRF is normally bound to NMDA-Rs; upon calcium influx it dissociates from the receptor and directly activates ERK signaling.

In this study, we sought to determine the pathway through which NMDA-Rs act to decrease Aβ production by investigating the signaling molecules linking NMDA-Rs to ERK activation, by identifying the subunit composition of NMDA-Rs that initiate this response, and by distinguishing the differential roles of ERK1 and ERK2 isoforms in NMDA-R-dependent Aβ production. The ultimate goal of these experiments was to identify specific molecular players key to decreasing Aβ production caused by glutamatergic signaling.

MATERIALS AND METHODS

Animals

The mice used for these studies were hemizygous *APPswe/PS1ΔE9* (APP/PS1; Jankowsky et al., 2001, 2004) and bred on a wild-type C3H/B6 background or littermate controls (WT). Original transgenic breeders were purchased from Jackson Laboratory (Bar Harbor, Maine), and colonies were maintained at Washington University. Equal numbers of male and female mice were used in each study at 2-4 months of age. All studies were performed in accordance with the guidelines of AAALAC and the Institutional Animal Care and Use Committee (IACUC) at Washington University.

Aβ Microdialysis

In vivo microdialysis was performed in awake and behaving APP/PS1 mice as previously described (Cirrito et al., 2003, 2011). Briefly, guide cannulas (BR-style, Bioanalytical Systems, West Lafayette, IN) were stereotaxically implanted above the left hippocampus, coordinates bregma -3.1mm, 2.5mm lateral to midline, and 1.2mm below dura at a 12° angle. The cannulas were securely affixed to the head with dental cement, and microdialysis probes (BR-2, 2mm, 38kDa MWCO, Bioanalytical Systems) were inserted into the hippocampus through the guide cannula. In APP/PS1 mice, probes were perfused with artificial cerebrospinal fluid (aCSF; 1.3mM $CaCl_2$, 1.2mM $MgSO_4$, 3mM KCl, 04mM KH_2PO_4, 25mM $NaHCO_3$, and 122mM NaCl, pH 7.35) with 0.15% bovine serum albumin (BSA; Sigma-Aldrich, St. Louis, MO) at a rate of 1.0μL/min with samples of hippocampal ISF collected every 90 minutes during basal collection or every hour during treatment. Basal sampling began at least 16 hours following surgery. These experiments took place under constant light conditions to diminish circadian-related fluctuation in Aβ levels. At the conclusion of the experiment, all ISF samples were analyzed for $A\beta_{x\text{-}40}$ levels by sandwich ELISA.

Compounds

Reverse microdialysis was used to administer compounds directly into the hippocampus. Drugs were diluted into the perfusion buffer of artificial CSF and 0.15% BSA, allowing the drugs to diffuse into the brain continuously for the duration of the experiment at the same time that Aβ is collected. Due to the complexity of determining the final concentration of compound delivered to the brain, only the starting concentrations of drugs in the perfusion buffer are given. We estimate approximately 10% of the drug is delivered across the probe membrane where it is further

diluted in the brain CSF. NMDA (40μM), MK801 (100μM), and ifenprodil (50μM) were purchased from Sigma. KT5720 (800nM), KN-93 (50μM), Go6983 (1μM), Ro25-6981 (5μM), and TCN201 (100μM) were purchased from Tocris Bioscience (Ellisville, MO).

Aβ Sandwich ELISAs

ISF samples were analyzed for $A\beta_{x\text{-}40}$ or $A\beta_{x\text{-}42}$ concentration using methods previously described (Fisher et al., 2016). A mouse monoclonal anti-$A\beta_{40}$ capture antibody (mHJ2) or anti-$A\beta_{42}$ capture antibody (mHJ7.4) made in-house was used in conjunction with a biotinylated central domain detection antibody (mHJ5.1) and streptavidin-poly-HRP-40 (Fitzgerald Industries, Acton, MA). Super Slow ELISA TMB (Sigma) was then used to develop, and absorbance was read by a BioTek Epoch plate reader at 650 nm. The same assay can be used for both human and murine $A\beta_{x\text{-}40}$. Standard curves for ELISAs were generated using synthetic human $A\beta_{40}$ or $A\beta_{42}$ (American Peptide, Sunnyvale, CA). Basal levels of ISF Aβ levels were calculated by averaging the Aβ concentrations taken every 90 minutes for 9 hours prior to drug treatment. All Aβ levels for each mouse were then normalized by calculating percent of basal for each point. Mean ± SEM per group are shown.

AAV Vector Production

The packaging cell line, HEK293, was maintained in Dulbecco's modified Eagles medium (DMEM), supplemented with 5% fetal bovine serum (FBS), 100 units/ml penicillin, 100mg/ml streptomycin in 37°C incubator with 5% CO_2. The cells were plated at 30-40% confluence in CellSTACS (Corning, Tewksbury, MA) 24 h before transfection (70-80% confluence when transfection). 730mg pAAV2/8, 1180 mg pHelper, and 590mg rAAV transfer plasmid

containing the gene of interest were co-transfected into HEK293 cells using the calcium phosphate precipitation procedure (Zolotukhin et al., 2002). The cells were incubated at 37°C for 3 days before harvesting. The cells were lysed by three freeze/thaw cycles. The cell lysate was treated with 25 U/ml of Benzonaze at 37ºC for 30 min followed by iodixanol gradient centrifugation. The iodixanol gradient fraction was further purified by column chromatography. HiTrap Q column (GE Healthcare) was used for AAV8. The eluate was concentrated with Vivaspin 20 100K concentrator (Sartorius Stedim, Bohemia, NY). Vector titer was determined by Dot blot assay.

Viral Injections and tissue lysis

APP/PS1 mice aged 2-4 months old were stereotaxically injected unilaterally into anterior and posterior sites of hippocampus with shERK1, shERK2, or shScrambled. Injection coordinates for the anterior site were -1.65mm anterior/posterior, -1.2mm medial/lateral, and -1.75mm dorsal/ventral. Injection coordinates for the posterior site were -2.9mm anterior/posterior, -2.7mm medial/lateral, and -2.2mm dorsal/ventral. Virus was injected at a rate of 0.5µL/min with 2µL/injection site. After two weeks to allow for viral integration and gene knockdown, mice were sacrificed and perfused with 4% paraformaldehyde, followed by brain dissection and snap-freezing of the hippocampus on dry ice. Tissue was homogenized by sonication at a 10:1 volume:wet weight in 150mM NaCl, 50mM Tris, pH 7.4, 0.5% deoxycholic acid, 0.1% SDS, 1% Triton X-100, 2.5mM EDTA, and protease inhibitors.

Western blotting

SDS PAGE and Western blotting was used to determine the amount of ERK1 and ERK2 knockdown in the hippocampus. Gel electrophoresis of 20μg protein samples was performed under reducing conditions using 4-12% Bis-Tris NuPAGE gels (ThermoFisher Scientific, Waltham, MA) and then transferred to nitrocellulose membrane. Blots were probed for p44/p42 MAPK (aka ERK; 1:1000; Cell Signaling Technology, Danvers, MA) and tubulin (1:2500; Sigma). HRP-conjugated donkey anti-rabbit IgG (1:250; Cell Signaling Technology, Danvers, MA) and HRP-conjugated Amersham ECL sheep anti-mouse IgG (1:500; GE Healthcare, Chicago, IL) were used as secondary antibodies. Membranes were developed using SuperSignal West Pico Substrate (ThermoFisher) and imaged using the Kodak ImageStation 440CF (Rochester, NY). Band intensity was quantified using the Kodak 1D Image Analysis software, and normalized using tubulin signals as loading controls. Values shown are these normalized band intensities relative to the experimental control group. Mean ± SEM per group are shown.

Statistical Analysis

Data in figures are presented as mean ± SEM. Prism 6.0b for Mac OS X (GraphPad, San Diego, CA) was used for all statistical analyses. Two-tailed unpaired *t*-tests were used to compare between two groups. One-way or two-way ANOVA was used when comparing one or two independent variables, respectively, between multiple groups. Analysis of microdialysis experiments was performed by averaging the final three data points of a specific treatment period and using one-way or two-way ANOVA with Dunnett's correction for multiple comparisons. Values were accepted as significant is $p \leq 0.05$.

RESULTS

Receptor subunit composition is not a factor in NMDA-R Aβ regulation

Despite highly similar amino acid sequences, the GluN2A and GluN2B NMDA-R subunits often exhibit distinct binding partners, pharmacological properties, and cellular roles (Zhang and Luo, 2013). A number of highly selective subunit-specific antagonists have been developed to differentiate the effects of GluN2A versus GluN2B due to the hypothesis that subunit composition determines receptor signaling for either neuronal survival or death (Hardingham, 2006). Which subunit is responsible for ERK activation is a well-studied question, but a consensus is yet to be reached (Krapivinsky et al., 2003; Ivanov et al., 2006b; Li et al., 2006). In order to determine if NMDA-Rs activate ERK and decrease Aβ production through subunit-specific signaling, we administered subunit-specific antagonists to an Alzheimer's mouse model using hippocampal microdialysis (Fig. 2.1 A,B). In order to assess soluble ISF Aβ levels before plaque formation, we used young, 2 to 4 month-old APPswe//*PS1Δe9* hemizygous (APP/PS1) mice (Jankowsky et al., 2001, 2004).

Subunit-specific antagonists were administered directly into the hippocampus using reverse microdialysis for 6 hours following collection of basal ISF samples. NMDA (40μM starting concentration) was then added for an additional 18 hours. Two different, highly selective GluN2B antagonists were used: Ro25-6981 (>1000-fold specificity over GluN2A) and ifenprodil (>400-fold specificity over GluN2A). Neither antagonist prevented the decrease in Aβ levels seen with NMDA treatment (Fig. 2.1 A,B). Development of a GluN2A-specific antagonist has not yielded as much success as with GluN2B antagonists. Recent studies, however, have identified a potent GluN2A antagonist, TCN201, which noncompetitively blocks GluN2A-

containing receptors in a manner dependent on the GluN1-agonist concentration (Edman et al., 2012). As seen with the GluN2B antagonists, blocking GluN2A signaling did not influence the effect of NMDA treatment on ISF Aβ levels. Importantly, NMDA failed to decrease Aβ levels when all NMDA-Rs were blocked with MK801, a noncompetitive NMDA-R antagonist. Together, these results argue that neither GluN2A-containing nor GluN2B-containing receptors alone are responsible for NMDA-Rs' effect on Aβ. Instead, it is likely that both populations of receptors redundantly signal to regulate Aβ production. It is important to note, however, that these subunit-specific antagonists do not completely inhibit NMDA-R currents. Additionally, the selectivity of TCN201 for GluN2A subunits depends on the GluN1 agonist concentration.

ERK1 or ERK2 is sufficient for NMDA-R-mediated Aβ regulation

The two prominent isoforms of ERK, ERK1 and ERK2, display both overlapping and distinct roles in cellular signaling. Until the development of targeted genetic inactivation of either gene, these ERK isoforms have been considered functionally identical due to their close homology. Isoform-specific ERK knockout and knockdown studies, however, demonstrated that ERK1 and ERK2 have distinct characteristics. Pharmacological tools frequently used to manipulate ERK activity, such as the inhibitors U0126 and FR180204, act equally on all ERKs and therefore fail to distinguish specific ERK isoform roles.

In order to determine if NMDA-R-ERK signaling acts on Aβ in an isoform-specific manner, we stereotaxically injected purified short-hairpin RNA (shRNA) against ERK1 or ERK2 packaged into adeno-associated virus serotype 8 (AAV8) and driven by a U6 promoter to knockdown expression of ERK1 or ERK2 in the hippocampus of young APP/PS1. Western blot

analysis showed that AAV-transduction of shRNA against ERK1 (shERK1) resulted in a decrease by about 45% compared to controls injected with scrambled shRNA (shScrambled), while ERK2 expression decreased by approximately 42% (shERK2; Fig. 2.2A). Microdialysis probes were then implanted into the hippocampus of these shERK1 and shERK2 mice and 40μM NMDA was infused into the brain via reverse microdialysis. If NMDA-Rs acted on Aβ through a specific ERK isoform, we would expect that decreased expression of this isoform would attenuate the decrease in Aβ seen following NMDA treatment. However, NMDA treatment led to indistinguishable decreases in ISF Aβ levels in all groups, regardless of ERK1 or ERK2 knockdown (Fig. 2.2B). These results indicate that NMDA-Rs do not signal to regulate Aβ through a specific ERK isoform and that either ERK1 or ERK2 is sufficient to see effects on Aβ following NMDA treatment. Our RNAi approach, however, only decreased expression of each ERK isoform and did not abolish EKR1 or ERK2 activity entirely. It is possible that the remaining ERK expression allowed sufficient signaling to mediate NMDA-R signaling, obscuring our results.

NMDA-R-ERK signaling to Aβ does not require PKA, CaMKII, or PKC

ERK phosphorylates an array of cellular targets and regulates a large variety of signaling cascades and cellular roles. Despite its multifarious functions, ERK mediates very distinct, selective pathways. Precise and exquisite regulation of ERK activation is achieved through controlled intensity, duration, and subcellular localization of signaling (Pouysségur et al., 2002). This means that the decrease in Aβ levels observed in our experiments is likely mediated by a very specific pathway from NMDA-Rs to ERK phosphorylation. By identifying the signaling

molecules necessary to connect NMDA-Rs to ERK to Aβ, we can define select targets that could be used to modify Aβ levels.

NMDA-Rs have been observed to signal to ERK through a variety of pathways. Studies of glutamatergic regulation of synaptic plasticity were the first to link calcium influx through NMDA-Rs to ERK activation (Bading and Greenberg, 1991; Xia et al., 1996). Chandler et al. (2000) found that, depending on the level of receptor stimulation, NMDA-Rs exerted bidirectional control of ERK activation. The stimulatory pathway was dependent on the activation of calcium/calmodulin-dependent kinase II (CaMKII; Chandler et al., 2000). Further studies supported these results. For example, NMDA-R signaling was shown to control AMPA-R trafficking during synaptic plasticity through CaMKII-dependent activation of ERK (Zhu et al., 2002a). CaMKII connected to NMDA-Rs through binding to the postsynaptic density 95 (PSD95) complex where it decreased the activity of p135 synaptic Ras-GTPase activating protein (SynGAP; Chen et al., 1998). Later, synaptic NMDA-Rs specifically were found to activate ERK through CaMKII (Hardingham, 2006). Additionally, NMDA-Rs were found to activate ERK through protein kinase A (PKA) activation during LTP in hippocampal slices (Banko et al., 2004). Protein kinase C (PKC) has also been linked to NMDA-R-dependent ERK activation (Park et al., 2010).

We utilized pharmacological small-molecule inhibitors of these signaling molecules to determine if their activity was necessary for NMDA-Rs to signal through ERK to lower Aβ levels. CaMKII was inhibited with KN-93 (50μM) before and during treatment with 40μM NMDA via reverse microdialysis in young APP/PS1 mice. Alone, CaMKII inhibition increased ISF Aβ levels up to 200% over basal levels (Fig. 2.3A,B). At 6 hours of treatment, Aβ levels appeared to reach a plateau, although it is possible that levels would have increased further with

longer KN-93 treatment. These results indicate that basal levels of CaMKII activation normally act to decrease Aβ levels. However, NMDA treatment still decreased Aβ even with CaMKII inhibition, meaning that CaMKII is not required for the pathway of interest. ISF Aβ levels were unchanged following inhibition of either PKA (KT5720; 500nM) or PKC (Gö6983; 1μM). As with CaMKII, neither PKA nor PKC inhibition prevented NMDA treatment from lowering Aβ levels (Fig. 2.3A,B).

These results argue that NMDA-Rs do not activate ERK and regulate Aβ production through CaMKII, PKC, or PKA. There are caveats to these experiments, however. While the use of reverse microdialysis allows us to bypass the BBB, it also prevents us from knowing the specific concentration of drug that is administered to the hippocampus. We referenced previous *in vitro* studies and the published IC_{50} values for the inhibitors used, but we cannot be sure that the target was fully inhibited. Treatment with KN-93 increased Aβ levels without NMDA, suggesting that CaMKII was indeed inhibited. Inhibition of PKA and PKC, however, did not affect Aβ. This could mean that PKA or PKC signaling is not involved in Aβ regulation, or it could be clue that the targets were not engaged by their respective inhibitors. These results would be bolstered by secondary measures of kinase inhibition.

DISCUSSION

Studies carried out in our lab and in others have implicated NMDA-Rs, the receptors essential for mediating synaptic plasticity, in the regulation of Aβ production; specifically, high levels of NMDA-R activation initiate an ERK-mediated signaling cascade that increases non-amyloidogenic processing of APP (Lesné et al., 2005; Hoey et al., 2009; Verges et al., 2011). In an

effort to dissect this pathway, we primarily used microdialysis in APP/PS1 mice to demonstrate that decreases in Aβ following NMDA treatment is not due to a specific NMDA-R subunit (Fig. 2.1) nor is it the result of discrete signaling through either ERK1 or ERK2 (Fig. 2.2). Additionally, we have shown that NMDA-Rs do not activate ERK through CaMKII, PKA, or PKC activation to affect APP processing (Fig. 2.3).

NMDA-Rs mediate opposing roles in the context of cellular fate. While NMDA-Rs are responsible for synaptic plasticity, activate pro-survival genes, and protect against oxidative stress, they are also known to activate pro-death signaling and facilitate excitotoxicity (Hardingham and Bading, 2010). The mechanistic switch that determines the ultimate direction of NMDA-R signaling is still under investigation. The degree of NMDA-R activation and the amount of calcium allowed to enter the cell has been proposed as an explanation for these differential effects (Lipton and Kater, 1989; Chandler et al., 2000; Poo et al., 2000) as have the cellular localization of NMDA-Rs (Sattler et al., 2000; Ivanov et al., 2006b; Papadia et al., 2008; Hardingham and Bading, 2010) and the NMDA-R subunit composition (Krapivinsky et al., 2003; Li et al., 2006; Liu et al., 2007). Because NMDA-R activation can be either protective or toxic through a mechanism that is as yet undetermined, the use of a NMDA-R agonist to decrease Aβ production is clearly not a feasible option as an AD therapeutic. Instead, a safer, more selective target must be identified. To this aim, we sought to address the population of NMDA-Rs responsible for the desired effects on Aβ.

While there is evidence that synaptic NMDA-Rs mediate protective NMDA-R signaling, selectively targeting synaptic versus extrasynaptic NMDA-Rs is not possible in the complex environment of a living brain. To achieve greater experimental control over receptor populations, we turned to an *in vitro* system. In an *in vitro* setting, use-dependent antagonists allow for the selective activation of synaptic or extrasynaptic receptors. However, we were unable to perform these

experiments after failing to reliably reproduce the effects we observed *in vivo* following NMDA treatment in a tissue culture model. Indeed, NMDA treatment did not have consistent effects on extracellular Aβ levels in the multiple cellular systems we tested: neuro2A cells, a mouse neuroblastoma cell line expressing APP, SH-SY5Y cells, a human neuroblastoma cell line, and primary hippocampal neurons from wild-type mice (data not shown). Indeed, the type of medium used as well as the presence of the supplement B27 appeared to have large effects on Aβ levels following treatment with NMDA, NMDA-R antagonists, or ERK inhibitors. Thus, we were unable to specifically target extrasynaptic versus synaptic NMDA-Rs in the context of Aβ production.

The type of GluN2, the main regulatory subunit, present in a NMDA-R shapes the receptor's temporal and spatial properties. GluN2A subunits are associated with protective signaling pathways such as CREB and ERK phosphorylation, while GluN2B-containing receptors are thought to oppose these survival signals and mediate excitotoxicity (Krapivinsky et al., 2003; Zhang and Luo, 2013). Furthermore, GluN2A-containing receptors are enriched in synaptic sites and GluN2B-containig receptors in extrasynaptic locations, though this distinction is not perfect (Petralia et al., 2010; Petralia and S., 2012). We used subunit-specific antagonists in order to differentiate between GluN2A and GluN2B signaling and found that antagonizing either subunit was not enough to prohibit NMDA treatment from decreasing Aβ levels. These results differ somewhat from previous studies that found that synaptic NMDA-R activation promoted increased α-secretase activity (Hoey et al., 2009) and that extrasynaptic NMDA-R signaling elevated β-secretase APP processing (Bordji et al., 2010). Both of these studies targeted NMDA-R subpopulations *in vitro* and did not examine a subunit-specific effect, however. It could be that the differential effects on Aβ observed by these groups is due entirely to NMDA-R location and not composition, or that these signaling pathways operate differently *in vitro* and *in vivo*.

Similar to NMDA-Rs, ERK signaling has a hand in an extensive number of cellular processes, making it a less than ideal target for therapeutic intervention. ERK has long been suspected to play a beneficial role in the regulation of Aβ production, but a selective pathway has yet to be defined (Mills et al., 1997; Goodenough et al., 2000; Manthey et al., 2001; Zhu et al., 2002b). Specificity could be gained if ERK's effect on Aβ production is exclusively carried out through one of the ERK isoforms. Using virally driven RNAi to knockdown either ERK1 or ERK2 in the hippocampus of APP/PS1 prior to performing microdialysis, we found that neither isoform is necessary for NMDA-Rs to regulate Aβ production. The use of shRNA against ERK1 or ERK2 was only able to reduce expression of these isoforms by less than half, however.

In addition to testing isoform-specificity, we searched for the signaling pathway linking NMDA-Rs to ERK activation. Because ERK cascades are responsible for specific cellular responses, a high level of regulation must be achieved through precise localization via scaffold proteins and specific docking sites that allow the binding of certain activators and regulators (Pouysségur et al., 2002). We tested the top three candidates that have been shown to link NMDA-Rs to ERK phosphorylation in previous studies: CaMKII, PKA, and PKC. Using inhibitors of these signaling molecules, we demonstrated that none was necessary for NMDA-Rs to activate ERK and decrease Aβ production. One possible explanation for this is that there is redundancy in this pathway and inhibition of no one signal is enough to block the effect. Additionally, due to the constraints of reverse microdialysis, it is possible that our pharmacological inhibition of these signaling molecules was incomplete. Future experiments may involve genetic targeting to more reliably silence CaMKII, PKA, or PKC signaling.

Unlike CaMKII, PKA, or PKC, RasGRF, a Ras-specific GDP/GTP exchange factor and Ras activator, is directly attached to NMDA-Rs. RasGRF has been found to both activate and

inhibit ERK signaling depending on the RasGRF isoform activated. Krapivinsky et al. showed that RasGRF1 bound to the GluN2B subunit, inhibited ERK activity, and promoted LTD (Krapivinsky et al., 2003). On the other hand, a different group used RasGRF isoform-specific knockout mice to demonstrate that RasGRF2 associated with NR2A, stimulated ERK, and promoted LTP (Li et al., 2006; Feig, 2011). Future experiments will need to be done to target RasGRF and determine if it is necessary for NMDA-R-regulation of Aβ. Because there are no pharmacological inhibitors developed against RasGRF, a genetic strategy will need to be used. RasGRF$^{-/-}$ mice have been developed and could be bred with APP/PS1 to determine the effect of RasGRF on Aβ pathology.

CONCLUSIONS

Amyloid-β production and release into the extracellular space is a pivotal process contributing to the pathogenesis of AD. Factors that regulate this process are therefore of great interest as targets for therapeutic intervention. Though NMDA-R signaling and ERK activation have been shown to decrease production of Aβ, neither NMDA-Rs nor ERK is a viable drug candidate due to their many cellular roles. We sought to explore this pathway in order to identify a more selective, viable candidate for pharmacological targeting. Ultimately, we found that NMDA-R-dependent Aβ regulation is not achieved through specific NMDA-R subunits, through either ERK isoform, or through CaMKII, PKA, or PKC signaling. Future experiments will address the roles of synaptic versus extrasynaptic NMDA-Rs as well as RasGRF activation of ERK.

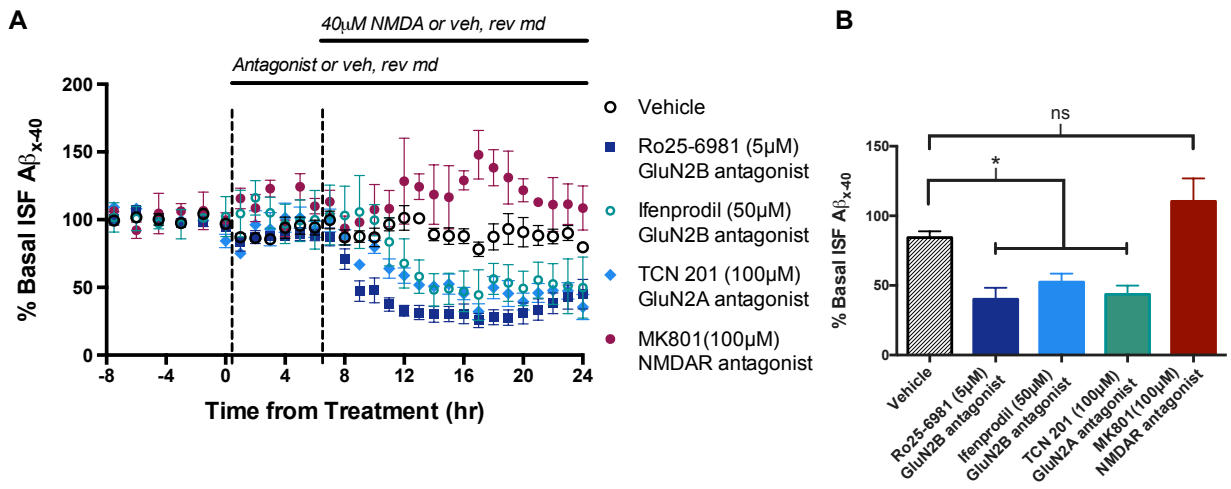

Figure 2.1: Subunit-specific antagonism does not affect ISF Aβ levels. A,B) 2-4 month old APP/PS1 were treated with aCSF (vehicle), Ro25-6981 (5μM; GluN2B antagonist), ifenprodil (50μM, GluN2B antagonist), TCN 201 (100μM; GluN2A antagonist), or MK801 (100μM; universal NMDA-R antagonist) for 6 hours, followed by 18 hours of co-treatment of antagonist with NMDA using microdialysis (n=4-8 mice/group). The last 3 time points of each treatment were averaged, and the percent change in ISF Aβ levels at the end of NMDA treatment versus the basal period of sampling was graphed. No antagonist significantly changed ISF Aβ levels on its own. The addition of NMDA to subunit-specific antagonists (Ro25-6981, ifenprodil, and TCN 201) decreased ISF Aβ levels by approximately 45%, and there was no difference between these antagonists. Only treatment with MK801 blocked the effect of NMDA on ISF Aβ.

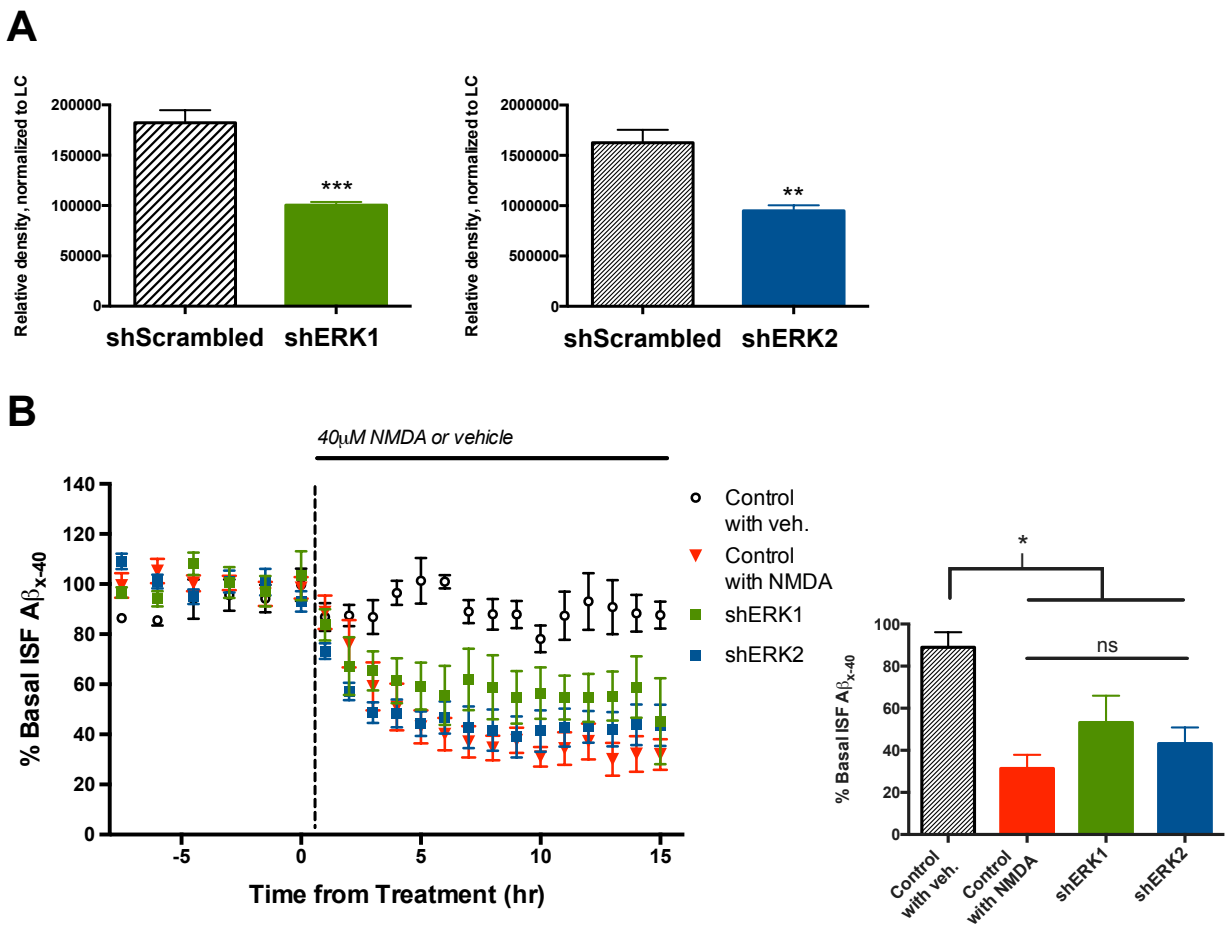

Figure 2.2: ERK1 or ERK2 knockdown is insufficient to alter NMDA-R regulation of ISF Aβ levels. A) ERK isoform knockdown was achieved using AAV delivery of shRNA targeted against either ERK1 (shERK1) or ERK2 (shERK2) or carrying a nonsense shRNA for control (shScrambled; n=8 mice/group). Western blot analysis of the hippocampal lysates was used to quantify the amount of ERK1 or ERK2 protein following knockdown as compared to shScrambled tissue. The shRNA targeted against ERK1 decreased ERK1 protein levels by 44.87% (p=0.0007) and shRNA against ERK2 decreased its expression by 41.62% (p=0.0029). **B)** Young APP/PS1 mice with no viral injection, ERK1 knockdown, or ERK1 knockdown were

administered NMDA or vehicle (aCSF) for 15 hours via reverse microdialysis. NMDA treatment decreased ISF Aβ levels by the same amount regardless of isoform knockdown.

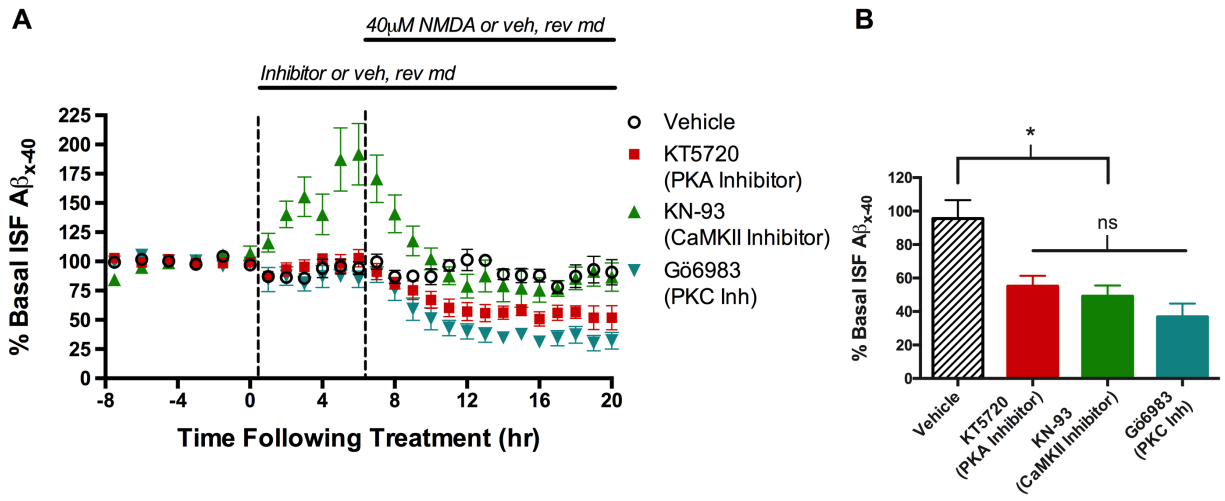

Figure 2.3: Inhibition of PKA, CaMKII, or PKC does not abrogate NMDA's effects on ISF Aβ levels.

A,B) Young APP/PS1 mice were pre-treated with either KT5720 (800nM; PKA inhibitor), KN-93 (50μM; CaMKII inhibitor), Gö6983 (1μM; PKC inhibitor), or vehicle (aCSF) for 6 hours before co-treatment with NMDA for 14 hours. The last 3 time points of each treatment were averaged, and the percent change in ISF Aβ levels at the end of NMDA treatment versus the end of inhibitor alone treatment was graphed. Though CaMKII inhibition increased ISF Aβ levels on its own, ultimately NMDA treatment leads to similar decreases in ISF Aβ levels following CaMKII, PKA, and PKC inhibition.

Chapter 3

AMPA-ergic Regulation of Amyloid-β Levels in an Alzheimer's Disease Mouse Model

PREFACE

This chapter contains a manuscript in preparation:

Hettinger JC, Lee H, Bu G, Holtzman DM, Cirrito JR. AMPA-ergic regulation of amyloid-β levels in an Alzheimer's disease mouse model. Manuscript in preparation.

Author contributions for the citation above:

JCH, JRC, DMH, and GB designed the research. JCH and HL performed the research. JCH analyzed the data and JCH and JRC wrote the paper.

ABSTRACT

Extracellular accumulation and aggregation of the Aβ peptide into toxic multimers is a key event in Alzheimer's disease pathogenesis. Aβ aggregation is concentration-dependent, with higher concentrations of Aβ much more likely to form toxic species. The processes that regulate extracellular levels of Aβ therefore stand to directly affect onset of AD pathology. Studies from our lab and others have demonstrated that synaptic activity is a critical regulator of Aβ production through both presynaptic and postsynaptic mechanisms. AMPA receptors (AMPA-Rs), as the most abundant ionotropic glutamate receptors, have the potential to greatly impact Aβ levels. By performing in vivo microdialysis in APP/PS1 mice, we found that AMPA-R activation decreases interstitial fluid (ISF) Aβ levels in a dose-dependent manner. Moreover, the effect of AMPA treatment involves three distinct pathways. Tonic, steady-state activity of AMPA-Rs normally promotes higher ISF Aβ concentrations. Evoked AMPA-R activity, however, decreases Aβ levels both by stimulating glutamatergic transmission and activating downstream NMDA receptor (NMDA-R) signaling or, with longer treatment, by acting independently of NMDA-R activity. Surprisingly, we found this latter, direct AMPA pathway of Aβ regulation is achieved through increased Aβ clearance rather than suppressed production. Understanding the pathways that regulate and maintain Aβ levels prior to AD pathology may provide insights into disease pathogenesis.

SIGNIFICANCE STATEMENT

Alzheimer’s disease pathology accumulates over many years. Synaptic activity is a strong regulator of brain Aβ concentration that influences if and when Aβ will aggregate. The

relationship between synaptic activity and Aβ levels has many facets. Synaptic transmission drives Aβ secretion into the brain ISF, while neurotransmitter receptor activation regulates Aβ levels independently of transmission. Here, we show that AMPA-Rs regulate Aβ via several pathways. AMPA-Rs and NMDA-Rs cooperate to suppress processing of APP into Aβ. Furthermore, AMPA treatment decreases Aβ levels through enhanced clearance, thus linking synaptic activity to Aβ clearance for the first time. These data emphasize that Aβ regulation by synaptic activity involves a number of independent pathways that together determine extracellular Aβ levels.

INTRODUCTION

Alzheimer's disease (AD) follows a protracted course with pathology detected years, even decades before clinical symptoms manifest. The preclinical stage of AD appears to be initiated by the aggregation of the peptide amyloid-β (Aβ) into toxic oligomers, thereby triggering a host of biochemical and cellular pathological events (Hardy and Higgins, 1992; Sperling et al., 2011; Musiek and Holtzman, 2015). The shift from normal production of soluble Aβ to its pathogenic aggregation is heavily influenced by Aβ's extracellular concentration. Consequently, the rate at which Aβ is produced and secreted from the neuron, as well as its clearance from the extracellular space, is directly linked to the formation of toxic amyloid species (Meyer-Luehmann et al., 2003; Yan et al., 2009; Bero et al., 2011).

Our lab and others have shown that an important regulator of extracellular Aβ levels is synaptic activity (Kamenetz et al., 2003; Cirrito et al., 2005b). Elevated synaptic activity drives clathrin-mediated endocytosis at the presynaptic membrane, thereby increasing endocytosis of

the amyloid precursor protein (APP) and subsequent Aβ generation (Cirrito et al., 2008). At the systems level, the regional distribution of amyloid plaque deposition in AD brains correlates with default mode network connectivity, suggesting that chronic high levels of network activity contribute to plaque formation (Buckner et al., 2005, 2009). However, not all increased neuronal activity results in increased Aβ concentrations. Indeed, a number of postsynaptic receptors have been shown to decrease Aβ production. Stimulation of serotonin receptors activates the extracellular regulated kinase (ERK) signaling pathway, which enhances α-secretase activity and non-amyloidogenic APP processing (Cirrito et al., 2011; Fisher et al., 2016). Similarly, M1 muscarinic acetylcholine receptors decrease Aβ levels by enhancing α-secretase activity through protein kinase C (PKC) activation (Davis et al., 2010; Fisher, 2012). NMDA receptor (NMDA-R) activation regulates Aβ levels bidirectionally – low concentrations of NMDA elevate Aβ levels through increased presynaptic membrane endocytosis, while higher concentrations of NMDA decrease Aβ production through dendritic, calcium-dependent signaling and increased α-secretase activity (Cirrito et al., 2011). These experiments show that the relationship between neuronal activity and Aβ production is complex, with even the same receptors in some cases having opposing effects depending on the extent of activation.

AMPA receptors (AMPA-Rs) are the predominant postsynaptic glutamate-gated ion channels and are responsible for the majority of fast excitatory transmission in the CNS, making them well positioned to impact the relationship between Aβ levels and synaptic activity. AMPA-Rs are composed of four subunits (GluA1-GluA4) in a dimers-of-dimers assembly to make up heteromeric, tetrameric complexes (Chater and Goda, 2014). Within the hippocampus, the majority of AMPA-Rs are made up of either GluA1 and -2 heteromers, GluA2 and -3 heteromers, or GluA1 homomers (Wenthold et al., 1996). The vast majority of AMPA-Rs in the

hippocampal pyramidal cells are heteromers containing RNA-edited GluA2 subunits. The presence of this subunit is highly significant to the biophysical properties of the receptor as it yields the receptor impermeable to calcium (Sommer et al., 1991). The existence of calcium-permeable GluA1 homomeric receptors remains controversial in the field, as is their possible physiological role (Lu et al., 2009). Biochemical studies show a small, functional population of calcium-permeable AMPA-Rs, likely extrasynaptic (Wenthold et al., 1996), while conditional genetic deletions of each subunit imply that these receptors have no significant effect on AMPA-R currents (Lu et al., 2009). This question continues to be pertinent as even a small population of AMPA-Rs with the ability to initiate intracellular calcium signaling could have an impact on glutamatergic transmission.

AMPA-Rs are pivotal actors in mediating synaptic plasticity and determining synaptic strength. In short, a synapse is strengthened with the insertion of AMPA-Rs into the membrane or weakened when they are endocytosed. AMPA-R trafficking in and out of the postsynaptic membrane is therefore highly dynamic. Phosphorylation and dephosphorylation of receptor subunits regulates receptor trafficking through a number of kinases and phosphatases such as CaMKII, PKA, calcineurin, and PKC (for review see Shepherd and Huganir, 2007). Also important to determining AMPA-R localization and activity is a troop of AMPA-R-binding intracellular and extracellular proteins, including proteins with and without PDZ domains (for review see Braithwaite et al., 2000). An additional route for AMPA-R regulation is receptor desensitization. AMPA-Rs are rapidly desensitized in a matter of milliseconds following agonist exposure, leading to short-term depression (Trussell et al., 1993). Dissociation of desensitized receptors from anchoring proteins results in their fast diffusion out the synaptic membrane and allows speedy recovery from synaptic depression (Constals et al., 2015).

In addition to their well-established role as the primary agents of postsynaptic depolarization, growing evidence suggests AMPA-Rs can act as independent activators of second messenger signaling (Wang and Durkin, 1995; Wang et al., 1997; Perkinton et al., 1999a; Hartmann et al., 2004; Rao and Finkbeiner, 2007). AMPA-R activation, for example, has been found to activate ERK signaling through a pathway that is sensitive to pertussis toxin, suggesting the participation of G protein (Wang and Durkin, 1995; Hayashi et al., 1999) Within retinal ganglion cells, AMPA-R activation has the ability to suppress the inward current through the c-GMP gated channel, again likely mediated by a G-protein (Kawai and Sterling, 1999). Furthermore, spontaneous, synaptic glutamatergic transmission maintains dendritic spines through undefined trophic signals that rely on AMPA-Rs, indicating some signaling initiated by the receptors (McKinney et al., 1999). These studies and others provide convincing evidence that AMPA-Rs have the ability to influence the cell through more than just sodium conductance and depolarization.

The most obvious and fundamental symptoms of AD are deficits in learning and memory. Studies in both human subjects and mouse models have shown that these deficits are at least in part mediated by Aβ-induced synaptic changes (Guntupalli et al., 2016b). Increased Aβ levels caused by overexpression of APP caused increased AMPA-R endocytosis and synaptic depression in a manner mimicking the natural processes of LTD (Hsieh et al., 2006). Increased calcium signaling following Aβ treatment decreased PKC-mediated phosphorylation of GluR2 subunits (Liu et al., 2010), and Aβ oligomers induced GluR1 dephosphorylation via calcineurin, which was associated with spatial memory deficits (Miñano-Molina et al., 2011). GluR3 was also shown to be important in Aβ-induced AMPA-R dysfunction; treatment with Aβ oligomers blocked LTP only in GluA3-expressing neurons (Reinders et al., 2016). APP knock-in AD

mouse models display downscaling of AMPA-R currents with age as well as deficits in LTP and LTD (Chang et al., 2006). Because deficits in AMPA-R function is clearly linked to AD pathology, positive AMPA-R modulators (AMPAkines) are being considered as AD therapeutics that could strengthen excitatory transmission and synaptic plasticity (Swanson, 2009). In aged rats, AMPAkine treatment rescued dendritic loss and memory deficits associated with aging (Lauterborn et al., 2016).

Most of the research involving AMPA-Rs and AD has focused on the deleterious effect of pathological amyloid species on AMPA-Rs (Chang et al., 2006; Hsieh et al., 2006; Shepherd and Huganir, 2007), while the inverse relationship, that of AMPA-R's effects on Aβ, has received much less attention. A notable exception is a compelling study by Hoey et al. (2013), which reported increased non-amyloidogenic processing of APP following AMPA treatment in vitro. Given the AMPA-R's dominant role in synaptic transmission and its active signaling capabilities, we hypothesized that AMPA-Rs regulate Aβ metabolism.

Using in vivo microdialysis, we found that baseline AMPA-R activity maintains higher levels of Aβ, whereas evoked activation of AMPA-Rs leads to reduced Aβ levels in the interstitial fluid (ISF) of the mouse hippocampus. Interestingly, the effect of exogenous AMPA treatment resolves into two phases. Initially, AMPA-Rs decrease Aβ levels through synaptic release of glutamate and downstream activation of NMDA-Rs. After prolonged treatment with AMPA, however, Aβ levels are reduced through an NMDA-R-independent pathway that does not rely on presynaptic transmission. Surprisingly, we found that AMPA-Rs directly influence Aβ levels by altering Aβ clearance, implicating synaptic activity with clearance mechanisms. This is the first instance of a synaptic activity-related process regulating Aβ clearance as opposed

to Aβ production. These findings highlight the complexity behind the overlapping pathways regulating extracellular Aβ levels.

MATERIALS AND METHODS

Animals

The mice used for these studies were hemizygous *APPswe/PS1ΔE9* (APP/PS1; Jankowsky et al., 2001, 2004) and bred on a wild-type C3H/B6 background or littermate controls (WT). Original transgenic breeders were purchased from Jackson Laboratory (Bar Harbor, Maine), and colonies were maintained at Washington University. Equal numbers of male and female mice were used in each study at 2-4 months of age. All studies were performed in accordance with the guidelines of AAALAC and the Institutional Animal Care and Use Committee (IACUC) at Washington University.

Aβ Microdialysis

In vivo microdialysis was performed in awake and behaving APP/PS1 mice as previously described (Cirrito et al., 2003, 2011). Briefly, guide cannulas (BR-style, Bioanalytical Systems, West Lafayette, IN) were stereotaxically implanted above the left hippocampus, coordinates bregma -3.1mm, 2.5mm lateral to midline, and 1.2mm below dura at a 12° angle. The cannulas were securely affixed to the head with dental cement, and microdialysis probes (BR-2, 2mm, 38kDa MWCO, Bioanalytical Systems) were inserted into the hippocampus through the guide cannula. In APP/PS1 mice, probes were perfused with artificial cerebrospinal fluid (aCSF;

1.3mM $CaCl_2$, 1.2mM $MgSO_4$, 3mM KCl, 04mM KH_2PO_4, 25mM $NaHCO_3$, and 122mM NaCl, pH 7.35) with 0.15% bovine serum albumin (BSA; Sigma-Aldrich, St. Louis, MO) at a rate of 1.0μL/min with samples of hippocampal ISF collected every 90 minutes during basal collection or every hour during treatment. Because WT murine Aβ concentrations are lower than in transgenic mice, microdialysis was run at 0.5μL/min and samples collected every 3 hours to increase concentration of each sample. Basal sampling began at least 16 hours following surgery. These experiments took place under constant light conditions to diminish circadian-related fluctuation in Aβ levels. At the conclusion of the experiment, all ISF samples were analyzed for $A\beta_{x\text{-}40}$ or $A\beta_{x\text{-}42}$ levels by sandwich ELISA.

Compounds

Reverse microdialysis was used to administer compounds directly into the hippocampus. Drugs were diluted into the perfusion buffer of artificial CSF and 0.15% BSA, allowing the drugs to diffuse into the brain continuously for the duration of the experiment at the same time that Aβ is collected. Due to the complexity of determining the final concentration of compound delivered to the brain, only the starting concentrations of drugs in the perfusion buffer are given. We estimate approximately 10% of the drug is delivered across the probe membrane where it is further diluted in the brain CSF. AMPA (0.5, 2, 5, and 10μM), MK801 (100μM), NMDA (40μM), and thiorphan (10μM) were purchased from Sigma. Cyclothiazide (CTZ; 300μM), FK506 (10mg/kg), CP-465022 (2, 5mg/kg), tetrodotoxin (TTX; 5μM), NBQX (100μM), and GM6001 (25μM) were purchased from Tocris Bioscience (Ellisville, MO). LY411575 (Sigma) was diluted in corn oil and administered subcutaneously at 5 mg/kg. FK506 was serially diluted in DMSO then propylene glycol and administered subcutaneously at 10mg/kg. CP-465022 was diluted in water

and administered at both 2- and 5mg/kg subcutaneously. Recombinant mouse IL-6 protein was obtained from Millipore Sigma (Temecula, CA). Recombinant hexafluoroisopropanol (HFIP)-$A\beta_{40}$ was purchased from rPeptide and reconstituted in DMSO.

Aβ Sandwich ELISAs

ISF samples were analyzed for $A\beta_{x\text{-}40}$ or $A\beta_{x\text{-}42}$ concentration using methods previously described (Fisher et al., 2016). A mouse monoclonal anti-$A\beta_{40}$ capture antibody (mHJ2) or anti-$A\beta_{42}$ capture antibody (mHJ7.4) made in-house was used in conjunction with a biotinylated central domain detection antibody (mHJ5.1) and streptavidin-poly-HRP-40 (Fitzgerald Industries, Acton, MA). Super Slow ELISA TMB (Sigma) was then used to develop, and absorbance was read by a BioTek Epoch plate reader at 650 nm. The same assay can be used for both human and murine $A\beta_{x\text{-}40}$. Standard curves for ELISAs were generated using synthetic human $A\beta_{40}$ or $A\beta_{42}$ (American Peptide, Sunnyvale, CA). Basal levels of ISF Aβ levels were calculated by averaging the Aβ concentrations taken every 90 minutes for 9 hours prior to drug treatment. All Aβ levels for each mouse were then normalized by calculating percent of basal for each point. Mean ± SEM per group are shown.

Western blotting

Guide cannula implantation and microdialysis were performed as described above using 2-4 month old APP/PS1 mice. 5μM AMPA or vehicle was administered to APP/PS1 mice via reverse microdialysis for 8 or 14 hours. Immediately following treatment, perfusion buffer was changed to aCSF containing 0.1% Evans Blue dye for 30 minutes. During this period, the area of the hippocampus directly surrounding the microdialysis probe was dyed blue, approximating the

area of tissue affected by reverse microdialysis drug delivery. Following the 30-minutes of Evans Blue administration, the mice were sacrificed and the dyed tissue surrounding the probe was microdissected and snap frozen on dry ice, generating approximately 5-7mg of tissue per mouse. The collected hippocampal tissue was homogenized by sonication at a 10:1 volume:wet weight in 150mM NaCl, 50mM Tris, pH 7.4, 0.5% deoxycholic acid, 0.1% SDS, 1% Triton X-100, 2.5mM EDTA, and protease inhibitors. Gel electrophoresis of 20μg protein samples was performed under reducing conditions using 4-12% Bis-Tris NuPAGE gels (ThermoFisher Scientific, Waltham, MA) and then transferred to nitrocellulose membrane. Blots were probed for glial fibrillary acidic protein (GFAP; 1:500; ThermoFisher), low density lipoprotein receptor-related protein 1 (LRP1; 1:5000; Abcam, Cambridge, MA), insulin-degrading enzyme (IDE; 1ug/mL; Abcam), neprilysin (1:1000; Millipore), matrix metalloproteinase-9 (MMP-9; 1:1000; Millipore, Billerica, MA), C-terminal fragments of APP (1:1000; Sigma), β-amyloid 1-16 (6E10; 1:500; BioLegend, San Diego, CA), glutamate receptor 2 (GluR2; 1:1000; Millipore), tubulin (1:2500; Sigma), and glyceraldehyde 3-phosphate dehydrogenase (GAPDH; 1:10,000; Sigma). HRP-conjugated goat anti-rabbit IgG (1:1000; Cell Signaling Technology, Danvers, MA) and HRP-conjugated Amersham ECL sheep anti-mouse IgG (1:500; GE Healthcare, Chicago, IL) were used as secondary antibodies. Membranes were developed using SuperSignal West Pico Substrate (ThermoFisher) or Lumigen-TMA6 (GE Healthcare) and imaged using the Kodak ImageStation 440CF (Rochester, NY). Band intensity was quantified using the Kodak 1D Image Analysis software, and normalized using tubulin or GAPDH signals as loading controls. Values shown are these normalized band intensities relative to the experimental control group. Mean ± SEM per group are shown.

Quantitative Real-Time PCR (qPCR)

Using the same tissue preparation as used for Western blotting (described above), APP/PS1 mice were treated with 5μM AMPA for 8 or 14 hours, followed by 30 minutes of 0.1% Evans Blue solution via reverse microdialysis. Dyed tissue around the probe was microdissected and frozen. Quantitative PCR was performed as described previously (Fisher et al., 2016). The RNeasy Mini Kit (Qiagen, Valencia, CA) was used to extract RNA, which was then reverse transcribed with a High Capacity cDNA Reverse Transcription kit (ThermoFisher). The Harvard Medical School Primer Bank was used to design primers (Wang and Seed, 2003; Spandidos et al., 2008, 2010). Real-time detection of PCR product was performed using the Fast SYBR Green Master Mix (Applied Biosystems, Foster City, CA) in ABI 7900HT (Applied Biosystems) with the default thermal cycling program. *cFos* was used as a positive control due to its established role as a mark of neuronal activity (Kaczmarek, 1993). *Gapdh* was used as a reference gene for relative expression calculations. Relative mRNA levels were calculated using the comparative Ct method using the formula $2^{-\Delta\Delta Ct}$. Mean ± SEM per group are shown.

Histology

2-4 month-old wild-type mice (n=6 per group) or APP/PS1 mice (n=3 per group) were treated with 8 hours or 14 hours, respectively, of AMPA or artificial CSF via reverse microdialysis then immediately transcardially perfused with ice-cold phosphate buffer saline (PBS) with 0.3% heparin. Brains were removed, fixed in 4% paraformaldehyde for 24 hours at 4°C, then placed in 30% sucrose prior to freezing and sectioning. Coronal brain sections 50μm wide were sliced in 300μm intervals using a freezing sliding microtome. Sections were then immunostained to

visualize astrocytes or microglia using antibodies against glial fibrillary acidic protein (GFAP; 1:500, ThermoFisher) as an astrocytic marker or against ionized calcium-binding adaptor molecule 1 (Iba1; 1:500; Wako Laboratory Chemicals, Richmond, VA) as a microglial marker. Biotinylated secondary antibody, horseradish peroxidase-conjugated streptavidin, and DAB reaction (Sigma) were used to develop. Brain sections were imaged with a Nanozoomer slide scanner (Hamamatsu Photonics, Bridgewater, NJ). Staining density was qualitatively evaluated by blinded observers and vehicle- and AMPA-treated groups were compared. Images shown are representative.

Aβ Elimination Half-Life

Half-life of ISF Aβ was measured using methods described previously (Cirrito et al., 2003). Microdialysis was performed as detailed above and basal ISF Aβ levels were collected. Reverse microdialysis was then used to treat APP/PS1 mice with either 5μM AMPA or vehicle for 14 hours, followed by co-administration with LY411575, a potent and selective γ-secretase inhibitor (Sigma; 5mg/kg in corn oil, subcutaneous injection) to block Aβ production. ISF Aβ levels were measured using sandwich ELISA, and the half-life was calculated using the slope of the semi-log plot of percent change in Aβ levels versus time. The slope was calculated based only on Aβ values that were continually decreasing, excluding points at which levels plateaued. Mean ± SEM per group are shown.

Aβ Uptake Assay

BV2 microglial cell line was generously provided by Kristen Funk (Washington University in St. Louis, St. Louis, MO) and cultured in DMEM supplemented with 2% FBS. Cultures were

maintained in at 5% CO_2 humidified atmosphere of 37°C. BV2 cells were plated at a concentration of $1X10^5$cells/mL in 12-well plates. Cells were treated with either AMPA (0.1-25μM) or murine IL-6 (2-25ng) for 14 hours followed by 4 hours of co-treatment with 500nM HFIP-Aβ_{40} added directly to the medium. The cells were then washed 3 times with PBS, trypsinized, and lysed in RIPA buffer, and sonicated. The concentration of Aβ_{40} was then quantified via ELISA.

MesoScale Discovery (MSD) Multiplex Cytokine Assay

Hippocampal tissue was collected from APP/PS1 mice treated with either vehicle (n=7) or AMPA (n=-9) for 14 hours via reverse microdialysis. Only tissue directly surrounding the probe was used. Tissue was homogenized following the manufacturer protocol in 500mM NaCl, 50mM Tris, pH 7.4, 0.5% deoxycholic acid, 0.1% SDS, 1% Triton X-100, 2mM EDTA, and protease inhibitors (MesoScale Discovery, Rockville, MD, USA). Samples were assayed for interleukin (IL)-1β, IL-6, and tumor necrosis factor (TNF)-α using a custom MSD Proinflammatory Panel multiplex assay using the manufacturer's protocol. Samples were assayed duplicate. Data analysis was performed using MSD Workbench software.

Experimental Design and Statistical Analysis

Mice were randomly assigned into treatment groups, with equal numbers of male and females. In addition, littermates were split between groups. Based on power analyses for detecting changes in ISF Aβ in microdialysis experiments, we used n=4-8 mice per treatment group. A full description of statistical tests and the number of mice used can be found in the figure legends. Two-tailed unpaired *t*-tests were used to compare between two groups. One-way or two-way

ANOVA was used when comparing one or two independent variables, respectively, between multiple groups. The appropriate correction for multiple comparisons was used (Sidak, Tukey, or Bonferroni; refer to figure legends). Analysis of microdialysis experiments was performed by averaging the final three data points of a specific treatment period and using one-way or two-way ANOVA with an appropriate correction for multiple comparisons. Values were accepted as significant is $p \leq 0.05$. Data in figures are presented as mean ± SEM. Prism 6.0b for Mac OS X (GraphPad, San Diego, CA) was used for all statistical analyses.

RESULTS

Local administration of AMPA decreases ISF Aβ in a dose-dependent manner

Both synaptic activity and NMDA-Rs have distinct, established roles in regulating Aβ, but the involvement of AMPA-R signaling in Aβ regulation has been largely unexplored. To address this, we used in vivo microdialysis to measure the concentration of ISF Aβ in the hippocampus of mice (Cirrito et al., 2003, 2008). Crucially, this technique allows us to monitor changes in ISF Aβ levels over time in freely moving mice with functional glutamatergic synapses and intact neuronal networks. Through reverse microdialysis, we are also able to locally and continuously deliver small-molecule compounds, such as AMPA, into the hippocampus without needing to cross the blood-brain barrier.

Using microdialysis in the hippocampus of young, plaque-free (2-4 month old) *APPswe/PS1Δe9* hemizygous (APP/PS1) mice (Jankowsky et al., 2001, 2004), we collected hourly samples of ISF while infusing AMPA in increasing concentrations from 0.5μM to 10μM for 8 hours each (Fig. 3.1A). AMPA delivered at 0.5μM or 2μM had no effect on ISF Aβ. However, beginning with the 5μM AMPA concentration, ISF Aβ levels gradually decreased over

time before stabilizing at a 32% decrease from baseline levels. An even greater decrease is seen following 10μM AMPA treatment, with levels of Aβ stabilizing at a 75% decrease from baseline levels (Fig. 3.1A). In the following experiments, we used 5μM AMPA in order to observe both increases and decreases in ISF Aβ levels following AMPA treatment. 5μM AMPA decreases ISF $A\beta_{42}$ similarly to $A\beta_{40}$, indicating that AMPA acts on both species of Aβ in the same manner (Fig. 3.1B). Next, wild-type (WT) mice were treated with 5μM AMPA to eliminate potential confounds due to the transgenes in APP/PS1 mice. Murine ISF Aβ levels in WT animals reacted to 5μM AMPA treatment similarly to APP/PS1 mice with a 45% decrease from baseline levels (Fig. 3.1C).

AMPA-Rs rapidly desensitize following AMPA or glutamate exposure (Trussell et al., 1993). One possible explanation for the observed effect on ISF Aβ, therefore, could be reduced activity due to decreased AMPA-R signaling. To test this possibility, we treated the APP/PS1 mice with cyclothiazide (CTZ), a thiazide diuretic, which inhibits desensitization and potentiates AMPA-mediated glutamate currents (Yamada and Rothman, 1992). The mice were pre-treated with CTZ for 4 hours before and then during treatment with increasing doses of AMPA (0.5μM-5μM) lasting four hours each (Fig. 3.1D). Potentiated AMPA-R signaling enhanced the suppression in ISF Aβ levels with AMPA treatment starting at just 0.5μM, a dose that had no effect on ISF Aβ without CTZ. This decrease is dose-dependent, with a maximal decrease in ISF Aβ of 83% from basal levels (Fig. 3.1D). These data indicate that the observed decrease in ISF Aβ is due to AMPA-R activity and not desensitization. Along with desensitization, decreased AMPA-R signaling and resulting reduced activity could be caused by AMPA-R internalization following excessive AMPA exposure, as is observed in LTD. One of the key phosphatases identified for receptor dephosphorylation and subsequent endocytosis is calcineurin, also known

as protein phosphatase 2B (Mulkey et al., 1994; Beattie et al., 2000). To determine if AMPA treatment causes calcineurin-mediated AMPA-R internalization, we pre-treated APP/PS1 mice with FK506, a calcineurin inhibitor, before co-treating with 5μM AMPA (Fig. 3.1E). Calcineurin inhibition did not block the decrease in ISF Aβ caused by AMPA exposure, suggesting that loss of AMPA-R signaling through endocytosis is not responsible for the effect of AMPA on Aβ. It is important to note, however, that calcineurin is likely not the only signaling molecule regulating AMPA-R internalization.

AMPA decreases Aβ levels through multiple distinct pathways

The exogenous application of AMPA through reverse microdialysis allows us to directly and selectively target AMPA-Rs. However, infusion of AMPA does not necessarily reproduce endogenous AMPA-R signaling. To address this, we treated mice with NBQX, a competitive AMPA-R antagonist (Fig. 3.2A). When baseline levels of AMPA-R signaling were blocked, ISF Aβ levels decreased by 32%, suggesting that AMPA-R activation increases Aβ during normal activity. To confirm these results, we also used a non-competitive AMPA-R antagonist, CP-465022. As with the competitive antagonist, ISF Aβ levels decreased by approximately 32% (Fig. 3.2B).

Next, we treated mice with tetrodotoxin (TTX) for 16 hours to prevent the production of action potentials and therefore block evoked presynaptic release of glutamate (Fig. 3.2C). Following 16 hours of TTX treatment, we co-infused TTX with NBQX. As previously reported, treatment with TTX alone decreased ISF Aβ levels by about 40% from basal levels (Cirrito et al., 2005b). Blocking AMPA-Rs in addition to TTX treatment lead to a further decrease in Aβ levels of 33% despite the cessation of presynaptic activity (Fig. 3.2C). Thus, AMPA-R signaling

mediated by receptors activated during steady-state, tonic levels of activity appears to normally repress ISF Aβ levels independently of evoked glutamatergic signaling. Interestingly, antagonizing basally active AMPA-Rs induced a full effect on ISF Aβ levels regardless if action potentials were intact or blocked with TTX, suggesting that basal AMPA-ergic regulation of Aβ is driven by spontaneous glutamate release via miniature EPSCs ("minis") as opposed to evoked activity.

We next determined the extent to which AMPA-mediated Aβ regulation relies on presynaptic activity. As before, mice were pre-treated with TTX followed by co-treatment with TTX and AMPA. During the initial 8 hours of TTX and AMPA treatment, the decrease in Aβ levels caused by AMPA treatment (Fig. 3.2D) was abolished. However, a longer AMPA treatment of 14 hours significantly decreased ISF Aβ levels by 30% of post-TTX levels (Fig. 3.2C). These results imply that, initially, evoked glutamatergic transmission is necessary for AMPA treatment to decrease ISF Aβ. With longer treatment, however, ISF Aβ levels are reduced through postsynaptic AMPA-R signaling alone, without the need of action potentials or further glutamatergic activity stimulation.

Given that high levels of NMDA-R activation result in decreased Aβ levels through calcium–dependent ERK signaling (Hoey et al., 2009; Verges et al., 2011), we hypothesized that AMPA treatment might reduce ISF Aβ levels through the indirect activation of NMDA-Rs expressed on downstream postsynaptic neurons. To determine the contribution of NMDA-Rs to the changes in Aβ levels following AMPA treatment, mice were pre-treated with MK801, an NMDA-R open channel blocker, via reverse microdialysis for 6 hours before co-treatment with MK801 and 5μM AMPA (Fig. 3.2E). Initially, co-application of MK801 and AMPA did not show an AMPA-related change in Aβ levels. However, after 8 hours of AMPA administration

Aβ levels began to decline, reaching 50% by hour 14 (Fig. 3.2E). These data imply that AMPA's effects on ISF Aβ levels are dependent on NMDA-R signaling for only a limited period. After prolonged treatment with AMPA, Aβ levels are decreased through a NMDA-R-independent mechanism.

In consideration of these results, we questioned if AMPA-R signaling might be responsible for any part of NMDA-Rs' effect on Aβ levels. To test this, we first treated the mice with 100μM NBQX, a competitive AMPA-R antagonist, through reverse microdialysis then co-treated with NMDA (Fig. 3.2A). As observed in previous experiments (Verges et al., 2011), 40μM NMDA reduced ISF Aβ levels to approximately 50% of basal levels within 6 hours of treatment, even in the presence of an AMPA-R antagonist (Fig. 3.2A). Though the effect of AMPA treatment on ISF Aβ in part relies on NMDA-R involvement, the opposite does not appear true; NMDA treatment decreases Aβ levels independently from AMPA-R activation. To ensure the specificity of AMPA treatment, animals were treated with NBQX to block AMPA-Rs prior to the addition of AMPA. As was expected, NBQX completely blocked the effect of AMPA-Rs on Aβ (Fig. 3.2A).

AMPA treatment results in long-lasting changes in ISF Aβ levels

Previous data show that activation of NMDA-R signaling rapidly decreases ISF Aβ levels by approximately 50% (Verges et al., 2011). Once NMDA is no longer administered, ISF Aβ gradually returns to baseline levels within 30 hours. AMPA treatment, however, results in a longer-lasting change in Aβ levels. APP/PS1 mice were treated with 5μM AMPA in the microdialysis perfusion buffer for 8 hours. After this period, AMPA treatment ended and Aβ levels were monitored every 1-2 hours for an additional 44 hours (Fig. 3.3A). Levels of ISF Aβ

decreased steadily during the AMPA treatment and continued to decrease for 3 hours into the washout period to reach a maximal decrease of 60% from basal levels. From this trough, Aβ levels very gradually increased for the duration of the washout, reaching a level only 35% decreased from basal levels after 44 hours of recovery (Fig. 3.3A). The washout study was terminated after a total of 60 hours of ISF collection due to limitations in the reliable duration of microdialysis experiments, so it is possible that Aβ levels may completely recover from AMPA treatment with a longer washout period. A recovery in ISF Aβ suggests that AMPA treatment does not cause major cell death and that the area surrounding the microdialysis probe continues to function normally following treatment.

APP/PS1 mice were treated with AMPA for 8 hours followed by co-administration with NBQX (Fig. 3.3B). The decrease in Aβ levels following AMPA application did not recover to baseline levels with the addition of NBQX despite the cessation of AMPA-R activation. Because the Aβ decrease was preserved without AMPA-ergic transmission, the effect on Aβ is likely due to a long-lasting intracellular event and not a feed-forward increase in continued glutamatergic transmission. This observed long-lived change in Aβ levels was initiated by an AMPA treatment period of only 30 minutes, which resulted in a 30% decrease in ISF Aβ (Fig. 3.3C).

Transcription of APP processing-related genes and the levels of APP fragments are unchanged following AMPA treatment

We demonstrated above that extended treatment with AMPA influences ISF Aβ levels without the need for NMDA-R activation. NMDA-Rs are often associated with intracellular signaling and transcriptional regulation, while AMPA-Rs are generally thought of in terms of

neuronal depolarization. However, there is growing evidence to suggest that AMPA-Rs may also play an active role in cellular signaling. For example, Plant et al. (2006) found that transient calcium signaling through calcium-permeable AMPA-Rs promotes the maintenance of long-term potentiation (LTP). Additionally, AMPA-R signaling, independent of depolarization, is sufficient to activate the transcription factor CREB as well as to initiate ERK signaling (Perkinton et al., 1999b; Santos et al., 2006; Rao and Finkbeiner, 2007). Given these results, the AMPA-R-dependent decrease in ISF Aβ that we observe could be due to the initiation of a signaling cascade by AMPA-Rs. First, we tested if AMPA-Rs affect the transcription of genes related to APP processing or Aβ clearance (Fig. 3.4A,B). APP/PS1 mice were administered 5μM AMPA for 8 or 14 hours by reverse microdialysis. At the end of treatment, probes were infused with Evans Blue for 30-minutes to mark the surrounding tissue reached by reverse microdialysis. The dyed hippocampal tissue was lysed and used for quantitative real-time PCR (qPCR) for a selection of genes involved in Aβ metabolism. Expression of the immediate early gene, *cFos*, was used as a control due to its increased expression following glutamatergic transmission (Kaczmarek, 1993). As expected, AMPA treatment increased the expression of *cFos* in both the 8- and 14-hour groups. However, we found no significant changes in the expression of *APP*, in genes related to α-secretase (*ADAM10* and *ADAM17*), in genes related to β-secretase (*BACE1*), nor in genes related to ϒ-secretase (*PS1, PS2, PSEN2, APH1, BSG,* and *NIC*) following 8 or 14 hours of AMPA treatment (Fig. 3.4A,B). Further, AMPA treatment did not change expression in *ERK1* or *ERK2* or in genes associated with Aβ clearance (*LRP1, LRPR, AQP4, NEP, MMP2,* and *MMP9*). Finally, none of the AMPA-R subunits genes (*GRIA1-4*) were altered by AMPA treatment (Fig. 3.4A,B).

Extended treatment with AMPA promotes increased ISF Aβ clearance but not Aβ production

To the best of our knowledge, all previous studies investigating the relationship between synaptic signaling and alterations in Aβ levels, including several from our laboratory, have found that synaptic signaling primarily affects Aβ production (Cirrito et al. 2003; Cirrito et al. 2005; Fisher et al. 2016; Kamenetz et al. 2003; Bero et al. 2011; Yan et al. 2009; Wei et al. 2010). However, after 14 hours of AMPA administration, we found no change in full-length APP levels or in the cleavage product β-C-terminal fragment (β-CTF) as determined by Western blot (Fig. 3.5A). In combination with the lack of transcriptional changes in production-related genes (Fig. 3.4A,B), these data lead us to hypothesize that extended treatment with AMPA could regulate Aβ clearance.

Aβ is eliminated from the ISF through five main pathways: receptor-mediated transport across the blood brain barrier (BBB), enzymatic degradation, cellular uptake, glymphatic-mediated clearance, or passive bulk-flow clearance (for reviews see Tanzi et al., 2004; Holtzman et al., 2011; Tarasoff-Conway et al., 2015). If any of these pathways is targeted by AMPA treatment, the rate of ISF Aβ clearance could increase. To test this possibility, we measured half-life of ISF Aβ in mice treated with either 5μM AMPA or vehicle using reverse microdialysis (Fig. 3.5B,C). After 14 hours, mice were subcutaneously injected with LY411575, a potent γ-secretase inhibitor that rapidly inhibits Aβ production. LY411575 enters the brain and within 15 minutes reaches a concentration approximately 200-fold in excess of its IC_{50} for γ-secretase inhibition (Cirrito et al., 2003). The rate of decrease in Aβ levels was then measured for both groups using the slope of the semi-log plot of percentage baseline Aβ levels versus time (Fig. 3.5C). Interestingly, the half-life of ISF Aβ was significantly shorter by over 30% in mice

receiving AMPA treatment ($t_{1/2}$= 0.93 hr) than those in the control group ($t_{1/2}$= 1.38 hr), indicating that AMPA treatment increases the clearance of ISF Aβ (Fig. 3.5D). It is important to note that 6 of 12 AMPA-treated mice had ISF Aβ levels decrease so much that a reliable half-life could not be calculated. If this greater decrease following AMPA treatment was also due to enhanced clearance, then the observed significance of AMPA on Aβ elimination rate would be enhanced, meaning we could be underestimating the effect of AMPA on Aβ clearance.

Next, we measured the levels of key proteins involved in Aβ clearance in the hippocampal tissue surrounding the microdialysis probe for mice treated with 14 hours of AMPA or vehicle (Fig. 3.6A). Similar to the qPCR experiments (Fig. 3.4B), only the positive control cFos showed a significant change in protein levels with AMPA treatment (Fig. 3.6A). Though these data suggest that none of the Aβ clearance-related proteins selected is involved in AMPA-mediated regulation of Aβ, Western blots do not detect cell type-specific changes in protein levels, alterations in protein function, or changes in protein localization. To test if AMPA treatment increases protease activity and thus Aβ degradation, we pre-treated APP/PS1 mice with the neprilysin inhibitor, thiorphan, or with the broad-spectrum metalloproteinase (MMP) inhibitor, GM6001, before co-treating with AMPA. Inhibition of neprilysin or all MMP family members blocks Aβ clearance pathways as well as potentially inhibits α-secretase, which increases ISF Aβ levels when those agents are administered singly (Fig. 3.6B). Importantly, the addition of AMPA still decreased Aβ by a comparable amount as observed without protease inhibitors, indicating that AMPA does not affect proteolytic degradation of Aβ through these proteases.

Another possible clearance route is the uptake of extracellular Aβ by microglial phagocytosis. We utilized a BV2 cell culture model to test the effect of AMPA treatment on

microglial Aβ uptake (Fig. 3.6C). BV2 cells are retroviral immortalized mouse microglial cells that share many similar functions with primary microglia (Bocchini et al., 1992; Henn et al., 2009; Stansley et al., 2012). These cells were treated with various concentrations of AMPA, ranging from 01μM to 25μM, for 14 hours followed by 4 hours of treatment with synthetic $A\beta_{40}$ (500nM). The cells were thoroughly washed, trypsinized to digest surface-bound Aβ, and lysed for intracellular Aβ quantification. No change in the amount of Aβ taken up by the BV2 cells was observed following AMPA treatment of any concentration. While these data suggest that AMPA treatment does not directly affect microglial phagocytosis of Aβ, there are a number of caveats. For instance, AMPA treatment could be affecting clearance by acting on multiple cell types, including microglia. Additionally, BV2 cells do not exhibit the same degree of activation following stimulation as primary microglia (Stansley et al., 2012).

AMPA-R activation does not induce inflammation

A potential concern is that AMPA treatment decreases ISF Aβ by causing cellular toxicity and/or creating a lesion through increased glutamatergic activity (Olney et al., 1986). If AMPA does cause cellular damage, an inflammatory response would involve the recruitment and activation of microglia and astrocytes (Eng et al., 1992; Denes et al., 2007; Hanisch and Kettenmann, 2007). To monitor inflammatory responses, mice were treated with 5μM AMPA or with vehicle for 8 or 14 hours before brains were collected and fixed in 4% formaldehyde. The brains were stained for Iba1, a marker of microglia (Ito et al., 2001), and GFAP, a marker for astrocytes (Bush et al. 1999; Eng et al. 1992). As expected, we found increased Iba1 and GFAP staining around the microdialysis probe tract, but no change in staining density between the AMPA-treated and vehicle-treated tissue at either time point (Fig. 3.7A). For confirmation, we

measured protein levels of GFAP and CD45, another microglial marker (Bennett et al. 2016), using hippocampal lysates from APP/PS1 mice treated with either 5μM AMPA or vehicle for 14 hours (Fig. 3.7B). In agreement with the immunostaining results, AMPA treatment did not increase GFAP or CD45 protein levels, indicating a lack of glial recruitment (Fig. 3.7B). In addition to monitoring the glial response, we measured pro-inflammatory cytokines levels in the hippocampal lysates of mice following AMPA treatment. Though IL-1β and TNF-α levels were unchanged, the levels of IL-6 showed a dramatic increase of over 500% (Fig. 3.7C). IL-6 is a neuropoietic cytokine with both neuromodulatory and neuroprotective roles, known to be induced by neuronal activity (Sallmann et al., 2000; Juttler et al., 2002; Erta et al., 2012). Without a visible increase in gliosis and with no significant increase in IL-1β or TNF-α, there does not appear to be a broad inflammatory response. These data, along with the partial recovery of ISF Aβ in the 44 hours sampled following AMPA treatment (Fig. 3.3A), strongly suggest AMPA is not causing widespread toxicity accounting for the effects on Aβ observed in these experiments.

DISCUSSION

In this study, we provide evidence that evoked AMPA-R signaling decreases extracellular Aβ concentration through two different pathways. The first of these pathways acts on Aβ through an indirect network effect; AMPA-R stimulation leads to increased glutamatergic transmission, including elevated NMDA-R signaling on the postsynaptic neuron. It has been previously shown that NMDA-Rs regulate Aβ levels by using calcium as a second messenger to activate ERK and increase α-secretase activity. Second, we found that AMPA-Rs can also influence Aβ levels independently of NMDA-Rs. This purely AMPA-R-mediated pathway takes longer to recruit and

increases the rate of ISF Aβ clearance. Gene expression and protein levels of many primary clearance-related molecules remain unchanged, possibly indicating cell-type specific changes or alterations in protein function or localization. This is obviously an important area for future study.

Exogenous application of AMPA decreases ISF Aβ through postsynaptic signaling

We found that infusion of AMPA directly into the hippocampus of APP/PS1 mice through reverse microdialysis decreases ISF Aβ levels by up to 75% following the maximal dose of 10μM. Treatment with AMPA induces a potent, long-lasting effect on Aβ levels, with even a brief application initiating a full response. AMPA-Rs, therefore, appear to be significant regulators of Aβ levels in the extracellular space. Factors that influence extracellular levels of Aβ have the potential to directly influence AD pathogenesis by altering the likelihood of Aβ to aggregate (Lomakin et al., 1997). That AMPA increases activity but suppresses Aβ levels is somewhat surprising considering previous reports that synaptic activity drives production of Aβ. Treatment with the $GABA_A$ receptor antagonist picrotoxin, high levels of potassium chloride, or electrical stimulation promotes Aβ secretion into the extracellular space (Kamenetz et al., 2003; Cirrito et al., 2005b, 2008). In a more physiological setting, increasing activity within the barrel cortex through vibrissal stimulation results in higher levels of ISF Aβ in APP/PS1 mice (Tampellini et al., 2010a; Bero et al., 2011). In humans, the highest levels of amyloid deposition are found in brain regions with the highest baseline metabolic activity (Buckner et al., 2005).

Considering these findings, it would be reasonable to hypothesize that AMPA-Rs, as excitatory channels, should increase Aβ levels. Paradoxically, however, we found increasing

AMPA-R activation through exogenous AMPA treatment significantly decreases ISF Aβ. Because AMPA-Rs are susceptible to rapid desensitization, we considered the possibility that AMPA-Rs act on Aβ levels through induced synaptic depression (Yamada and Rothman, 1992; Trussell et al., 1993). However, when receptor desensitization was blocked with cyclothiazide, the decrease in Aβ in response to AMPA was potentiated. Receptor desensitization only limited Aβ suppression, and receptor activation is directly responsible for the reduction of Aβ levels.

Though general increases in synaptic activity upregulate Aβ production, the activation of certain postsynaptic signaling systems can alter APP processing to yield varied effects on Aβ levels, particularly when α-secretase is targeted and Aβ production is precluded. As mentioned above, serotonin receptor activation decreases Aβ levels through PKA and ERK activation (Cirrito et al., 2011; Fisher et al., 2016). The serotonin receptor illustrates the specificity involved in Aβ regulation; only the G_s-linked receptors decrease Aβ whereas the other G-protein coupled serotonin receptors have no effect or may even increase Aβ (Fisher et al., 2016). Additionally, M1 muscarinic acetylcholine (mACh) receptor agonists decrease Aβ production, and knocking out this receptor leads to increased levels of Aβ in the brain as well as increased amyloid pathology (Jones et al., 2008; Davis et al., 2010; Fisher, 2012). Within the glutamate receptor family, muscarinic glutamate receptor 5 has been shown to trigger Aβ production (Kim et al., 2010; Hamilton et al., 2014), and NMDA-Rs can modulate Aβ levels bidirectionally (Lesné et al., 2005; Hoey et al., 2009; Verges et al., 2011). Clearly, postsynaptic effects on Aβ are varied and markedly context-specific.

Spontaneous and evoked AMPA-R activation differentially regulate Aβ levels

In these studies we have shown that AMPA-R regulation of Aβ levels is multifarious. When basal AMPA-R activity is antagonized, ISF Aβ decreases by 20%. The same decrease occurs even after action potentials are blocked and evoked synaptic transmission is inhibited, indicating that the basal AMPA-R signaling that increases Aβ levels is likely due to spontaneous transmission. Conversely, application of AMPA via reverse microdialysis stimulates evoked glutamatergic transmission as well as direct AMPA-R activation. In this scenario, AMPA-R activation decreases Aβ levels. This dual effect of AMPA-Rs depending on the mode of transmission has been seen in various contexts. Sara and colleagues (2011) utilized a use-dependent AMPA-R antagonist to show that spontaneous and evoked transmission activate discrete populations of AMPA-Rs. Additionally, several studies have found that receptors that respond differentially to spontaneous and evoked transmission are physically and functionally distinct (Murphy et al., 1994; Sutton et al., 2004, 2006, 2007; Atasoy et al., 2008; Sutton and Schuman, 2009). Intriguingly, spontaneous activity appears to suppress protein synthesis while evoked activity stimulates translation. Another possible explanation is that the effects of AMPA-Rs on Aβ are dependent on relative levels of AMPA-R activation. During basal transmission, a smaller set of AMPA-Rs is active compared to the AMPA-Rs targeted by action potentials or exogenous AMPA treatment.

Extended AMPA treatment decreases ISF Aβ half-life

Adding an additional layer of complexity, exogenous AMPA treatment appears to act on Aβ levels through two different pathways. Within the first 8 hours of treatment, AMPA's ability to modulate Aβ levels is dependent on NMDA-R signaling. This pathway relies on presynaptic

activity to increase glutamatergic transmission, thus stimulating NMDA-R activation on downstream neurons to decrease Aβ production in these cells (Hoey et al., 2009; Verges et al., 2011). The reverse is not true, however; AMPA-Rs do not appear to play a role in NMDA-R-mediated decreases in Aβ. Following longer periods of AMPA treatment, a novel pathway by which AMPA-Rs influence Aβ independently of both presynaptic activity and NMDA-Rs emerges.

As detailed above, studies regarding synaptic and postsynaptic regulation of Aβ have primarily addressed the effects of activity on Aβ production. However, we did not detect changes in APP processing-related gene expression or in APP fragment levels following either 8 or 14 hours of AMPA treatment. Instead, using microdialysis along with a potent inhibitor of ϒ-secretase, we found that treatment with AMPA for 14 hours decreased the half-life of ISF Aβ, implying that AMPA-Rs can modulate Aβ levels through increased clearance. However this effect is accomplished, it does not appear to involve glial recruitment, a broad inflammatory response, or changes in key clearance-related proteins. We did find that one proinflammatory cytokine, IL-6, increased dramatically following AMPA treatment. IL-6 has been shown to have both normal physiological as well as inflammatory, pathological roles in the CNS (Gadient and Otten, 1997; Erta et al., 2012; Gruol, 2015; Wang et al., 2015) and has been shown to increase in response to neuronal depolarization (Sallmann et al., 2000; Juttler et al., 2002). Furthermore, IL-6 signaling has been linked to increased clearance of Aβ through microglial phagocytosis (Chakrabarty et al., 2010; Wang et al., 2015). Given the substantial increase in IL-6 following AMPA treatment, this signaling pathway clearly calls for future study.

Though both production and clearance determine the steady state levels of Aβ in the extracellular space, late-onset AD (LOAD) is primarily characterized by dysfunctions in Aβ

clearance (Mawuenyega et al., 2010; Tarasoff-Conway et al., 2015). In 2003, we found that ISF Aβ half-life as measured by microdialysis is doubled in an aged APP transgenic model compared to young animals (Cirrito et al., 2003). In human studies, metabolic labeling and CNS analysis revealed impaired clearance rates in participants with LOAD, though Aβ production was unaltered (Mawuenyega et al., 2010). Furthermore, many of the genetic factors associated with LOAD are related to clearance, including *APOE, CLU, CR1, and CD33*. Given the evident prominence of Aβ clearance in AD, our results highlight the importance of understanding the ways in which synaptic activity impinges on previous clearance-related studies.

CONCLUSIONS

There are clearly numerous mechanisms that together regulate levels of Aβ. Though the confluence of these various synaptic-mediated pathways appears to result in increased Aβ, we propose that certain postsynaptic signaling pathways, such as those described in these studies, act as protective mechanisms that aid in maintaining Aβ homeostasis. The failure of these Aβ-suppressing pathways may contribute to the breakdown of homeostasis that ultimately results in the build-up of pathology. Indeed, glutamatergic transmission is one of the first systems targeted by toxic species of amyloid as the disease progresses (Olney et al., 1997; Francis, 2003; Lacor et al., 2007; Marcello et al., 2008).

As the dominant excitatory ionotropic receptors in the brain, AMPA-Rs have the potential to greatly influence extracellular Aβ levels and amyloid pathology. We have found that activation of AMPA-Rs initiates a varied and complex response in which opposing pathways act concurrently to regulate Aβ levels. Soluble, monomeric Aβ production is a normal process of

every brain. Even those brains destined to develop AD pathology produce Aβ for decades without formation of toxic aggregates. The point at which Aβ becomes pathogenic is likely influenced by a number of factors, including the loss of homeostatic pathways. Identifying and understanding how, early in our lives, Aβ levels are controlled may give us clues to disease etiology or even prevention.

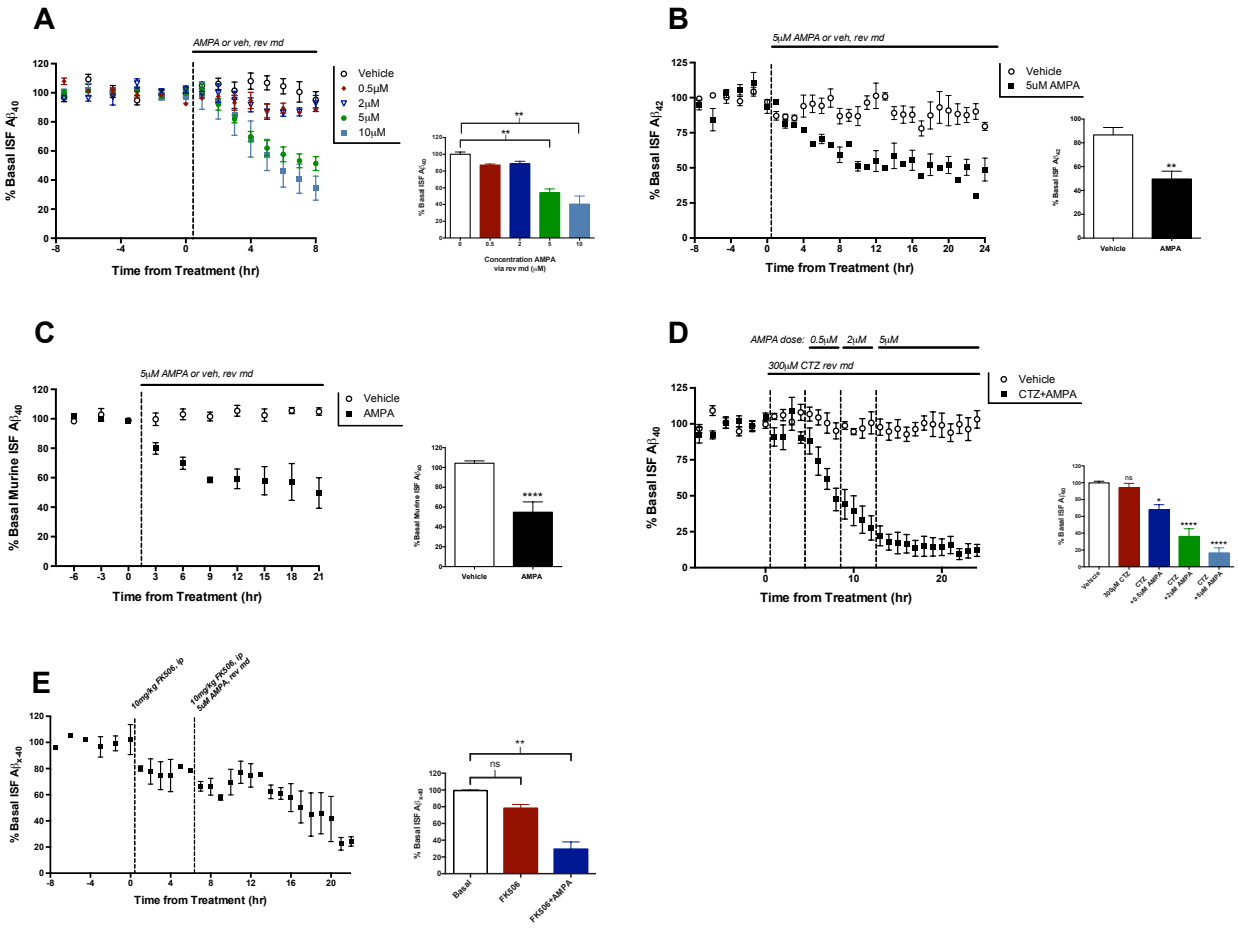

Figure 3.1: AMPA treatment decreases levels of ISF Aβ levels. A) Varying doses of AMPA or vehicle (artificial CSF) were administered to 2-4 month-old APP/PS1 mice via reverse microdialysis (rev md), and changes in interstitial fluid (ISF) $A\beta_{40}$ were measured using ELISA. AMPA has a dose-dependent effect on ISF Aβ levels. Though treatment with 0.5μM and 2μM AMPA did not alter ISF Aβ levels significantly (n=3, n=5 respectively), treatment with 5μM AMPA decreased levels 31.7±9.5% (p=0.015, n=4, one-way ANOVA, Dunnet's *post hoc* test), and 10μM AMPA decreased levels by 73.8±12.2% (p<0.0001, n=2, , one-way ANOVA, Dunnet's *post hoc* test). **B)** APP/PS1 mice (n=4) were treated with 5μM AMPA for 24 hours and ISF $A\beta_{42}$ levels decreased by 37.0±9.4% (p<0.0043, two-tailed t-test). **C)** Wild-type, littermate C3H/B6 mice were dosed with 5μM AMPA using rev md and levels of murine ISF $A\beta_{40}$ levels

decreased by 49.4±8.4% ($p<0.0001$, n=6, two-tailed t-test). **D)** APP/PS1 mice were treated with 300μM cyclothiazide (CTZ) for 4 hours (n=6), after which increasing doses of AMPA (0.5, 2, and 5μM) were added to the perfusion buffer. CTZ administered alone did not change ISF Aβ levels. Aβ levels decreased 31.9±11.1% ($p=0.030$, , one-way ANOVA, Dunnet's *post hoc* test) by 0.5μM AMPA, 63.6±11.1% ($p<0.0001$, , one-way ANOVA, Dunnet's *post hoc* test) by 2μM, and maximally decreased 83.2±11.1% ($p<0.0001$, , one-way ANOVA, Dunnet's *post hoc* test) when treated with 5μM AMPA. **E)** APP/PS1 mice (n=3) were administered FK506 (10mg/kg), a calcineurin inhibitor, via intraperitoneal (i.p.) injection and levels of Aβ were monitored for 6 hours, followed by another i.p. injection of FK506 concurrent with AMPA treatment via reverse microdialysis for 16 hours. Aβ levels did not significantly decrease with FK506 alone ($p=0.148$, one-way ANOVA, Tukey *post hoc* test) but did decrease when additionally treated with AMPA ($p=0.0063$, one-way ANOVA, Tukey *post hoc* test). Data plotted as mean ± SEM.

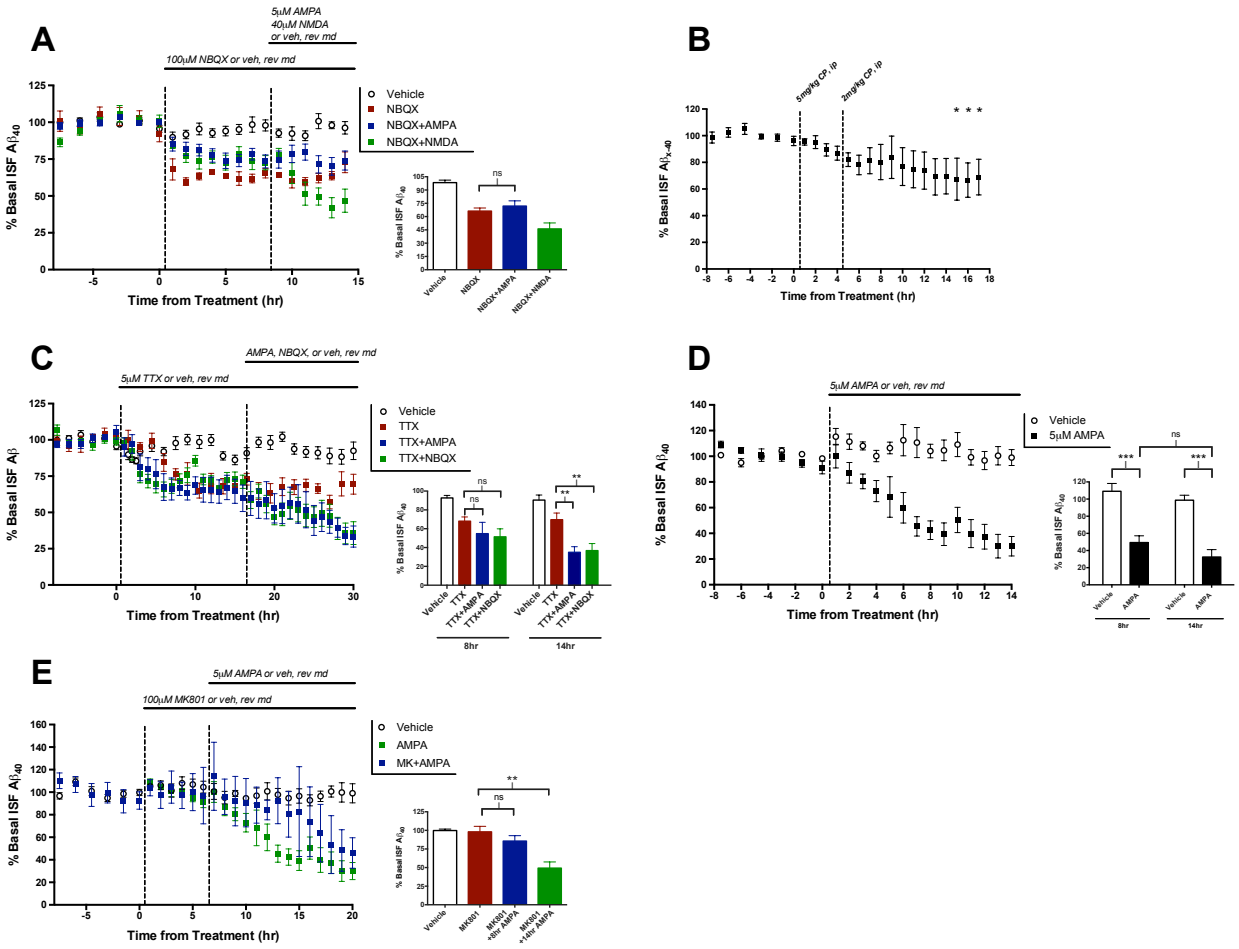

Figure 3.2: AMPA treatment alters Aβ levels through multiple pathways. A) APP/PS1 mice (n=6) were treated with 100μM NBQX, an AMPA receptor antagonist, for 8 hours then co-treated with either 40μM NMDA (n=6), 5μM AMPA (n=7), or vehicle (n=12). After 6 hours of co-treatment with NBQX, the addition of AMPA had no effect on Aβ levels, though NMDA still reduced Aβ by 37.5±3.3% ($p<0.0001$, one-way ANOVA, Bonferroni *post hoc* test). **B)** Mice (n=6) were administered CP465022, a non-competitive AMPA-R antagonist via i.p. injection twice while ISF Aβ was monitored. The first injection (5mg/kg) was given 4 hours before a subsequent 2mg/kg injection. The average of the last 3 hours of treatment was significantly reduced by 29.6±13.1% compared to the average of the last 3 hours of basal collection

(p=0.0475, two-tailed t-test). **C)** Animals (n=6 per group) were treated with 5μM tetrodotoxin (TTX) for 16 hours then co-treated with TTX and either 5μM AMPA, 100μM NBQX, or vehicle for an additional 14 hours. After 8 hours of co-treatment, ISF Aβ levels remained unchanged in all groups. After 14 hours co-treatment with AMPA reduced Aβ levels by 34.6±9.9% (p=0.0027, two-way ANOVA, Sidak *post hoc* test) and co-treatment with NBQX reduced levels by 32.8±9.3% (p=0.0027, two-way ANOVA, Sidak *post hoc* test). **D)** APP/PS1 mice were treated with either 5μM AMPA (n=7) or vehicle (n=5) for 14 hours, leading to a decrease in ISF Aβ levels of 66.3±11.8% (p=0.0001, two-way ANOVA, Sidak *post hoc* test). **E)** 100μM MK801 was administered by reverse microdialysis for 6 hours to APP/PS1 mice followed by co-administration with 5μM AMPA or vehicle, which lead to a decrease in ISF Aβ levels of 48.8±10.0% (p=0.0013; n=5, one-way ANOVA, Tukey *post hoc* test). Data plotted as mean ± SEM.

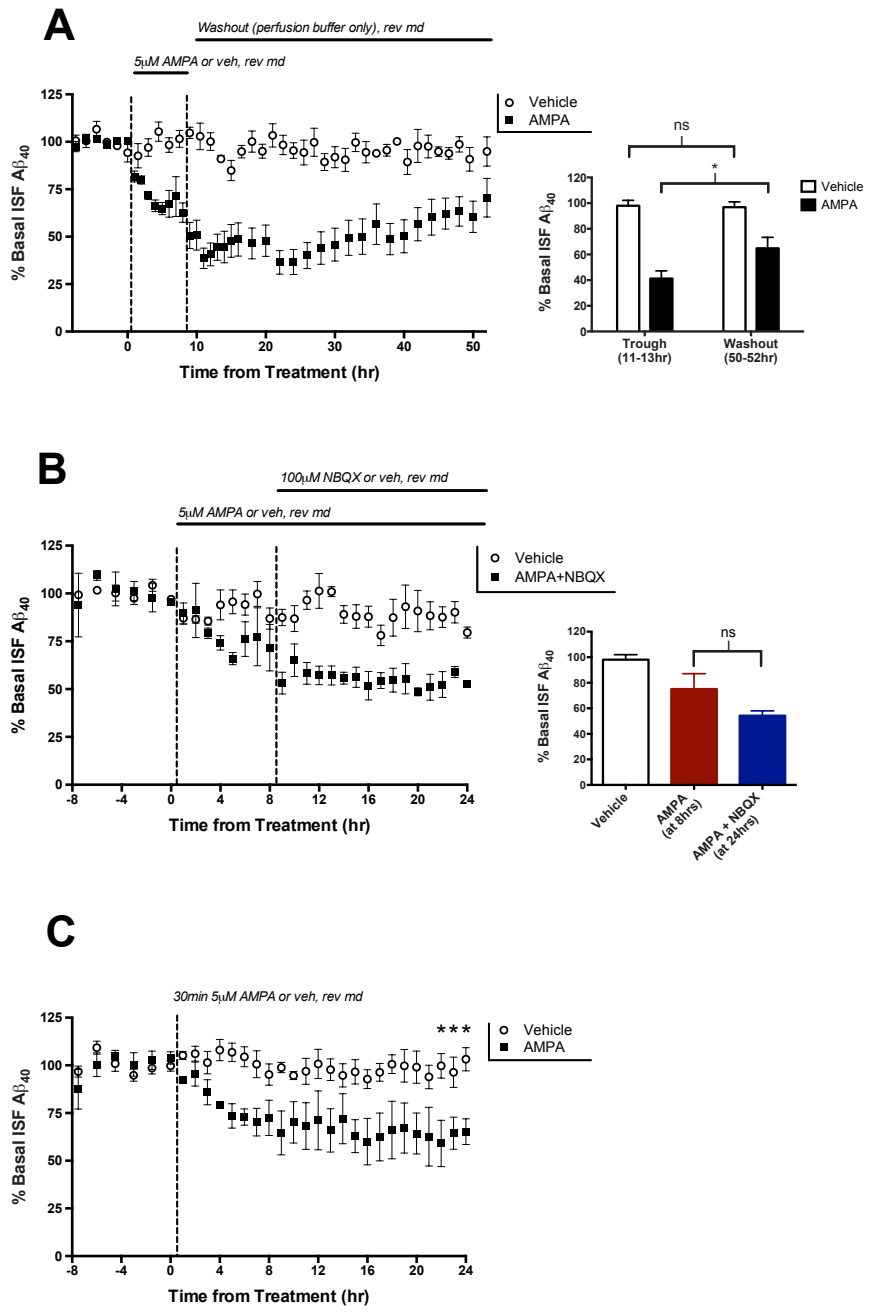

Figure 3.3: AMPA treatment results in potent, long-lasting decreases in ISF Aβ levels that slowly recover. A) APP/PS1 mice (n=5) were treated with 5μM AMPA using reverse microdialysis for 8 hours resulting in a decrease in ISF Aβ levels of 32.7±3.0% from baseline. After 8 hours, AMPA was removed from the microdialysis perfusion buffer. Aβ levels continued

to decline for 3 hours post-treatment to reach a maximum reduction of 56.7±1.7% from baseline. For the next 40 hours, ISF Aβ levels gradually increased. When the experiment was ended at 52 hours, ISF Aβ levels had increased 23.5±3.0% to reach 64.8±3.0% of basal levels, which was a significant increase from the lowest Aβ levels post-treatment (p=0.0245, two-way ANOVA, Sidak *post hoc* test). **B)** APP/PS1 mice (n=3) were treated with 5μM AMPA followed by co-treatment with AMPA and 100μM NBQX for 14 hours. The addition of NBQX did not alter the decrease in Aβ levels caused by AMPA treatment (one-way ANOVA, Sidak *post hoc* test). **C)** 5μM AMPA was infused by rev md into APP/PS1 mice for a 30-minute period, after which the syringe was replaced with artificial CSF for 24 hours. AMPA treatment caused a 41.30±9.45% decrease in ISF Aβ levels in the 22-24 hours after 30-minute dosage (n=3, p=0.035, two-tailed t-test). Data plotted as mean ± SEM.

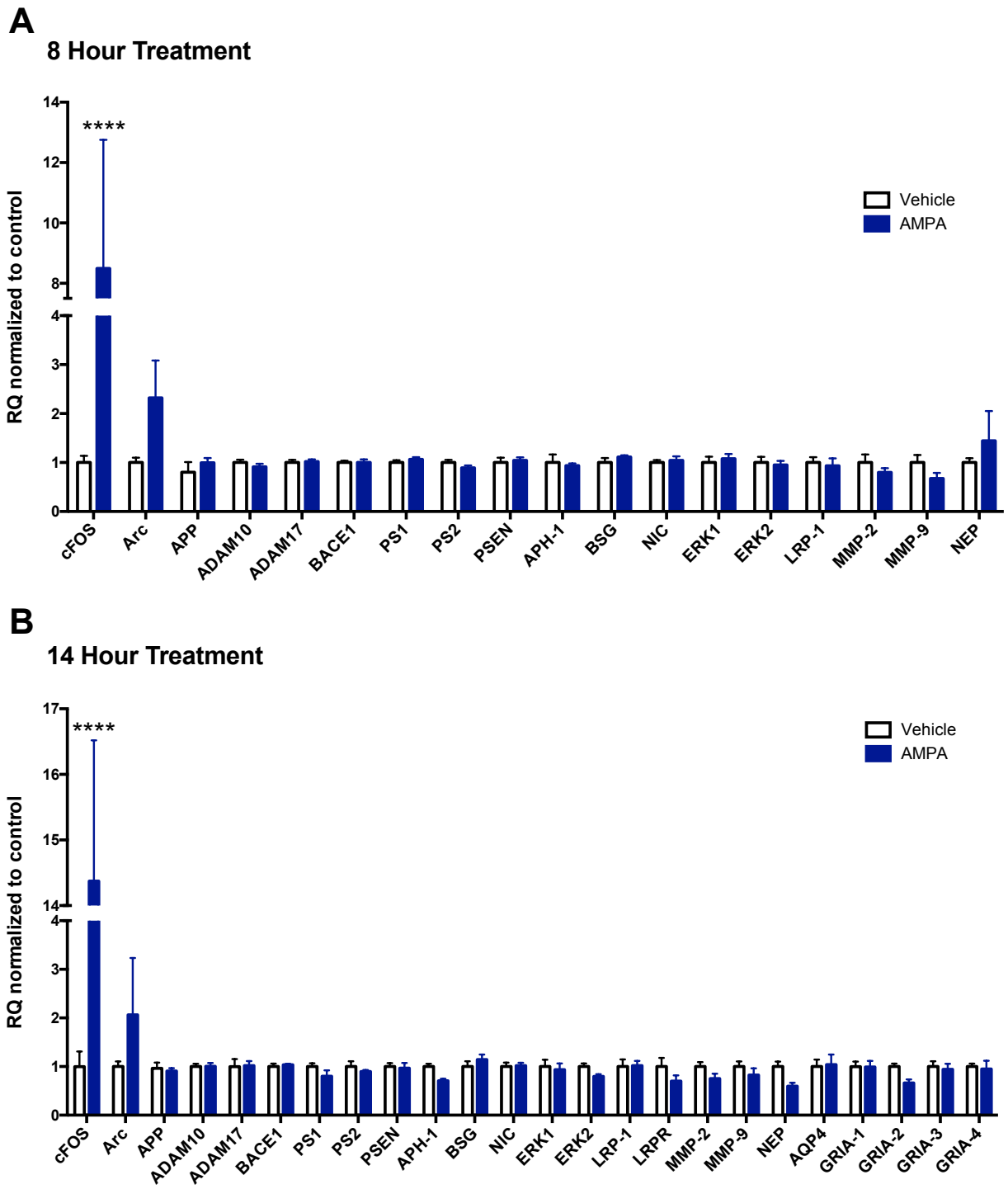
A
8 Hour Treatment
RQ normalized to control
****
Vehicle
AMPA
cFOS
Arc
APP
ADAM10
ADAM17
BACE1
PS1
PS2
PSEN
APH-1
BSG
NIC
ERK1
ERK2
LRP-1
MMP-2
MMP-9
NEP
B
14 Hour Treatment
RQ normalized to control
****
Vehicle
AMPA
cFOS
Arc
APP
ADAM10
ADAM17
BACE1
PS1
PS2
PSEN
APH-1
BSG
NIC
ERK1
ERK2
LRP-1
LRPR
MMP-2
MMP-9
NEP
AQP4
GRIA-1
GRIA-2
GRIA-3
GRIA-4

Figure 3.4: 8 and 14 hour AMPA treatment does not alter expression of genes related to Aβ metabolism. 5μM AMPA or vehicle was given to 2-4 month old APP/PS1 mice for 8 hours **(A)** or 14 hours **(B**; n=6 per group) before the hippocampal tissue surrounding the microdialysis probe was collected and analyzed with quantitative PCR. **A)** qPCR analysis revealed no differences in expression for major genes involved in Aβ production and clearance between mice treated with AMPA or vehicle. Expression of *cFos*, a marker for neuronal activity, increased 7.5±3.7 fold ($p<0.0001$, two-way ANOVA, Sidak *post hoc* test) for the AMPA-treated group over *cFos* expression in controls, though this difference was not significant. **B)** After 14 hours of AMPA treatment, expression of genes involved in Aβ processing was not changed as shown by qPCR analysis. AMPA-treated animals showed a 14.4±1.8 fold increase in *cFos* expression over controls ($p<0.0001$, two-way ANOVA, Sidak *post hoc* test). Data plotted as mean ± SEM.

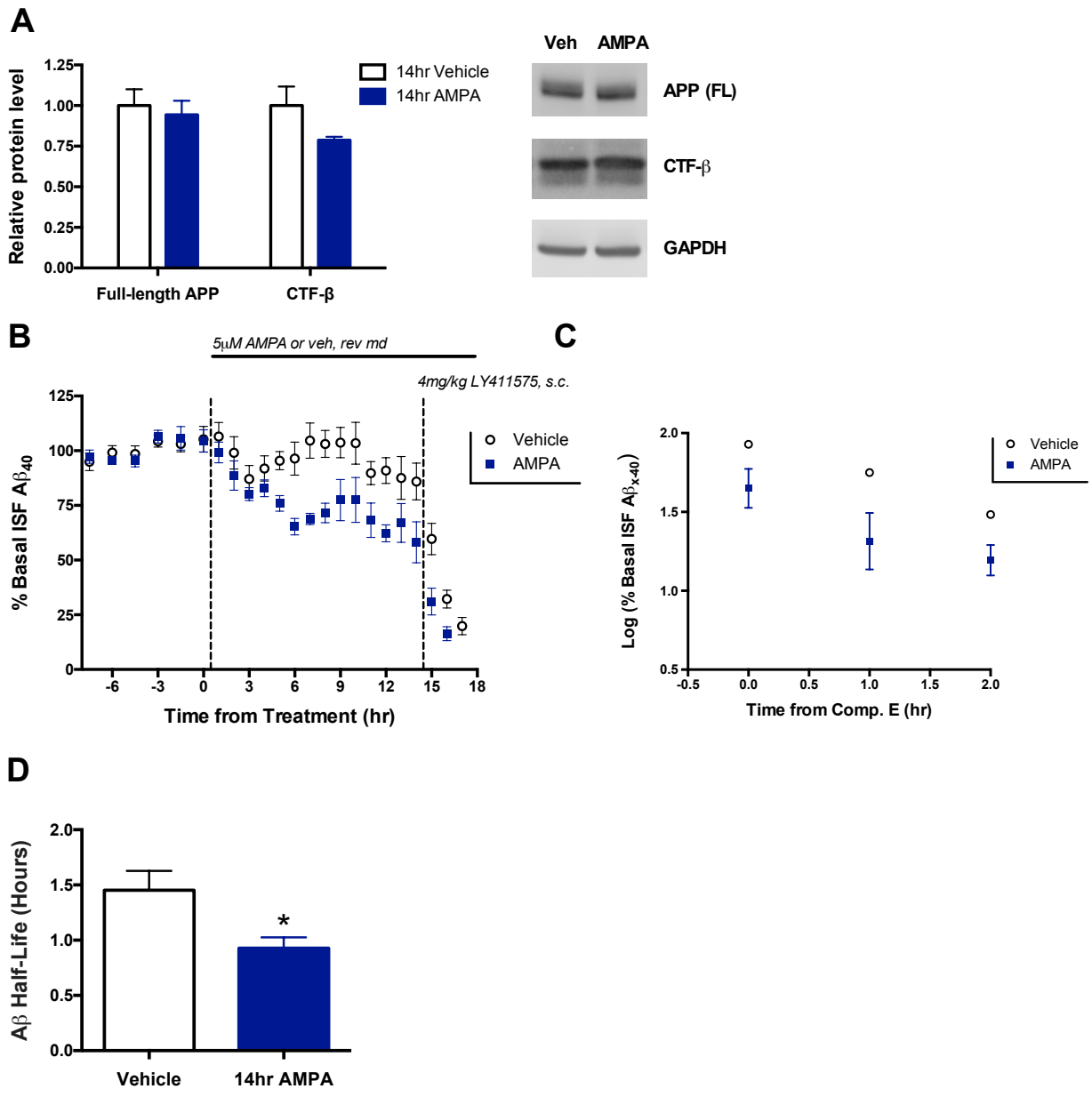

Figure 3.5: Extended treatment with AMPA decreases Aβ levels through clearance, not production. **A)** 2-4 month old APP/PS1 mice were treated with either 5μM AMPA (n=6) or aCSF (n=8) via reverse microdialysis for 14 hours. Tissue surrounding the microdialysis probe was analyzed via Western blot for full-length APP and β-CTF, and no significant change was observed between treatment groups (two-way ANOVA, Sidak *post hoc* test). Bands were

normalized to GAPDH and displayed relative to control. Blot images are representative examples. **B)** APP/PS1 mice were treated with 14 hours of AMPA (n=6) or vehicle (n=7). With microdialysis collection ongoing, animals were administered a 4mg/kg subcutaneous (s.c.) injection of LY411575, a ϒ-secretase inhibitor, or vehicle (corn oil). **C)** The log of the last three microdialysis samples collected following LY411575 treatment were plotted in order to calculate ISF Aβ half-life. **D)** ISF Aβ half-life for each treatment group was calculated by taking the slope of the semi-log plot of concentration versus time for the time points between drug delivery and the plateauing of Aβ concentrations. Mice treated with 5μM AMPA had an Aβ half-life of 0.9±0.1 hours compared to a half-life of 1.5±0.2 hours for the mice treated with aCSF ($p=0.0298$, two-tailed t-test). Data plotted as mean ± SEM.

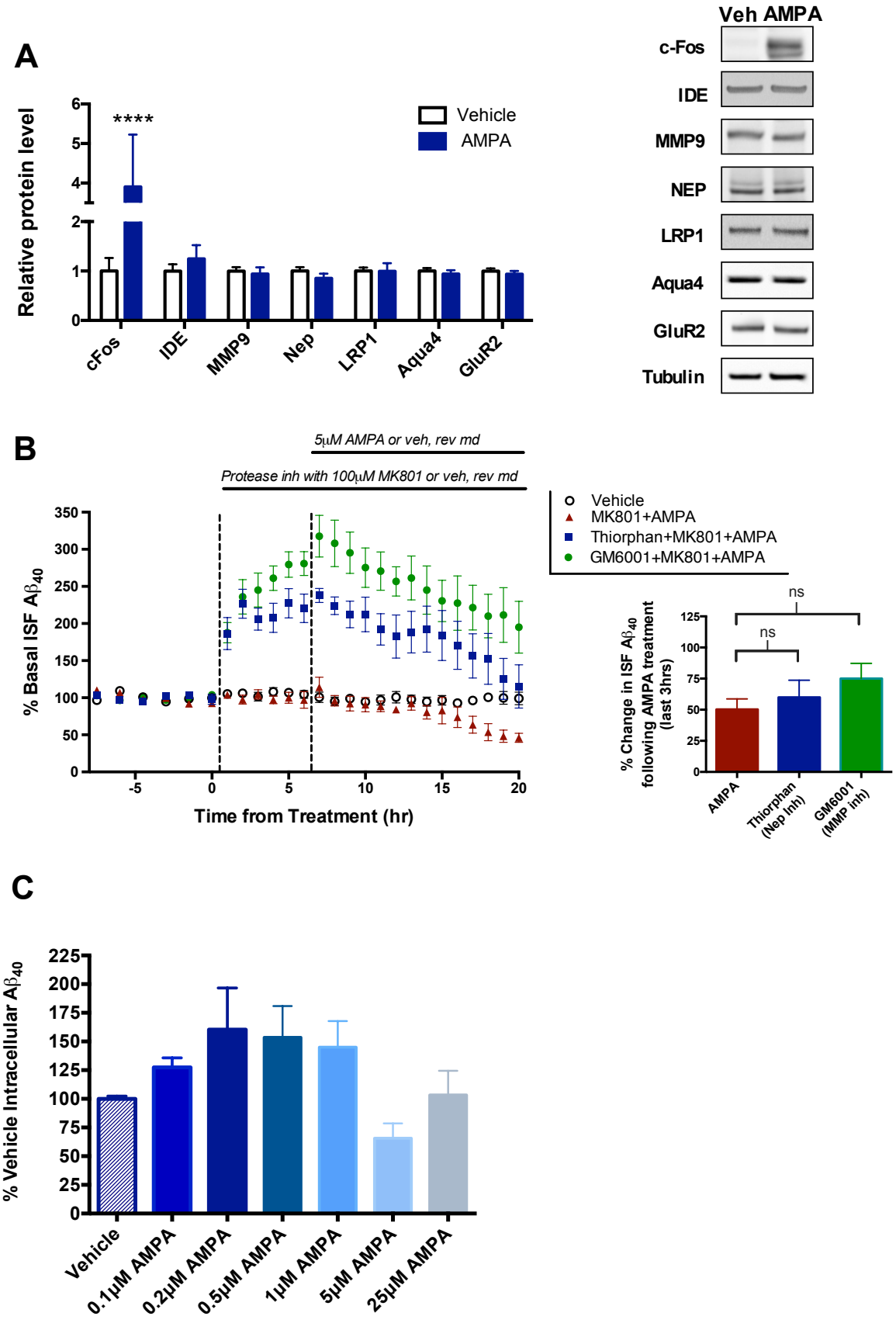
A
Relative protein level
****
Vehicle
AMPA
cFos
IDE
MMP9
Nep
LRP1
Aqua4
GluR2
Veh AMPA
c-Fos
IDE
MMP9
NEP
LRP1
Aqua4
GluR2
Tubulin
B
5μM AMPA or veh, rev md
Protease inh with 100μM MK801 or veh, rev md
% Basal ISF Aβ40
Time from Treatment (hr)
Vehicle
MK801+AMPA
Thiorphan+MK801+AMPA
GM6001+MK801+AMPA
% Change in ISF Aβ40 following AMPA treatment (last 3hrs)
ns
ns
AMPA
Thiorphan (Nep Inh)
GM6001 (MMP inh)
C
% Vehicle Intracellular Aβ40
Vehicle
0.1μM AMPA
0.2μM AMPA
0.5μM AMPA
1μM AMPA
5μM AMPA
25μM AMPA

Figure 3.6: AMPA-mediated decrease in Aβ not due to changes in clearance-related proteins or proteases. A) 2-4 month old APP/PS1 mice were treated with either 5μM AMPA (n=6) or aCSF (n=8) via reverse microdialysis for 14 hours. Tissue surrounding the microdialysis probe was analyzed via Western blot to determine levels of proteins involved in Aβ elimination and clearance. Bands were normalized to GAPDH and displayed relative to control. Blot images are representative examples. cFos protein expression was increased 2.9±0.4 fold ($p<0.0001$, two-way ANOVA, Sidak *post hoc* test) in the AMPA group compared to the controls. No other proteins showed a significant difference between treatment groups. **B)** Reverse microdialysis was used to treat APP/PS1 mice (n=7) with 10μM thiorphan (neprilysin inhibitor), 25μM GM6001 (broad-spectrum MMP inhibitor), or vehicle for 6 hours, followed by 14 hours of co-treatment with 5μM AMPA. The Aβ concentrations in the last 3 hours of each treatment were averaged and the differences between the end of inhibitor/vehicle treatment and after the addition of AMPA were compared. Inhibiting protease activity with thiorphan or GM6001 did not alter the decrease in ISF Aβ levels observed following AMPA treatment ($p=0.40$, one-way ANOVA, Dunnet's *post hoc* test). **C)** BV2 microglial cells were treated with various doses of AMPA (0.1μM-25μM) for 14 hours, followed by a 4 hour co-incubation with AMPA and 500nM recombinant HFIP-$A\beta_{40}$. Cells were lysed and internalized Aβ was measured with ELISA. Treatment with AMPA did not affect the amount of Aβ taken up by the BV2 cells ($p=0.30$, one-way ANOVA, Dunnett *post hoc* test). Data plotted as mean ± SEM.

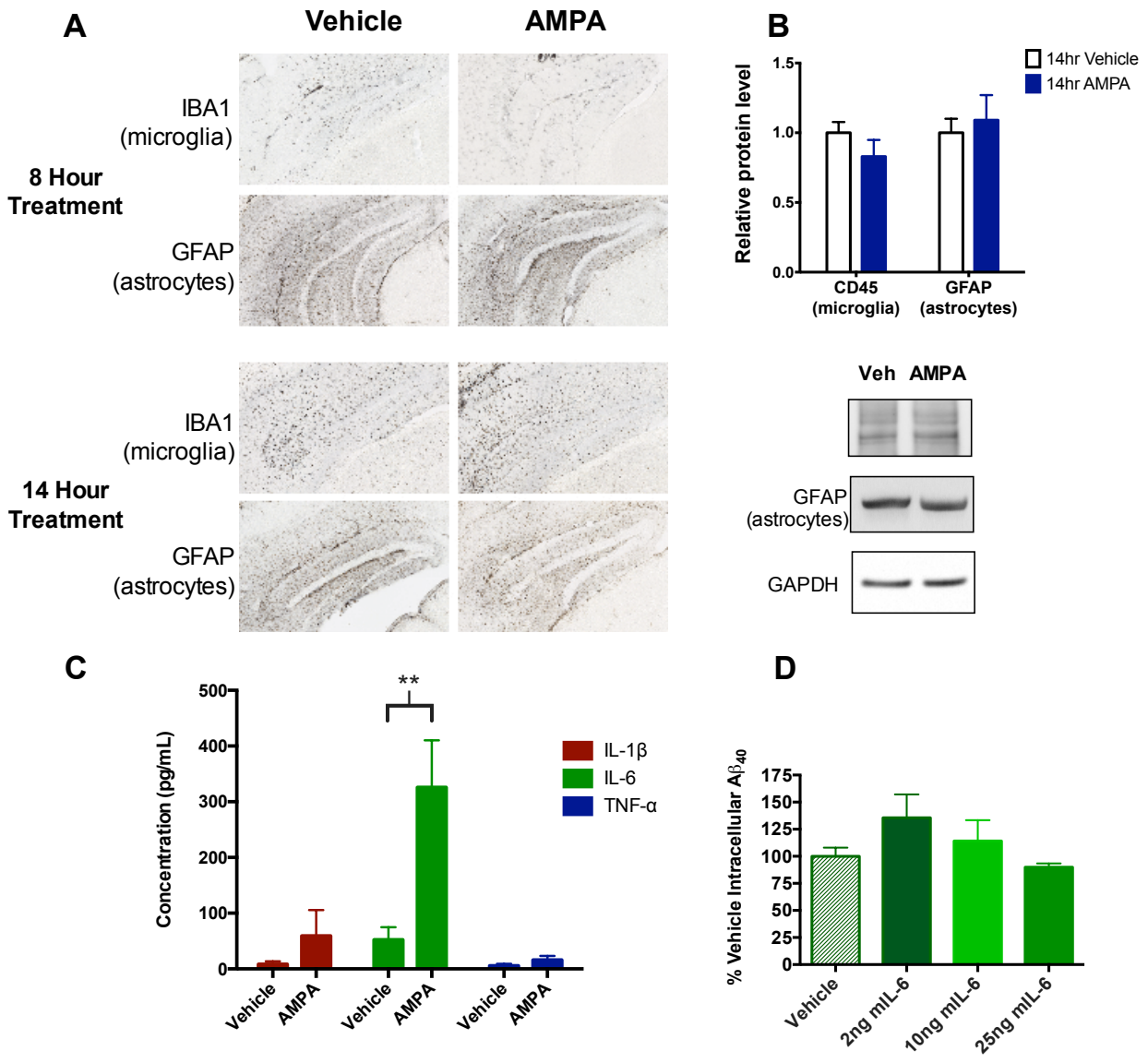

Figure 3.7: Glial recruitment unchanged and IL-6 levels enhanced following AMPA treatment. A) Wild-type C3H/B6 mice (for the 8 hour treatment, n=6 per group) or APP/PS1 mice (for the 14 hour treatment, n=3 per group) were implanted with microdialysis probes and treated with either 5μM AMPA or aCSF for 8 or 14 hours. Brain sections were immunostained with DAB using anti-GFAP antibody to mark astrocytes or anti-Iba1 antibody to mark microglia. Immunoreactivity between control and AMPA-treated sections were compared, and representative images are shown. **B)** 2-4 month old APP/PS1 mice were treated with either 5μM

AMPA (n=6) or aCSF (n=8) via reverse microdialysis for 14 hours. Tissue surrounding the microdialysis probe was analyzed via Western blot for GFAP or CD45, markers of astrocytes and microglia, respectively, and no difference was observed between treatment groups (two-way ANOVA, Sidak *post hoc* test). Bands were normalized to GAPDH and displayed relative to control. Blot images are representative examples. **C)** As in Fig. 7B, APP/PS1 mice were treated with either 5μM AMPA (n=9) or vehicle (n=7) for 14 hours, and hippocampal lysates were analyzed for pro-inflammatory cytokines using a MSD multiplex assay. Levels of IL-1β ($p=0.991$, two-way ANOVA, Sidak *post hoc* test) and TNF-α ($p=0.999$, two-way ANOVA, Sidak *post hoc* test) were unchanged. IL-6 levels were significantly elevated following AMPA treatment, increasing from 52.3 to 773.8pg/mL ($p=0.0014$, two-way ANOVA, Sidak *post hoc* test). **D)** BV2 microglial cells were treated with various doses of recombinant mouse IL-6 (2-25ng) for 14 hours, followed by a 4 hour co-incubation with IL-6 and 500nM recombinant HFIP-$A\beta_{40}$. Cells were lysed and internalized Aβ was measured with ELISA. Treatment with IL-6 did not affect the amount of Aβ taken up by the BV2 cells ($p=0.352$, one-way ANOVA, Dunnett *post hoc* test). Data plotted as mean ± SEM.

Chapter 4

Conclusions and Future Directions

CONCLUSIONS

Homeostatic regulation of brain Aβ levels is of upmost importance when considering AD pathogenesis. Disruption of any of the fine-tuned controls that constantly strive to keep Aβ in check could tip the scales toward amyloid pathology. Synaptic activity is known to be an important regulator of the production of Aβ, through both pre- and postsynaptic mechanisms. Studies have found that presynaptic activity drives Aβ production while postsynaptic receptor activation has a more nuanced role. The goal of the experiments described herein was to explore the regulation of Aβ levels by postsynaptic glutamatergic transmission through NMDA- and AMPA-R activity. These questions were addressed *in vivo* using adult APP/PS1 mouse models of AD to maintain an intact network of connections throughout the experiments.

We sought to define the route through which high levels of NMDA-R activation leads to decreased production of Aβ through ERK activation with the hopes of identifying a suitable target for therapeutic intervention. We first investigated the individual contributions of the GluN2A and GluN2B subunits of NMDA-Rs as these subunits have been found to give the receptor unique signaling properties and cellular roles (Hardingham, 2006; Zhang and Luo, 2013). Using subunit-specific NMDA-R antagonists, we showed that blocking either type of receptor was insufficient to prevent NMDA treatment from decreasing Aβ levels in the ISF, which could only be accomplished by the noncompetitive NMDA-R channel blocker MK801 (Fig. 2.1). These results indicate that neither a particular receptor subunit is necessary for Aβ regulation by NMDA-Rs nor is the activation of a full population of NMDA-Rs. Next, we used virally driven shRNA against either ERK1 or ERK2 to knockdown expression of each ERK isoform in the hippocampus. As with the NMDA-R subunits, we found no specificity in NMDA-R regulation of Aβ levels (Fig. 2.2).

Again in an effort to find a selective target behind the NMDA-R-mediated decrease in Aβ production, we inhibited a number of signaling molecules known to link NMDA-R activation to ERK phosphorylation using pharmacological antagonists. With this method, we found that NMDA-Rs do not act on ERK and then Aβ through signaling to CaMKII, PKC, or PKA (Fig. 2.3). Though we ultimately failed to define the pathway linking NMDA-R activation to Aβ regulation, we were able to rule out a number of possibilities that will be useful when considering postsynaptic activity's link to the maintenance of Aβ homeostasis.

Knowing that NMDA-Rs have the capability to largely influence Aβ levels, we turned our attention to the study of AMPA-R activation and Aβ regulation in Chapter 3. Though we initially hypothesized that AMPA treatment would increase Aβ levels through synaptic activity-related, presynaptic acceleration of APP processing, we found that the regulation of Aβ by AMPA-Rs is quite complex and involves at least three different pathways. First, endogenous AMPA-R activity, as targeted by AMPA-R antagonism, enhanced ISF Aβ levels (Fig. 3.2A). Again, we believed this to be due to increased activity. However, the effect was seen even after action potentials were blocked with tetrodotoxin, ruling out this explanation (Fig. 3.2C). With evoked neurotransmitter release prohibited, the only AMPA-Rs activation remaining to influence Aβ levels must be caused by spontaneous release. The concept that spontaneous glutamate release might precipitate a cellular response independent of evoked transmission is not new. In fact, a number of studies have shown that spontaneous release can have effects distinct from evoked release by activating spatially segregated postsynaptic targets (Sutton et al., 2006, 2007; Atasoy et al., 2008; Sutton and Schuman, 2009; Kavalali et al., 2011; Sara et al., 2011; Kavalali, 2014). Indeed, spontaneously activated AMPA-Rs have an important role in maintaining dendritic spine density through signaling that does not require evoked transmission (McKinney

et al., 1999). Our results indicate that increasing Aβ levels may be another independent role for spontaneous AMPA-ergic signaling.

The two remaining pathways we identified by which AMPA-Rs regulate Aβ levels are the result of evoked glutamatergic transmission. Using reverse microdialysis to bath hippocampal cells with AMPA, we found that increasing doses of AMPA decreased ISF Aβ levels in a dose-dependent manner (Fig. 3.1A). This was managed in part by an overall increase in glutamatergic signaling, resulting in an action potential-dependent activation of NMDA-Rs and subsequent NMDA-R-dependent decrease in Aβ production (Fig. 3.2C,E; Verges et al., 2011). Much of this pathway is already described in previous publications and in Chapter 2. Downstream activation of NMDA-Rs, however, was not the only method by which AMPA treatment decreased Aβ levels. We found that prolonged treatment with AMPA resulted in decreased Aβ even with NMDA-Rs or action potentials blocked (Fig. 3.2C-E). Furthermore, this decrease was shown to be the result of enhanced Aβ clearance, not decreased production as we hypothesized. How clearance is targeted is still unanswered, although we have data to suggest that it is not through changes in levels of clearance-related proteins (Fig. 3.6A) or through increased proteolytic activity of neprilysin or MMPs (Fig. 3.6B).

That AMPA-R activation is capable of altering Aβ clearance is a surprising finding because the vast majority, if not all, other studies have linked synaptic activity to the regulation of Aβ through changes in Aβ production (Kamenetz et al., 2003; Buckner et al., 2005; Cirrito et al., 2005b, 2008, 2011; Jones et al., 2008; Hoey et al., 2009, 2013; Bordji et al., 2010; Kim et al., 2010; Tampellini et al., 2010b; Verges et al., 2011; Fisher, 2012; Das et al., 2013; Sheline et al., 2014; Tampellini, 2015; Fisher et al., 2016). Amyloid-β clearance, however, has been found to have particular importance in the etiology of late-onset AD (LOAD). Studies in both animals

models and humans have observed impaired clearance, rather than production, with age and disease (Cirrito et al., 2003; Mawuenyega et al., 2010; Tarasoff-Conway et al., 2015). Furthermore, the *APOEε4* allele, the strongest genetic risk factor for LOAD, is associated with impaired Aβ clearance (Castellano et al., 2011), as are many of the lesser genetic risk factors identified through GWAS (e.g. *CD33*, *CLU*, *CR1*, *PICALM*, and *BIN1*; for review see Tanzi, 2012). These data raise the interesting possibility that alterations in synaptic activity and specifically AMPA-R signaling may be playing a role in the observed deficits in clearance that are so prevalent in LOAD.

Because AMPA-Rs are the most numerous excitatory receptors in the brain and the major mediators of basal excitatory transmission, their ability to enhance Aβ clearance could have profound implications. Evidence from rodent studies suggests that AMPA-R expression decreases with age, which could contribute to a loss of Aβ homeostasis if AMPA-R regulation becomes dysregulated (Shi et al., 2007; Gocel and Larson, 2013; Pandey et al., 2015). Furthermore, many studies have found that Aβ exposure downregulates AMPA-R expression, possibly contributing to a feed-forward increase in amyloid pathology (Chang et al., 2006; Hsieh et al., 2006; Liu et al., 2010; Miñano-Molina et al., 2011; Chater and Goda, 2014; Guntupalli et al., 2016a). Moreover, these results could implicate AMPA-R activity and changes in Aβ clearance to the finding that amyloid pathology is most severe in brain regions exhibiting the highest levels of synaptic activity (Raichle et al., 2001; Buckner et al., 2005, 2009). AMPA-R regulation of Aβ levels has the potential to significantly impact Aβ homeostasis and clearly merits further study.

FUTURE DIRECTIONS

When addressing such a broad topic as "glutamatergic regulation of Aβ," there are naturally numerous lines of study yet to be undertaken. I will describe those most pertinent to the results discussed in this document.

NMDA-R signaling and Aβ production

In my second chapter, I described my attempts to define the signaling pathway linking NMDA-R signaling to ERK activation and decreased Aβ production. Though I was able to eliminate a number of possibilities, I did not manage to identify a single part of the pathway that could act as a desirable target for therapeutics. Likely unexplored candidates by which NMDA-Rs signal to activate ERK are Ras-specific guanine nucleotide-releasing factor 1 and 2 (RasGRF1,2), highly homologous guanine nucleotide exchange factors (GEFs), that have been shown to directly couple NMDA-Rs to ERK (Krapivinsky et al., 2003; Tian et al., 2004; Hardingham, 2006; Ivanov et al., 2006b; Li et al., 2006; Vantaggiato et al., 2006; Bengtson et al., 2008; Feig, 2011). Though no pharmacological inhibitor exists for RasGRFs, the role of RasGRF1,2 in linking NMDA-R activation to Aβ regulation could be tested by knocking down expression of either protein using RNA interference, then monitoring the effects of NMDA treatment on ISF Aβ levels, similar to the approach used in Fig2.2. Also available are a number of mouse lines generated with either or both RasGRF1 or 2 deleted (Brambilla et al., 1997; Itier et al., 1998; Giese et al., 2001; Fernández-Medarde et al., 2002; Tian et al., 2004). These mice could be treated with NMDA to gauge if the effect on Aβ is still present without RasGRF signaling, or they could be crossbred with APP/PS1 mice to determine the impact of the deletion on amyloid pathology.

Astrocytic regulation of glutamatergic transmission

Previous findings along with the results discussed herein demonstrate the roles of both NMDA-Rs and AMPA-Rs in regulating Aβ levels. Within a functional tripartite synapse, the amount of NMDA-R and AMPA-R activation is carefully regulated through the uptake of glutamate from the extracellular space by astrocytes. Astrocytic function, therefore, likely plays an important role in glutamatergic Aβ regulation. Intriguingly, studies using both AD human tissue and AD animal models show irregular astrocytic glutamate uptake associated with amyloid pathology (Cross et al., 1987; Scott et al., 2002; Begni et al., 2004; Matos et al., 2008). Astrocytic uptake of glutamate is accomplished primarily through the two main astrocytic excitatory amino acid transporters (EAATs), EEAT1 and EAAT2 (Rothstein et al., 1996; Lehre and Danbolt, 1998). Manipulating EAAT activity either pharmacologically or genetically could mimic the changes in astrocytic glutamate uptake observed in AD, and changes in the effects of NMDA-R and AMPA-R activation on Aβ levels could be measured. How aberrant astrocytic glutamate uptake affects the regulation of Aβ by both NMDA-Rs and AMPA-Rs could yield insights into the break down of normal homeostatic mechanisms during the disease process.

AMPA-Rs, IL-6, and Aβ regulation

As described in chapter 3, we found that AMPA-R signaling enhances clearance of Aβ from the ISF. How this process is accomplished, however, is still largely unanswered. In searching for an inflammatory response following extended AMPA treatment, we found that levels of the proinflammatory cytokine IL-6 were greatly increased in mice treated with AMPA (Fig. 3.7C). Because neither IL-1β nor TNF-α were altered, AMPA appears to selectively act on IL-6 instead of creating a mass inflammatory response. This is of interest due to studies showing

that IL-6 signaling can increase clearance of Aβ through microglial phagocytosis (Chakrabarty et al., 2010; Wang et al., 2015). Overexpression of IL-6 in the brains of either neonatal or adult AD mouse models decreased plaque burden, though APP levels, APP processing, and steady-state Aβ generation were unchanged (Chakrabarty et al., 2010). In general, activated microglia exhibiting the M2 phenotype remove Aβ deposits from the extracellular space and have been shown to play a beneficial role in neurodegenerative diseases (Ries and Sastre, 2016; Tang and Le, 2016). IL-6 is known to be released in response to neuronal depolarization, explaining how AMPA treatment might lead to its increase (Sallmann et al., 2000; Juttler et al., 2002). We hypothesize that AMPA-R activation leads to IL-6 release, thereby stimulating microglial uptake of Aβ from the extracellular space. We are engaged in experiments that aim to block IL-6 signaling to determine its role in AMPA-R-mediated Aβ clearance *in vivo*. Another approach would be to test Aβ uptake in mixed primary cultures of both microglia and neurons in response to AMPA treatment.

Other mechanisms of AMPA-R-mediated Aβ regulation

IL-6 signaling is not the only candidate by which AMPA-Rs alter Aβ clearance. The low-density lipoprotein receptor-related protein 1 (LRP1), is an endocytic receptor expressed on neurons, vascular cells, and glia (Kanekiyo and Bu, 2014). LRP1 can directly bind Aβ and facilitate its transport from the extracellular space. Indeed, LRP1 has been linked to neuronal Aβ uptake (Kanekiyo et al., 2013), microglial Aβ phagocytosis (Kanekiyo et al., 2011; N'Songo et al., 2013), astrocytic Aβ uptake (Liu et al., 2017), and transcytosis across the endothelial cells of blood brain barrier (BBB; Deane et al., 2004; Kanekiyo et al., 2012; Storck et al., 2015). Mice with conditional, cell-specific LRP1 deletion have been generated, and could be used to

determine if AMPA-Rs regulate Aβ levels through LRP1 signaling. Alternatively, LRP1 binding to Aβ could be prohibited using an LRP1 blocking antibody.

The mechanism by which Aβ is degraded once it is taken up into neurons or glial cells has not been extensively defined. Microglial cultures can degrade phagocytosed Aβ through the autophagic pathway (Cho et al., 2014) and require lysosomal acidification (Majumdar et al., 2011). Lysosomal Aβ degradation has also been observed within neurons in AD animal models (Li et al., 2012; Xiao et al., 2014, 2015). If AMPA treatment does indeed increase cellular uptake of Aβ as we predict, then it is likely that lysosomal activity is increased following AMPA-R activation. One method to test this hypothesis is to quantify the colocalization of lysosomal proteins with Aβ using immunohistochemistry. Additionally, lysosomal activity could be blocked with cathepsin inhibitors.

Finally, we found that basal levels of AMPA-R activation normally act to increase ISF Aβ levels in the hippocampus (Fig. 3.2A,B) in a manner that does not rely on action potentials (Fig. 3.2C). We concluded that miniature, spontaneous events must drive increased Aβ through AMPA-R signaling. There are many follow-up questions raised by these findings. First, how do AMPA-Rs increase Aβ, through production or clearance? Also, does the magnitude or direction of basal AMPA-R regulation of Aβ change with age or disease status? What mediates the opposing effects of AMPA-R activation resulting from spontaneous or evoked transmission? Does the effect on Aβ levels simply rely on the number of AMPA-Rs activated, or is each type of transmission acting on a specific population of receptors? Could Aβ clearance through evoked AMPA-R signaling be simulated with the induction of long-term potentiation? The answers to these questions would fill their own dissertation and would help us further understand the interplay between normal brain functioning and Aβ regulation.

CLOSING REMARKS

The loss of Aβ homeostasis is a crucial event in AD pathogenesis, occurring decades before symptom development. As we learn more about AD pathology, a multitude of mechanisms working to keep Aβ levels in check have become apparent, with synaptic activity key among them. Even within this one category is a diversity of pathways. In this dissertation, we have explored the regulation of Aβ by NMDA- and AMPA-Rs, the receptors responsible for the majority of excitatory transmission and synaptic plasticity. By doing so, we have sought to understand how the normal workings of the brain may slowly and subtly set the stage for the amyloid cascade. By defining the mechanisms that constantly influence Aβ production and clearance, we can begin to pinpoint the factors responsible for AD pathogenesis and develop therapeutics against them.

REFERENCES

Arriagada PV, Growdon JH, Hedley-Whyte ET, Hyman BT (1992) Neurofibrillary tangles but not senile plaques parallel duration and severity of Alzheimer's disease. Neurology 42:631–639.

Atasoy D, Ertunc M, Moulder KL, Blackwell J, Chung C, Su J, Kavalali ET (2008) Spontaneous and evoked glutamate release activates two populations of NMDA receptors with limited overlap. J Neurosci 28:10151–10166.

Bading H, Greenberg ME (1991) Stimulation of protein tyrosine phosphorylation by NMDA receptor activation. Science 253:912–914.

Bakker ENTP, Bacskai BJ, Arbel-Ornath M, Aldea R, Bedussi B, Morris AWJ, Weller RO, Carare RO (2016) Lymphatic Clearance of the Brain: Perivascular, Paravascular and Significance for Neurodegenerative Diseases. Cell Mol Neurobiol 36:181–194.

Banko JL, Hou L, Klann E (2004) NMDA receptor activation results in PKA- and ERK-dependent Mnk1 activation and increased eIF4E phosphorylation in hippocampal area CA1. J Neurochem 91:462–470.

Baranello RJ, Bharani KL, Padmaraju V, Chopra N, Lahiri DK, Greig NH, Pappolla MA, Sambamurti K (2015) Amyloid-beta protein clearance and degradation (ABCD) pathways and their role in Alzheimer's disease. Curr Alzheimer Res 12:32–46.

Bateman RJ et al. (2012) Clinical and Biomarker Changes in Dominantly Inherited Alzheimer's Disease. N Engl J Med 367:795–804.

Beattie EC, Carroll RC, Yu X, Morishita W, Yasuda H, von Zastrow M, Malenka RC (2000) Regulation of AMPA receptor endocytosis by a signaling mechanism shared with LTD. Nat Neurosci 3:1291–1300.

Begni B, Brighina L, Sirtori E, Fumagalli L, Andreoni S, Beretta S, Oster T, Malaplate-Armand C, Isella V, Appollonio I, Ferrarese C (2004) Oxidative stress impairs glutamate uptake in fibroblasts from patients with Alzheimer's disease. Free Radic Biol Med 37:892–901.

Bell RD, Sagare AP, Friedman AE, Bedi GS, Holtzman DM, Deane R, Zlokovic B V (2007) Transport pathways for clearance of human Alzheimer's amyloid beta-peptide and apolipoproteins E and J in the mouse central nervous system. J Cereb Blood Flow Metab 27:909–918.

Bengtson CP, Dick O, Bading H (2008) A quantitative method to assess extrasynaptic NMDA receptor function in the protective effect of synaptic activity against neurotoxicity. BMC Neurosci 9:11.

Benilova I, Karran E, De Strooper B (2012) The toxic Aβ oligomer and Alzheimer's disease: an emperor in need of clothes. Nat Neurosci 15:349–357.

Bennett DA, Schneider JA, Wilson RS, Bienias JL, Arnold SE (2004) Neurofibrillary Tangles Mediate the Association of Amyloid Load With Clinical Alzheimer Disease and Level of Cognitive Function. Arch Neurol 61:378.

Bennetta ML, Bennetta C, Liddelowa SA, Ajami B, Zamanian JL, Fernhoff NB, Mulinyawe SB, Bohlen CJ, Adil A, Tucker A, L.Weissman I, Chang EF, Gordon L, Grant GA, Hayden Gephart MG, Barres BA (2016) New tools for studying microglia in the mouse and human CNS. Proc Natl Acad Sci 113:E1738-E1746.

Bero AW, Yan P, Roh JH, Cirrito JR, Stewart FR, Raichle ME, Lee J-M, Holtzman DM (2011) Neuronal activity regulates the regional vulnerability to amyloid-β deposition. Nat Neurosci 14:750–7561.

Bocchini V, Mazzolla R, Barluzzi R, Blasi E, Sick P, Kettenmann H (1992) An Immortalized Cell Line Expresses Properties of Activated Microglial Cells. J Neurosci Res 31:61–621.

Bordji K, Becerril-Ortega J, Nicole O, Buisson A (2010) Activation of extrasynaptic, but not synaptic, NMDA receptors modifies amyloid precursor protein expression pattern and increases amyloid-ß production. J Neurosci 30:15927–15942.

Braak H, Braak E (1991) Neuropathological stageing of Alzheimer-related changes. Acta Neuropathol 82:239–259.

Braithwaite SP, Meyer G, Henley JM (2000) Interactions between AMPA receptors and intracellular proteins. Neuropharmacology 39:919–930.

Brambilla R, Gnesutta N, Minichiello L, White G, Roylance AJ, Herron CE, Ramsey M, Wolfer DP, Cestari V, Rossi-Arnaud C, Grant SG, Chapman PF, Lipp HP, Sturani E, Klein R (1997) A role for the Ras signalling pathway in synaptic transmission and long-term memory. Nature 390:281–286.

Brody DL, Magnoni S, Schwetye KE, Spinner ML, Esparza TJ, Stocchetti N, Zipfel GJ, Holtzman DM (2008) Amyloid-beta dynamics correlate with neurological status in the injured human brain. Science 321:1221–1224.

Buckner RL, Sepulcre J, Talukdar T, Krienen FM, Liu H, Hedden T, Andrews-Hanna JR, Sperling RA, Johnson KA (2009) Cortical hubs revealed by intrinsic functional connectivity: mapping, assessment of stability, and relation to Alzheimer's disease. J Neurosci 29:1860–1873.

Buckner RL, Snyder AZ, Shannon BJ, LaRossa G, Sachs R, Fotenos AF, Sheline YI, Klunk WE, Mathis CA, Morris JC, Mintun MA (2005) Molecular, Structural, and Functional Characterization of Alzheimer's Disease: Evidence for a Relationship between Default Activity, Amyloid, and Memory. J Neurosci 25:7709–7717.

Bursavich MG, Harrison BA, Blain J-F (2016) Gamma Secretase Modulators: New Alzheimer's Drugs on the Horizon? J Med Chem 59:7389–7409.

Bush T, Puvanachandra N, Horner C, Polito A, Ostenfeld T, Svendsen C, Mucke L, Johnson M, Sofroniew M (1999) Leukocyte Infiltration, Neuronal Degeneration, and Neurite Outgrowth after Ablation of Scar-Forming, Reactive Astrocytes in Adult Transgenic Mice. Neuron 23:297–308.

Castellano JM, Kim J, Stewart FR, Jiang H, DeMattos RB, Patterson BW, Fagan AM, Morris JC, Mawuenyega KG, Cruchaga C, Goate AM, Bales KR, Paul SM, Bateman RJ, Holtzman DM (2011) Human apoE Isoforms Differentially Regulate Brain Amyloid- Peptide Clearance. Sci Transl Med 3:89ra57-89ra57.

Chakrabarty P, Jansen-West K, Beccard A, Ceballos-Diaz C, Levites Y, Verbeeck C, Zubair AC, Dickson D, Golde TE, Das P (2010) Massive gliosis induced by interleukin-6 suppresses A deposition in vivo: evidence against inflammation as a driving force for amyloid deposition. FASEB J 24:548–559.

Chandler LJ, Sutton G, Dorairajţ NR, Norwoodţ D (2000) N-Methyl D-Aspartate Receptor-mediated Bidirectional Control of Extracellular Signal-regulated Kinase Activity in Cortical Neuronal Cultures. J Biol Chem 276: 2627-2636.

Chang EH, Savage MJ, Flood DG, Thomas JM, Levy RB, Mahadomrongkul V, Shirao T, Aoki C, Huerta PT (2006) AMPA receptor downscaling at the onset of Alzheimer's disease pathology in double knockin mice. Proc Natl Acad Sci U S A 103:3410–3415.

Chater TE, Goda Y (2014) The role of AMPA receptors in postsynaptic mechanisms of synaptic plasticity. Front Cell Neurosci 8:401.

Chefer VI, Thompson AC, Zapata A, Shippenberg TS (2009) Overview of brain microdialysis. Curr Protoc Neurosci Chapter 7:Unit7.1.

Chen H-J, Rojas-Soto M, Oguni A, Kennedy MB (1998) A Synaptic Ras-GTPase Activating Protein (p135 SynGAP) Inhibited by CaM Kinase II. Neuron 20:895–904.

Cho M-H, Cho K, Kang H-J, Jeon E-Y, Kim H-S, Kwon H-J, Kim H-M, Kim D-H, Yoon S-Y (2014) Autophagy in microglia degrades extracellular β-amyloid fibrils and regulates the NLRP3 inflammasome. Autophagy 10:1761–1775.

Cirrito JR, Deane R, Fagan AM, Spinner ML, Parsadanian M, Finn MB, Jiang H, Prior JL, Sagare A, Bales KR, Paul SM, Zlokovic B V, Piwnica-Worms D, Holtzman DM (2005a) P-glycoprotein deficiency at the blood-brain barrier increases amyloid-beta deposition in an Alzheimer disease mouse model. J Clin Invest 115:3285–3290.

Cirrito JR, Disabato BM, Restivo JL, Verges DK, Goebel WD, Sathyan A, Hayreh D, D'Angelo G, Benzinger T, Yoon H, Kim J, Morris JC, Mintun MA, Sheline YI (2011) Serotonin signaling is associated with lower amyloid-β levels and plaques in transgenic mice and humans. Proc Natl Acad Sci U S A 108:14968–14973.

Cirrito JR, Kang J-E, Lee J, Stewart FR, Verges DK, Silverio LM, Bu G, Mennerick S, Holtzman DM (2008) Endocytosis is required for synaptic activity-dependent release of amyloid-beta in vivo. Neuron 58:42–51.

Cirrito JR, May PC, O'Dell MA, Taylor JW, Parsadanian M, Cramer JW, Audia JE, Nissen JS, Bales KR, Paul SM, DeMattos RB, Holtzman DM (2003) In Vivo Assessment of Brain Interstitial Fluid with Microdialysis Reveals Plaque-Associated Changes in Amyloid-{beta} Metabolism and Half-Life. J Neurosci 23:8844–8853.

Cirrito JR, Yamada K a, Finn MB, Sloviter RS, Bales KR, May PC, Schoepp DD, Paul SM, Mennerick S, Holtzman DM (2005b) Synaptic activity regulates interstitial fluid amyloid-beta levels in vivo. Neuron 48:913–922.

Constals A, Penn AC, Hosy E, Correspondence DC, Compans B, Toulmé E, Phillipat A, Bastien Marais S, Retailleau N, Hafner A-S, Oise Coussen F, Choquet D (2015) Glutamate-Induced AMPA Receptor Desensitization Increases Their Mobility and Modulates Short-Term Plasticity through Unbinding from Stargazin. Neuron 85:787–803.

Corder EH, Saunders AM, Strittmatter WJ, Schmechel DE, Gaskell PC, Small GW, Roses AD, Haines JL, Pericak-Vance MA (1993) Gene dose of apolipoprotein E type 4 allele and the risk of Alzheimer's disease in late onset families. Science 261:921–923.

Cross a. J, Slater P, Simpson M, Royston C, Deakin JFW, Perry RH, Perry EK (1987) Sodium dependent d-[3H]aspartate binding in cerebral cortex in patients with Alzheimer's and Parkinson's diseases. Neurosci Lett 79:213–217.

Cummings JL, Morstorf T, Zhong K (2014) Alzheimer's disease drug-development pipeline: few candidates, frequent failures. Alzheimers Res Ther 6:37.

Das U, Scott DA, Ganguly A, Koo EH, Tang Y, Roy S (2013) Activity-Induced Convergence of APP and BACE-1 in Acidic Microdomains via an Endocytosis-Dependent Pathway. Neuron 79:447–460.

Davis AA, Fritz JJ, Wess J, Lah JJ, Levey AI (2010) Deletion of M1 muscarinic acetylcholine receptors increases amyloid pathology in vitro and in vivo. J Neurosci 30:4190–4196.

De Felice FG, Velasco PT, Lambert MP, Viola K, Fernandez SJ, Ferreira ST, Klein WL (2007) Abeta oligomers induce neuronal oxidative stress through an N-methyl-D-aspartate receptor-dependent mechanism that is blocked by the Alzheimer drug memantine. J Biol Chem 282:11590–11601.

Deane R, Wu Z, Sagare A, Davis J, Du Yan S, Hamm K, Xu F, Parisi M, LaRue B, Hu HW, Spijkers P, Guo H, Song X, Lenting PJ, Van Nostrand WE, Zlokovic B V. (2004) LRP/Amyloid β-Peptide Interaction Mediates Differential Brain Efflux of Aβ Isoforms. Neuron 43:333–344.

De Strooper B, Karran E (2016) The Cellular Phase of Alzheimer's Disease. Cell 164:603–615.

De Strooper B, Vassar R, Golde T (2010) The secretases: enzymes with therapeutic potential in Alzheimer disease. Nat Rev Neurol 6:99–107.

Denes A, Vidyasagar R, Feng J, Narvainen J, McColl BW, Kauppinen RA, Allan SM (2007) Proliferating resident microglia after focal cerebral ischaemia in mice. J Cereb Blood Flow

Metab 27:1941–1953.

Doody RS, Raman R, Farlow M, Iwatsubo T, Vellas B, Joffe S, Kieburtz K, He F, Sun X, Thomas RG, Aisen PS, Siemers E, Sethuraman G, Mohs R (2013) A Phase 3 Trial of Semagacestat for Treatment of Alzheimer's Disease. N Engl J Med 369:341–350.

Edman S, McKay S, Macdonald LJ, Samadi M, Livesey MR, Hardingham GE, Wyllie DJA (2012) TCN 201 selectively blocks GluN2A-containing NMDARs in a GluN1 co-agonist dependent but non-competitive manner. Neuropharmacology 63:441–449.

Elder GA, Gama Sosa MA, De Gasperi R (2010) Transgenic mouse models of Alzheimer's disease. Mt Sinai J Med 77:69–81.

Eng LF, Yu AC, Lee YL (1992) Astrocytic response to injury. Prog Brain Res 94:353–365.

English JD, Sweatt JD (1996) Activation of p42 Mitogen-activated Protein Kinase in Hippocampal Long Term Potentiation. J Biol Chem 271:24329–24332.

Erta M, Quintana A, Hidalgo J (2012) Interleukin-6, a major cytokine in the central nervous system. Int J Biol Sci 8:1254–1266.

Esquerda-Canals G, Montoliu-Gaya L, Güell-Bosch J, Villegas S (2017) Mouse Models of Alzheimer's Disease. J Alzheimer's Dis 57:1171–1183.

Feig LA (2011) Regulation of Neuronal Function by Ras-GRF Exchange Factors. Genes Cancer 2:306–319.

Fernández-Medarde A, Esteban LM, Núñez A, Porteros A, Tessarollo L, Santos E (2002) Targeted disruption of Ras-Grf2 shows its dispensability for mouse growth and development. Mol Cell Biol 22:2498–2504.

Fisher A (2012) Cholinergic modulation of amyloid precursor protein processing with emphasis on M1 muscarinic receptor: perspectives and challenges in treatment of Alzheimer's disease. J Neurochem 120 Suppl:22–33.

Fisher JR, Wallace CE, Tripoli DL, Sheline YI, Cirrito JR (2016) Redundant Gs-coupled serotonin receptors regulate amyloid-β metabolism in vivo. Mol Neurodegener 11:45.

Francis PT (2003) Glutamatergic systems in Alzheimer's disease. Int J Geriatr Psychiatry 18:S15-21.

Gadient R, Otten U (1997) Interleukin-6 - a molecule with both beneficial and destructive potentials. Prog Neurobiol 52:379–390.

Games D et al. (1995) Alzheimer-type neuropathology in transgenic mice overexpressing V717F β-amyloid precursor protein. Nature 373:523–527.

Gangarossa G, Valjent E (2012) Regulation of the ERK pathway in the dentate gyrus by in vivo dopamine D1 receptor stimulation requires glutamatergic transmission. Neuropharmacology 63:1107–1117.

Giese KP, Friedman E, Telliez JB, Fedorov NB, Wines M, Feig LA, Silva AJ (2001) Hippocampus-dependent learning and memory is impaired in mice lacking the Ras-guanine-nucleotide releasing factor 1 (Ras-GRF1). Neuropharmacology 41:791–800.

Glen Iner GG, Wo CW (1984) Alzheimer's Disease and Down's Syndrome: Sharing of a Unique Cerebrovascular amyloid fibril protein. Biochem Biophys Res Commun 122.

Goate A et al. (1991) Segregation of a missense mutation in the amyloid precursor protein gene with familial Alzheimer's disease. Nature 349:704–706.

Gocel J, Larson J (2013) Evidence for loss of synaptic AMPA receptors in anterior piriform cortex of aged mice. Front Aging Neurosci 5:39.

Goldgaber D, Lerman M, McBride O, Saffiotti U, Gajdusek D (1987) Characterization and chromosomal localization of a cDNA encoding brain amyloid of Alzheimer's disease. Science 80:235.

Goodenough S, Engert S, Behl C (2000) Testosterone stimulates rapid secretory amyloid precursor protein release from rat hypothalamic cells via the activation of the mitogen-activated protein kinase pathway. Neurosci Lett 296:49–52.

Götz J, Chen F, van Dorpe J, Nitsch RM (2001) Formation of Neurofibrillary Tangles in P301L Tau Transgenic Mice Induced by Aβ42 Fibrils. Science 80:293

Gruol DL (2015) IL-6 regulation of synaptic function in the CNS. Neuropharmacology 96:42–54.

Guillozet AL, Weintraub S, Mash DC, Mesulam MM (2003) Neurofibrillary Tangles, Amyloid, and Memory in Aging and Mild Cognitive Impairment. Arch Neurol 60:729.

Guntupalli S, Widagdo J, Anggono V (2016a) Amyloid- β -Induced Dysregulation of AMPA Receptor Trafficking. Neural Plast 2016:1–12.

Guntupalli S, Widagdo J, Anggono V, Guntupalli S, Widagdo J, Anggono V (2016b) Amyloid- β -Induced Dysregulation of AMPA Receptor Trafficking. Neural Plast 2016:1–12.

Guo Q, Li H, Gaddam SSK, Justice NJ, Robertson CS, Zheng H (2012) Amyloid precursor protein revisited: neuron-specific expression and highly stable nature of soluble derivatives. J Biol Chem 287:2437–2445.

Haass C, Kaether C, Thinakaran G, Sisodia S (2012) Trafficking and proteolytic processing of APP. Cold Spring Harb Perspect Med Haass C, K:a006270.

Haass C, Lemere CA, Capell A, Citron M, Seubert P, Schenk D, Lannfelt L, Selkoe DJ (1995) The Swedish mutation causes early-onset Alzheimer's disease by beta-secretase cleavage within the secretory pathway. Nat Med 1:1291–1296.

Hamilton A, Esseltine JL, DeVries RA, Cregan SP, Ferguson SSG (2014) Metabotropic glutamate receptor 5 knockout reduces cognitive impairment and pathogenesis in a mouse model of Alzheimer's disease. Mol Brain 7:40.

Hanisch U-K, Kettenmann H (2007) Microglia: active sensor and versatile effector cells in the normal and pathologic brain. Nat Neurosci 10:1387–1394.

Hardingham GE (2006) 2B synaptic or extrasynaptic determines signalling from the NMDA receptor. J Physiol 572:614–615.

Hardingham GE, Bading H (2010) Synaptic versus extrasynaptic NMDA receptor signalling: implications for neurodegenerative disorders. Nat Rev Neurosci 11:682–696.

Hardingham GE, Fukunaga Y, Bading H (2002) Extrasynaptic NMDARs oppose synaptic NMDARs by triggering CREB shut-off and cell death pathways. Nat Neurosci 5:405–414.

Hardy JA, Higgins GA (1992) Alzheimer's disease: the amyloid cascade hypothesis. Science 256:184–185.

Hardy J, Selkoe DJ (2002) The amyloid hypothesis of Alzheimer's disease: progress and problems on the road to therapeutics. Science 297:353–356.

Hartmann B et al. (2004) The AMPA receptor subunits GluR-A and GluR-B reciprocally modulate spinal synaptic plasticity and inflammatory pain. Neuron 44:637–650.

Hayashi T, Umemori H, Mishina M, Yamamoto T (1999) The AMPA receptor interacts with and signals through the protein tyrosine kinase Lyn. Nature 397:72–76.

Henn A, Lund S, Hedtjärn M, Schrattenholz A, Pörzgen P, Leist M (2009) The suitability of BV2 cells as alternative model system for primary microglia cultures or for animal experiments examining brain inflammation. ALTEX 26:83–94.

Herber DL, Mercer M, Roth LM, Symmonds K, Maloney J, Wilson N, Freeman MJ, Morgan D, Gordon MN (2007) Microglial Activation is Required for Aβ Clearance After Intracranial Injection of Lipopolysaccharide in APP Transgenic Mice. J Neuroimmune Pharmacol 2:222–231.

Hoey SE, Buonocore F, Cox CJ, Hammond VJ, Perkinton MS, Williams RJ (2013) AMPA Receptor Activation Promotes Non- Amyloidogenic Amyloid Precursor. PLoS ONE 8:e78155.

Hoey SE, Williams RJ, Perkinton MS (2009) Synaptic NMDA receptor activation stimulates alpha-secretase amyloid precursor protein processing and inhibits amyloid-beta production. J Neurosci 29:4442–4460.

Holmes C, Boche D, Wilkinson D, Yadegarfar G, Hopkins V, Bayer A, Jones RW, Bullock R, Love S, Neal JW, Zotova E, Nicoll JA (2008) Long-term effects of Aβ42 immunisation in Alzheimer's disease: follow-up of a randomised, placebo-controlled phase I trial. Lancet 372:216–223.

Holtzman DM, Bales KR, Tenkova T, Fagan AM, Parsadanian M, Sartorius LJ, Mackey B, Olney J, McKeel D, Wozniak D, Paul SM (2000) Apolipoprotein E isoform-dependent amyloid deposition and neuritic degeneration in a mouse model of Alzheimer's disease. Proc Natl Acad Sci U S A 97:2892–2897.

Holtzman DM, Morris JC, Goate AM (2011) Alzheimer's disease: the challenge of the second century. Sci Transl Med 3:77.

Hsieh H, Boehm J, Sato C, Iwatsubo T, Tomita T, Sisodia S, Malinow R (2006) AMPAR removal underlies Abeta-induced synaptic depression and dendritic spine loss. Neuron 52:831–843.

Hunt DL, Castillo PE (2012) Synaptic plasticity of NMDA receptors: Mechanisms and functional implications. Curr Opin Neurobiol 22:496–508.

Iliff JJ, Wang M, Liao Y, Plogg BA, Peng W, Gundersen GA, Benveniste H, Vates GE, Deane R, Goldman SA, Nagelhus EA, Nedergaard M (2012) A paravascular pathway facilitates CSF flow through the brain parenchyma and the clearance of interstitial solutes, including amyloid β. Sci Transl Med 4:147ra111.

Itier J-M, Tremp GL, Léonard J-F, Multon M-C, Ret G, Schweighoffer F, Tocqué B, Bluet-Pajot M-T, Cormier V, Dautry F (1998) Imprinted gene in postnatal growth role. Nature 393:125–126.

Ito D, Tanaka K, Suzuki S, Dembo T, Fukuuchi Y (2001) Enhanced Expression of Iba1, Ionized Calcium-Binding Adapter Molecule 1, After Transient Focal Cerebral Ischemia In Rat Brain. Stroke 32:1208–1215.

Ivanov A, Pellegrino C, Rama S, Dumalska I, Salyha Y, Ben-Ari Y, Medina I (2006a) Opposing role of synaptic and extrasynaptic NMDA receptors in regulation of the extracellular signal-regulated kinases (ERK) activity in cultured rat hippocampal neurons. J Physiol 572:789–798.

Ivanov A, Pellegrino C, Rama S, Dumalska I, Salyha Y, Ben-Ari Y, Medina I (2006b) Opposing role of synaptic and extrasynaptic NMDA receptors in regulation of the extracellular signal-regulated kinases (ERK) activity in cultured rat hippocampal neurons. J Physiol 572:789–798.

Iwata N, Tsubuki S, Takaki Y, Shirotani K, Lu B, Gerard NP, Gerard C, Hama E, Lee HJ, Saido TC (2001) Metabolic regulation of brain Abeta by neprilysin. Science 292:1550–1552.

Jankowsky JL, Slunt HH, Gonzales V, Jenkins NA, Copeland NG, Borchelt DR (2004) APP processing and amyloid deposition in mice haplo-insufficient for presenilin 1. Neurobiol Aging 25:885–892.

Jankowsky JL, Slunt HH, Ratovitski T, Jenkins NA, Copeland NG, Borchelt DR (2001) Co-expression of multiple transgenes in mouse CNS: A comparison of strategies. Biomol Eng 17:157–165.

Jones CK, Brady AE, Davis AA, Xiang Z, Bubser M, Tantawy MN, Kane AS, Bridges TM, Kennedy JP, Bradley SR, Peterson TE, Ansari MS, Baldwin RM, Kessler RM, Deutch AY, Lah JJ, Levey AI, Lindsley CW, Conn PJ (2008) Novel selective allosteric activator of the M1 muscarinic acetylcholine receptor regulates amyloid processing and produces antipsychotic-like activity in rats. J Neurosci 28:10422–10433.

Ju Y-E, Ooms SJ, Sutphen C, Macauley SL, Zangrilli MA, Jerome G, Fagan AM, Mignot E, Zempel JM, Claassen JAHR, Holtzman DM (2017) Slow wave sleep disruption increases cerebrospinal fluid amyloid-b levels. Brain 211:387–393.

Juttler E, Tarabin V, Schwaninger M (2002) Interleukin-6 (IL-6): A Possible Neuromodulator Induced by Neuronal Activity. Neurosci 8:268–275.

Kaczmarek L (1993) Glutamate receptor-driven gene expression in learning. In: Acta Neurobiologiae Experimentalis, pp 187–196.

Kamenetz F, Tomita T, Hsieh H, Seabrook G, Borchelt D, Iwatsubo T, Sisodia S, Malinow R (2003) APP Processing and Synaptic Function. Neuron 37:925–937.

Kanekiyo T, Bu G (2014) The low-density lipoprotein receptor-related protein 1 and amyloid-beta clearance in Alzheimer's disease. Front Aging Neurosci 6:93.

Kanekiyo T, Cirrito JR, Liu C-C, Shinohara M, Li J, Schuler DR, Shinohara M, Holtzman DM, Bu G (2013) Neuronal Clearance of Amyloid- by Endocytic Receptor LRP1. J Neurosci 33:19276–19283.

Kanekiyo T, Liu C-C, Shinohara M, Li J, Bu G (2012) LRP1 in Brain Vascular Smooth Muscle Cells Mediates Local Clearance of Alzheimer's Amyloid-β. J Neurosci 32.

Kanekiyo T, Zhang J, Liu Q, Liu C-C, Zhang L, Bu G (2011) Heparan sulphate proteoglycan and the low-density lipoprotein receptor-related protein 1 constitute major pathways for neuronal amyloid-beta uptake. J Neurosci 31:1644–1651.

Kang J-E, Lim MM, Bateman RJ, Lee JJ, Smyth LP, Cirrito JR, Fujiki N, Nishino S, Holtzman DM (2009) Amyloid-beta dynamics are regulated by orexin and the sleep-wake cycle. Science 326:1005–1007.

Kavalali ET (2014) The mechanisms and functions of spontaneous neurotransmitter release. Nat Rev Neurosci 16:5–16.

Kavalali ET, Chung C, Khvotchev M, Leitz J, Nosyreva E, Raingo J, Ramirez DMO (2011) Spontaneous Neurotransmission: An Independent Pathway for Neuronal Signaling? Physiology 26:45-53.

Kawai F, Sterling P (1999) AMPA receptor activates a G-protein that suppresses a cGMP-gated current. J Neurosci 19:2954–2959.

Kim SH, Fraser PE, Westaway D, St George-Hyslop PH, Ehrlich ME, Gandy S (2010) Group II metabotropic glutamate receptor stimulation triggers production and release of Alzheimer's amyloid(beta)42 from isolated intact nerve terminals. J Neurosci 30:3870–3875.

Kitazawa M, Medeiros R, Laferla FM (2012) Transgenic mouse models of Alzheimer disease: developing a better model as a tool for therapeutic interventions. Curr Pharm Des 18:1131–1147.

Koo EH, Squazzo SL (1994) Evidence that production and release of amyloid beta-protein involves the endocytic pathway. J Biol Chem 269:17386–17389.

Kraft AW, Hu X, Yoon H, Yan P, Xiao Q, Wang Y, Gil SC, Brown J, Wilhelmsson U, Restivo JL, Cirrito JR, Holtzman DM, Kim J, Pekny M, Lee J-M (2013) Attenuating astrocyte activation accelerates plaque pathogenesis in APP/PS1 mice. FASEB J 27:187–198.

Krapivinsky G, Krapivinsky L, Manasian Y, Ivanov A, Tyzio R, Pellegrino C, Ben-Ari Y, Clapham DE, Medina I (2003) The NMDA receptor is coupled to the ERK pathway by a direct interaction between NR2B and RasGRF1. Neuron 40:775–784.

Kuhn P-H, Wang H, Dislich B, Colombo A, Zeitschel U, Ellwart JW, Kremmer E, Roßner S, Lichtenthaler SF (2010) ADAM10 is the physiologically relevant, constitutive α-secretase of the amyloid precursor protein in primary neurons. EMBO J 29:3020–3032.

Kurino M, Fukunaga K, Ushio Y, Miyamoto E (2002) Activation of Mitogen-Activated Protein Kinase in Cultured Rat Hippocampal Neurons by Stimulation of Glutamate Receptors. J Neurochem 65:1282–1289.

Lacor PN, Buniel MC, Furlow PW, Clemente AS, Velasco PT, Wood M, Viola KL, Klein WL (2007) Abeta oligomer-induced aberrations in synapse composition, shape, and density provide a molecular basis for loss of connectivity in Alzheimer's disease. J Neurosci 27:796–807.

Lauterborn JC, Palmer LC, Jia Y, Pham DT, Hou B, Wang W, Trieu BH, Cox CD, Kantorovich S, Gall CM, Lynch G (2016) Chronic Ampakine Treatments Stimulate Dendritic Growth and Promote Learning in Middle-Aged Rats. J Neurosci 36:1636–1646.

Lehre KP, Danbolt NC (1998) The Number of Glutamate Transporter Subtype Molecules at Glutamatergic Synapses: Chemical and Stereological Quantification in Young Adult Rat Brain. J Neurosci 18:8751–8757.

Lei Y, Han H, Yuan F, Javeed A, Zhao Y (2016) The brain interstitial system: Anatomy, modeling, in vivo measurement, and applications. Prog Neurobiol 157:230-246.

Lesné S, Ali C, Gabriel C, Croci N, MacKenzie ET, Glabe CG, Plotkine M, Marchand-Verrecchia C, Vivien D, Buisson A (2005) NMDA receptor activation inhibits alpha-secretase and promotes neuronal amyloid-beta production. J Neurosci 25:9367–9377.

Lewis J, Dickson DW, Lin W-L, Chisholm L, Corral A, Jones G, Yen S-H, Sahara N, Skipper L, Yager D, Eckman C, Hardy J, Hutton M, McGowan E (2001) Enhanced Neurofibrillary Degeneration in Transgenic Mice Expressing Mutant Tau and APP. Science 293:1487-1491.

Li H, Wei Y, Wang Z, Wang Q (2015) Application of APP/PS1 Transgenic Mouse Model for Alzheimer's Disease. J Alzheimer's Dis Park 5:1–4.

Li J, Kanekiyo T, Shinohara M, Zhang Y, LaDu MJ, Xu H, Bu G (2012) Differential regulation of amyloid-β endocytic trafficking and lysosomal degradation by apolipoprotein E isoforms.

J Biol Chem 287:44593–44601.

Li S, Tian X, Hartley DM, Feig LA (2006) Distinct roles for Ras-guanine nucleotide-releasing factor 1 (Ras-GRF1) and Ras-GRF2 in the induction of long-term potentiation and long-term depression. J Neurosci 26:1721–1729.

Lipton SA, Kater SB (1989) Neurotransmitter regulation of neuronal outgrowth, plasticity and survival. Trends Neurosci 12:265–270.

Liu CC, Hu J, Zhao N, Wang J, Na W, Cirrito JR, Kanekiyo T, Holtzman DM, Bu G (2017) Astrocytic LRP1 Mediates Brain Aβ Clearance and Impacts Amyloid Deposition. J Neurosci 37:4023-4031.

Liu S-J, Gasperini R, Foa L, Small DH (2010) Amyloid-β Decreases Cell-Surface AMPA Receptors by Increasing Intracellular Calcium and Phosphorylation of GluR2. J Alzheimer's Dis 21:655–666.

Liu Y, Wong TP, Aarts M, Rooyakkers A, Liu L, Lai TW, Wu DC, Lu J, Tymianski M, Craig AM, Wang YT (2007) NMDA receptor subunits have differential roles in mediating excitotoxic neuronal death both in vitro and in vivo. J Neurosci 27:2846–2857.

Lomakin A, Teplow DB, Kirschner DA, Benedek GB (1997) Kinetic theory of fibrillogenesis of amyloid beta-protein. Proc Natl Acad Sci U S A 94:7942–7947.

Lu W, Shi Y, Jackson AC, Bjorgan K, During MJ, Sprengel R, Seeburg PH, Nicoll RA (2009) Subunit composition of synaptic AMPA receptors revealed by a single-cell genetic approach. Neuron 62:254–268.

Mackenzie IR, Miller LA (1994) Senile plaques in temporal lobe epilepsy. Acta Neuropathol 87:504–510.

Majumdar A, Capetillo-Zarate E, Cruz D, Gouras GK, Maxfield FR (2011) Degradation of Alzheimer's amyloid fibrils by microglia requires delivery of ClC-7 to lysosomes. Mol Biol Cell 22:1664–1676.

Malinow R (2012) New developments on the role of NMDA receptors in Alzheimer's disease. Curr Opin Neurobiol 22:559–563.

Manthey D, Heck S, Engert S, Behl C (2001) Estrogen induces a rapid secretion of amyloid β precursor protein via the mitogen-activated protein kinase pathway. Eur J Biochem 268:4285–4291.

Marcello E, Epis R, Di Luca M (2008) Amyloid flirting with synaptic failure: towards a comprehensive view of Alzheimer's disease pathogenesis. Eur J Pharmacol 585:109–118.

Marcello E, Gardoni F, Mauceri D, Romorini S, Jeromin A, Epis R, Borroni B, Cattabeni F, Sala C, Padovani A, Di Luca M (2007) Synapse-associated protein-97 mediates alpha-secretase ADAM10 trafficking and promotes its activity. J Neurosci 27:1682–1691.

Masters CL, Simms G, Weinman NA, Multhaupt G, Mcdonald BL, Beyreuthert K (1985) Amyloid plaque core protein in Alzheimer disease and Down syndrome. Med Sci 82:4245–4249.

Matos M, Augusto E, Oliveira CR, Agostinho P (2008) Amyloid-beta peptide decreases glutamate uptake in cultured astrocytes: involvement of oxidative stress and mitogen-activated protein kinase cascades. Neuroscience 156:898–910.

Mawuenyega KG, Sigurdson W, Ovod V, Munsell L, Kasten T, Morris JC, Yarasheski KE, Bateman RJ (2010) Decreased clearance of CNS beta-amyloid in Alzheimer's disease. Science 330:1774.

McKinney RA, Capogna M, Dürr R, Gähwiler BH, Thompson and SM (1999) Miniature synaptic events maintain dendritic spines via AMPA receptor activation. Nat Neurosci 2:44–49.

Meyer-Luehmann M, Stalder M, Herzig MC, Kaeser SA, Kohler E, Pfeifer M, Boncristiano S, Mathews PM, Mercken M, Abramowski D, Staufenbiel M, Jucker M (2003) Extracellular amyloid formation and associated pathology in neural grafts. Nat Neurosci 6:370–377.

Miller DL, Papayannopoulos IA, Styles J, Bobin SA, Lin YY, Biemann K, Iqbal K (1993) Peptide Compositions of the Cerebrovascular and Senile Plaque Core Amyloid Deposits of Alzheimer′s Disease. Arch Biochem Biophys 301:41–52.

Mills J, Laurent Charest D, Lam F, Beyreuther K, Ida N, Pelech SL, Reiner PB (1997) Regulation of Amyloid Precursor Protein Catabolism Involves the Mitogen-Activated Protein Kinase Signal Transduction Pathway. J Neurosci 17:9415-22.

Miñano-Molina AJ, España J, Martín E, Barneda-Zahonero B, Fadó R, Solé M, Trullás R, Saura CA, Rodríguez-Alvarez J (2011) Soluble oligomers of amyloid-β peptide disrupt membrane trafficking of α-amino-3-hydroxy-5-methylisoxazole-4-propionic acid receptor contributing to early synapse dysfunction. J Biol Chem 286:27311–27321.

Mocanu M-M, Nissen A, Eckermann K, Khlistunova I, Biernat J, Drexler D, Petrova O, Schönig K, Bujard H, Mandelkow E, Zhou L, Rune G, Mandelkow E-M (2008) The Potential for β-Structure in the Repeat Domain of Tau Protein Determines Aggregation, Synaptic Decay, Neuronal Loss, and Coassembly with Endogenous Tau in Inducible Mouse Models of Tauopathy. J Neurosci 28:737-748.

Morris JC, Price JL (2001) Pathologic Correlates of Nondemented Aging, Mild Cognitive Impairment, and Early-Stage Alzheimer's Disease. J Mol Neurosci 17:101–118.

Mulkey RM, Endo S, Shenolikar S, Malenka RC (1994) Involvement of a calcineurin/ inhibitor-1 phosphatase cascade in hippocampal long-term depression. Nature 369:486–488.

Murphy TH, Blatter LA, Bhat R V, Fiore RS, Wier WG, Baraban JM (1994) Differential regulation of calcium/calmodulin-dependent protein kinase II and p42 MAP kinase activity by synaptic transmission. J Neurosci 14:1320–1331.

Musiek ES, Holtzman DM (2015) Three dimensions of the amyloid hypothesis: time, space and "wingmen." Nat Neurosci 18:800–806.

N'Songo A, Kanekiyo T, Bu G (2013) LRP1 plays a major role in the amyloid-β clearance in microglia. Mol Neurodegener 2013 81 8:P33.

Nagy Z, Esiri MM, Jobst KA, Morris JH, King EMF, McDonald B, Litchfield S, Smith A, Barnetson L, Smith AD (1995) Relative roles of plaques and tangles in the dementia of Alzheimer's disease: Correlations using three sets of neuropathological criteria. Dement Geriatr Cogn Disord 6:21–31.

Nakazawa T, Shimura M, Ryu M, Nishida K, Pagès G, Pouysségur J, Endo S (2008) ERK1 plays a critical protective role against N-methyl-D-aspartate-induced retinal injury. J Neurosci Res 86:136–144.

Oddo S, Caccamo A, Shepherd JD, Murphy MP, Golde TE, Kayed R, Metherate R, Mattson MP, Akbari Y, LaFerla FM (2003) Triple-transgenic model of Alzheimer's disease with plaques and tangles: intracellular Abeta and synaptic dysfunction. Neuron 39:409–421.

Oddo S, Vasilevko V, Caccamo A, Kitazawa M, Cribbs DH, LaFerla FM (2006) Reduction of soluble Abeta and tau, but not soluble Abeta alone, ameliorates cognitive decline in transgenic mice with plaques and tangles. J Biol Chem 281:39413–39423.

Olney JW, Collins RC, Sloviter RS (1986) Excitotoxic mechanisms of epileptic brain damage. Adv Neurol 44:857–877.

Olney JW, Wozniak DF, Farber NB (1997) Excitotoxic neurodegeneration in Alzheimer disease. New hypothesis and new therapeutic strategies. Arch Neurol 54:1234–1240.

Ottiz J, Harris HW, Guitart X, Terwilliger RZ, Haycock JW, Nestler EJ (1995) Extracellular Signal-Regulated Protein Kinases (ERKs) and ERK Kinase (MEK) in Brain: Regional Distribution and Regulation by Chronic Morphine. J Neurosci:1285–1297.

Pandey SP, Rai R, Gaur P, Prasad S (2015) Development- and age-related alterations in the expression of AMPA receptor subunit GluR2 and its trafficking proteins in the hippocampus of male mouse brain. Biogerontology 16:317–328.

Papadia S, Soriano FX, Léveillé F, Martel M-A, Dakin KA, Hansen HH, Kaindl A, Sifringer M, Fowler J, Stefovska V, McKenzie G, Craigon M, Corriveau R, Ghazal P, Horsburgh K, Yankner BA, Wyllie DJA, Ikonomidou C, Hardingham GE (2008) Synaptic NMDA receptor activity boosts intrinsic antioxidant defenses. Nat Neurosci 11:476–487.

Papouin T, Ladépêche L, Ruel J, Sacchi S, Labasque M, Hanini M, Groc L, Pollegioni L, Mothet J-P, Oliet SHR (2012) Synaptic and extrasynaptic NMDA receptors are gated by different endogenous coagonists. Cell 150:633–646.

Papouin T, Oliet SHR (2017) Synaptic and Extra-Synaptic NMDA Receptors in the CNS. In: Hashimoto K. (eds) The NMDA Receptors. Humana Press, Cham 30:19-49.

Park E-S, Kim S-Y, Youn D-H (2010) NMDA Receptor, PKC and ERK Mediate Fos Expression Induced by the Activation of Group I Metabotropic Glutamate Receptors in the Spinal Trigeminal Subnucleus Oralis. Mol Cells 30:461–466.

Perkinton MS, Sihra TS, Williams RJ (1999a) Ca(2+)-permeable AMPA receptors induce phosphorylation of cAMP response element-binding protein through a phosphatidylinositol 3-kinase-dependent stimulation of the mitogen-activated protein kinase signaling cascade in neurons. J Neurosci 19:5861–5874.

Perkinton MS, Sihra TS, Williams RJ (1999b) Ca(2+)-permeable AMPA receptors induce phosphorylation of cAMP response element-binding protein through a phosphatidylinositol 3-kinase-dependent stimulation of the mitogen-activated protein kinase signaling cascade in neurons. J Neurosci 19:5861–5874.

Petralia RS, S. R (2012) Distribution of Extrasynaptic NMDA Receptors on Neurons. Sci World J 2012:1–11.

Petralia RS, Wang YX, Hua F, Yi Z, Zhou A, Ge L, Stephenson FA, Wenthold RJ (2010) Organization of NMDA receptors at extrasynaptic locations. Neuroscience 167:68–87.

Plant K, Pelkey KA, Bortolotto ZA, Morita D, Terashima A, McBain CJ, Collingridge GL, Isaac JTR (2006) Transient incorporation of native GluR2-lacking AMPA receptors during hippocampal long-term potentiation. Nat Neurosci 9:602–604.

Poo M, Nishiyama M, Hong K, Mikoshiba K, Kato K (2000) Calcium stores regulate the polarity and input specificity of synaptic modification. Nature 408:584–588.

Postina R, Schroeder A, Dewachter I, Bohl J, Schmitt U, Kojro E, Prinzen C, Endres K, Hiemke C, Blessing M, Flamez P, Dequenne A, Godaux E, van Leuven F, Fahrenholz F (2004) A disintegrin-metalloproteinase prevents amyloid plaque formation and hippocampal defects in an Alzheimer disease mouse model. J Clin Invest 113:1456–1464.

Potter R, Patterson BW, Elbert DL, Ovod V, Kasten T, Sigurdson W, Mawuenyega K, Blazey T, Goate A, Chott R, Yarasheski KE, Holtzman DM, Morris JC, Benzinger TLS, Bateman RJ (2013) Increased in Vivo Amyloid-β42 Production, Exchange, and Loss in Presenilin Mutation Carriers. Sci Transl Med 5:189ra77.

Pouysségur J, Volmat V, Lenormand P (2002) Fidelity and spatio-temporal control in MAP kinase (ERKs) signalling. Biochem Pharmacol 64:755–763.

Price DL, Sisodia SS, Gandy SE (1995) Amyloid beta amyloidosis in Alzheimer's disease. Curr Opin Neurol 8:268–274.

Price JL, Morris JC (1999) Tangles and plaques in nondemented aging and ?preclinical? Alzheimer's disease. Ann Neurol 45:358–368.

Raichle ME, MacLeod AM, Snyder AZ, Powers WJ, Gusnard DA, Shulman GL (2001) A default mode of brain function. Proc Natl Acad Sci U S A 98:676–682.

Rao VR, Finkbeiner S (2007) NMDA and AMPA receptors: old channels, new tricks. Trends Neurosci 30:284–291.

Reinders NR, Pao Y, Renner MC, da Silva-Matos CM, Lodder TR, Malinow R, Kessels HW (2016) Amyloid-β effects on synapses and memory require AMPA receptor subunit GluA3. Proc Natl Acad Sci U S A 113:E6526–E6534.

Ries M, Sastre M (2016) Mechanisms of Aβ clearance and degradation by glial cells. Front Aging Neurosci 8:160.

Roberts KF, Elbert DL, Kasten TP, Patterson BW, Sigurdson WC, Connors RE, Ovod V, Munsell LY, Mawuenyega KG, Miller-Thomas MM, Moran CJ, Cross DT, Derdeyn CP, Bateman RJ, Bateman RJ (2014) Amyloid-β efflux from the central nervous system into the plasma. Ann Neurol 76:837–844.

Rothstein JD, Dykes-Hoberg M, Pardo CA, Bristol LA, Jin L, Kuncl RW, Kanai Y, Hediger MA, Wang Y, Schielke JP, Welty DF (1996) Knockout of Glutamate Transporters Reveals a Major Role for Astroglial Transport in Excitotoxicity and Clearance of Glutamate. Neuron 16:675–686.

Sallmann S, Jüttler E, Prinz S, Petersen N, Knopf U, Weiser T, Schwaninger M (2000) Induction of interleukin-6 by depolarization of neurons. J Neurosci 20:8637–8642.

Samuels IS, Saitta SC, Landreth GE (2009) MAP'ing CNS development and cognition: an ERKsome process. Neuron 61:160–167.

Santos AE, Duarte CB, Iizuka M, Barsoumian EL, Ham J, Lopes MC, Carvalho AP, Carvalho AL (2006) Excitotoxicity mediated by Ca2+-permeable GluR4-containing AMPA receptors involves the AP-1 transcription factor. Cell Death Differ 13:652–660.

Sara Y, Bal M, Adachi M, Monteggia LM, Kavalali ET (2011) Use-dependent AMPA receptor block reveals segregation of spontaneous and evoked glutamatergic neurotransmission. J Neurosci 31:5378–5382.

Sattler R, Xiong Z, Lu W-Y, MacDonald JF, Tymianski M (2000) Distinct Roles of Synaptic and Extrasynaptic NMDA Receptors in Excitotoxicity. J Neurosci 20:22–33.

Scott HL, Pow D V, Tannenberg AEG, Dodd PR (2002) Aberrant Expression of the Glutamate Transporter Excitatory Amino Acid Transporter 1 (EAAT1) in Alzheimer ' s Disease. 22:1–5.

Selkoe DJ, Hardy J (2016) The amyloid hypothesis of Alzheimer's disease at 25 years. EMBO Mol Med 8:595–608.

Sheline YI, West T, Yarasheski K, Swarm R, Jasielec MS, Fisher JR, Ficker WD, Yan P, Xiong C, Frederiksen C, Grzelak M V., Chott R, Bateman RJ, Morris JC, Mintun MA, Lee J-M, Cirrito JR (2014) An Antidepressant Decreases CSF Aβ Production in Healthy Individuals and in Transgenic AD Mice. Sci Transl Med 6.

Shepherd JD, Huganir RL (2007) The cell biology of synaptic plasticity: AMPA receptor trafficking. Annu Rev Cell Dev Biol 23:613–643.

Shi L, Adams MM, Linville MC, Newton IG, Forbes ME, Long AB, Riddle DR, Brunso-Bechtold JK (2007) Caloric restriction eliminates the aging-related decline in NMDA and AMPA receptor subunits in the rat hippocampus and induces homeostasis. Exp Neurol 206:70–79.

Shippenberg TS, Thompson AC (2001) Overview of microdialysis. Curr Protoc Neurosci Chapter 7:Unit7.1.

Shrestha BR, Vitolo O V., Joshi P, Lordkipanidze T, Shelanski M, Dunaevsky A (2006) Amyloid β peptide adversely affects spine number and motility in hippocampal neurons. Mol Cell Neurosci 33:274–282.

Sommer B, Köhler M, Sprengel R, Seeburg PH (1991) RNA editing in brain controls a determinant of ion flow in glutamate-gated channels. Cell 67:11–19.

Spandidos A et al. (2008) A comprehensive collection of experimentally validated primers for Polymerase Chain Reaction quantitation of murine transcript abundance. BMC Genomics 9:633.

Spandidos A, Wang X, Wang H, Seed B (2010) PrimerBank: a resource of human and mouse PCR primer pairs for gene expression detection and quantification. Nucleic Acids Res 38:D792-9.

Sperling RA et al. (2011) Toward defining the preclinical stages of Alzheimer's disease : Recommendations from the National Institute on Aging and the Alzheimer's Association workgroup. Alzheimer's Dement:1–13.

Stansley B, Post J, Hensley K, Beers D, Appel S, Barger S, Hamdheydari L, Mhatre M, Mou S, Pye Q, Stewart C, West M, West S, Williamson K, Hensley K (2012) A comparative review of cell culture systems for the study of microglial biology in Alzheimer's disease. J Neuroinflammation 2012 91 99:1176–1187.

Storck SE et al. (2015) Endothelial LRP1 transports amyloid-β1–42 across the blood-brain barrier. J Clin Invest 126:123–136.

Strittmatter WJ, Saunders AM, Schmechel D, Pericak-Vance M, Enghild J, Salvesen GS, Roses AD (1993) Apolipoprotein E: high-avidity binding to beta-amyloid and increased frequency of type 4 allele in late-onset familial Alzheimer disease. Proc Natl Acad Sci USA 90:1977–1981.

Sutton MA, Ito HT, Cressy P, Kempf C, Woo JC, Schuman EM (2006) Miniature Neurotransmission Stabilizes Synaptic Function via Tonic Suppression of Local Dendritic Protein Synthesis. Cell 125:785–799.

Sutton MA, Schuman EM (2009) Partitioning the synaptic landscape: distinct microdomains for spontaneous and spike-triggered neurotransmission. Sci Signal 2:19.

Sutton MA, Taylor AM, Ito HT, Pham A, Schuman EM (2007) Postsynaptic Decoding of Neural Activity: eEF2 as a Biochemical Sensor Coupling Miniature Synaptic Transmission to Local Protein Synthesis. Neuron 55:648–661.

Sutton MA, Wall NR, Aakalu GN, Schuman EM (2004) Regulation of dendritic protein synthesis by miniature synaptic events. Science 304:1979–1983.

Swanson GT (2009) Targeting AMPA and kainate receptors in neurological disease: therapies on the horizon? Neuropsychopharmacology 34:249–250.

Talantova M et al. (2013) Aβ induces astrocytic glutamate release, extrasynaptic NMDA receptor activation, and synaptic loss. Proc Natl Acad Sci U S A 110:E2518-27.

Tampellini D (2015) Synaptic activity and Alzheimer's disease: a critical update. Front Neurosci 9:423.

Tampellini D, Capetillo-Zarate E, Dumont M, Huang Z, Yu F, Lin MT, Gouras GK (2010a) Effects of synaptic modulation on beta-amyloid, synaptophysin, and memory performance in Alzheimer's disease transgenic mice. J Neurosci 30:14299–14304.

Tampellini D, Capetillo-Zarate E, Dumont M, Huang Z, Yu F, Lin MT, Gouras GK (2010b) Effects of synaptic modulation on beta-amyloid, synaptophysin, and memory performance in Alzheimer's disease transgenic mice. J Neurosci 30:14299–14304.

Tang Y, Le W (2016) Differential Roles of M1 and M2 Microglia in Neurodegenerative Diseases. Mol Neurobiol 53:1181–1194.

Tanzi R, Gusella J, Watkins P, Bruns G, St George-Hyslop P, Van Keuren M, Patterson D, Pagan S, Kurnit D, Neve R (1987) Amyloid beta protein gene: cDNA, mRNA distribution, and genetic linkage near the Alzheimer locus. Science (80) 235.

Tanzi RE (2012) The genetics of Alzheimer disease. Cold Spring Harb Perspect Med 2:a006296.

Tanzi RE, Moir RD, Wagner SL (2004) Clearance of Alzheimer's A?? peptide: The many roads to perdition. Neuron 43:605–608.

Tarasoff-Conway JM, Carare RO, Osorio RS, Glodzik L, Butler T, Fieremans E, Axel L, Rusinek H, Nicholson C, Zlokovic B V, Frangione B, Blennow K, Ménard J, Zetterberg H, Wisniewski T, de Leon MJ (2015) Clearance systems in the brain-implications for Alzheimer disease. Nat Rev Neurol 11:457–470.

Thinakaran G, Koo EH (2008) Amyloid precursor protein trafficking, processing, and function. J Biol Chem 283:29615–29619.

Tian X, Gotoh T, Tsuji K, Lo EH, Huang S, Feig L a (2004) Developmentally regulated role for Ras-GRFs in coupling NMDA glutamate receptors to Ras, Erk and CREB. EMBO J 23:1567–1575.

Trussell LO, Zhang S, Ramant IM (1993) Desensitization of AMPA receptors upon multiquantal neurotransmitter release. Neuron 10:1185–1196.

Turner PR, O'Connor K, Tate WP, Abraham WC (2003) Roles of amyloid precursor protein and its fragments in regulating neural activity, plasticity and memory. Prog Neurobiol 70:1–32.

Vantaggiato C, Formentini I, Bondanza A, Bonini C, Naldini L, Brambilla R (2006) ERK1 and ERK2 mitogen-activated protein kinases affect Ras-dependent cell signaling differentially. J Biol 5:14.

Verges DK, Restivo JL, Goebel WD, Holtzman DM, Cirrito JR (2011) Opposing synaptic regulation of amyloid-β metabolism by NMDA receptors in vivo. J Neurosci 31:11328–11337.

Verkhratsky A, Olabarria M, Noristani HN, Yeh C-Y, Rodriguez JJ (2010) Astrocytes in Alzheimer's disease. Neurotherapeutics 7:399–412.

Wang W-Y, Jia L-J, Luo Y, Zhang H-H, Cai F, Mao H, Xu W-C, Fang J-B, Peng Z-Y, Ma Z-W, Chen Y-H, Zhang J, Wei Z, Yu B-W, Hu S-F (2016) Location- and Subunit-Specific NMDA Receptors Determine the Developmental Sevoflurane Neurotoxicity Through ERK1/2 Signaling. Mol Neurobiol 53:216–230.

Wang W-Y, Tan M, Yu J-T, Tan L (2015) Role of pro-inflammatory cytokines released from microglia in Alzheimer's disease. Ann Transl Med 3:136.

Wang X, Seed B (2003) A PCR primer bank for quantitative gene expression analysis. Nucleic Acids Res 31:154.

Wang Y, Durkin JP (1995) alpha-Amino-3-hydroxy-5-methyl-4-isoxazolepropionic acid, but Not N-Methyl-D-aspartate, Activates Mitogen-activated Protein Kinase through G-protein beta Subunits in Rat Cortical Neurons. J Biol Chem 270:22783–22787.

Wang Y, Small DL, Stanimirovic DB, Morley P, Durkin JP (1997) AMPA receptor-mediated regulation of a Gi-protein in cortical neurons. Nature 389:502–504.

Wei W, Nguyen LN, Kessels HW, Hagiwara H, Sisodia S, Malinow R (2010) Amyloid beta from axons and dendrites reduces local spine number and plasticity. Nat Neurosci 13:190–196.

Weller RO, Subash M, Preston SD, Mazanti I, Carare RO (2007) Clearance of Aβ from the Brain in Alzheimer's Disease: Perivascular Drainage of Amyloid-β Peptides from the Brain and Its Failure in Cerebral Amyloid Angiopathy and Alzheimer's Disease. Brain Pathol 18:253–266.

Wenthold RJ, Petralia RS, Blahos J II, Niedzielski AS (1996) Evidence for multiple AMPA receptor complexes in hippocampal CA1/CA2 neurons. J Neurosci 16:1982–1989.

Wroge CM, Hogins J, Eisenman L, Mennerick S (2012) Synaptic NMDA receptors mediate hypoxic excitotoxic death. J Neurosci 32:6732–6742.

Wyss-Coray T (2006) Inflammation in Alzheimer disease: driving force, bystander or beneficial response? Nat Med 12:1005–1015.

Wyss-Coray T, Loike JD, Brionne TC, Lu E, Anankov R, Yan F, Silverstein SC, Husemann J (2003) Adult mouse astrocytes degrade amyloid-beta in vitro and in situ. Nat Med 9:453–457.

Xia Z, Dudek H, Miranti CK, Greenberg ME (1996) Calcium Influx via the NMDA Receptor Induces Immediate Early Gene Transcription by a MAP Kinase/ERK-Dependent Mechanism. J Neurosci 16:5425-5436.

Xiao Q, Yan P, Ma X, Liu H, Perez R, Zhu A, Gonzales E, Burchett JM, Schuler DR, Cirrito JR, Diwan A, Lee J-M (2014) Enhancing astrocytic lysosome biogenesis facilitates Aβ clearance and attenuates amyloid plaque pathogenesis. J Neurosci 34:9607–9620.

Xiao Q, Yan P, Ma X, Liu H, Perez R, Zhu A, Gonzales E, Tripoli DL, Czerniewski L, Ballabio A, Cirrito JR, Diwan A, Lee J-M (2015) Neuronal-Targeted TFEB Accelerates Lysosomal Degradation of APP, Reducing Aβ Generation and Amyloid Plaque Pathogenesis. J Neurosci 35:12137–12151.

Xie L, Kang H, Xu Q, Chen MJ, Liao Y, Thiyagarajan M, O'Donnell J, Christensen DJ, Nicholson C, Iliff JJ, Takano T, Deane R, Nedergaard M (2013) Sleep drives metabolite clearance from the adult brain. Science 342:373–377.

Yamada KA, Rothman SM (1992) Diazoxide blocks glutamate desensitization and prolongs excitatory postsynaptic currents in rat hippocampal neurons. J Physiol 458:409–423.

Yan P, Bero AW, Cirrito JR, Xiao Q, Hu X, Wang Y, Gonzales E, Holtzman DM, Lee J-M (2009) Characterizing the appearance and growth of amyloid plaques in APP/PS1 mice. J Neurosci 29:10706–10714.

Yan P, Hu X, Song H, Yin K, Bateman RJ, Cirrito JR, Xiao Q, Hsu FF, Turk JW, Xu J, Hsu CY, Holtzman DM, Lee J-M (2006) Matrix metalloproteinase-9 degrades amyloid-beta fibrils in vitro and compact plaques in situ. J Biol Chem 281:24566–24574.

Yoon S, Seger R (2006) The extracellular signal-regulated kinase: Multiple substrates regulate diverse cellular functions. Growth Factors 24:21–44.

Yu C-G, Yezierski RP, Joshi A, Raza K, Li Y, Geddes JW (2010) Involvement of ERK2 in traumatic spinal cord injury. J Neurochem 113:131–142.

Yu CG (2012) Distinct roles for ERK1 and ERK2 in pathophysiology of CNS. Front Biol (Beijing) 7:267–276.

Zhang X-M, Luo J-H (2013) GluN2A versus GluN2B: twins, but quite different. Neurosci Bull 29:761–772.

Zhang Y, Li P, Feng J, Wu M (2016) Dysfunction of NMDA receptors in Alzheimer's disease. Neurol Sci 37:1039–1047.

Zheng H, Koo EH, White K, Tessier-Lavigne M (2011) Biology and pathophysiology of the amyloid precursor protein. Mol Neurodegener 6:27.

Zhu JJ, Qin Y, Zhao M, Van Aelst L, Malinow R (2002a) Ras and Rap Control AMPA Receptor Trafficking during Synaptic Plasticity. Cell 110:443–455.

Zhu X, Lee H-G, Raina AK, Perry G, Smith MA (2002b) The Role of Mitogen-Activated Protein Kinase Pathways in Alzheimer's Disease. Neurosignals 11:270–281.

Zolotukhin S, Potter M, Zolotukhin I, Sakai Y, Loiler S, Fraites TJ, Chiodo VA, Phillipsberg T, Muzyczka N, Hauswirth WW, Flotte TR, Byrne BJ, Snyder RO (2002) Production and purification of serotype 1, 2, and 5 recombinant adeno-associated viral vectors. Methods 28:158–167.